

Jordan Journal of Mechanical and Industrial Engineering (JJMIE)

JJMIE is a high-quality scientific journal devoted to fields of Mechanical and Industrial Engineering. It is published by The Hashemite University in corporation with the Jordanian Scientific Research Support Fund.

EDITORIAL BOARD

Editor-in-Chief

Prof. **Nabil Anagreh**

Editorial board

Prof. **Mohammad Ahmad Hamdan**
University of Jordan

Prof. **Ibrahim A. Rawabdeh**
University of Jordan

Prof. **Amin Al Robaidi**
Al Balqa Applied University

Prof. **Naser Al-Hunuti**
University of Jordan

Prof. **Suhil Kiwan**
Jordan University of Science and Technology

Prof. **Mahmoud Abu-Zaid**
Mutah University

Assistant Editor

Dr. **Dr. Khalid Al-Widyan**
Hashemite University

Dr. **Ahmed Al-Ghandoor**
Hashemite University

Dr. **Osama Al Meanazel**
Hashemite University

THE INTERNATIONAL ADVISORY BOARD

Abu-Qudais, Mohammad
Jordan University of Science & Technology, Jordan

Abu-Mulaweh, Hosni
Purdue University at Fort Wayne, USA

Afaneh Abdul-Hafiz
Robert Bosch Corporation, USA

Afonso, Maria Dina
Institute Superior Tecnico, Portugal

Badiru, Adedji B.
The University of Tennessee, USA

Bejan, Adrian
Duke University, USA

Chalhoub, Nabil G.
Wayne State University, USA

Cho, Kyu-Kab
Pusan National University, South Korea

Dincer, Ibrahim
University of Ontario Institute of Technology,
Canada

Douglas, Roy
Queen's University, U. K

El Bassam, Nasir
International Research Center for Renewable
Energy, Germany

Haik, Yousef
United Arab Emirates University, UAE

Jaber, Jamal
Al- Balqa Applied University, Jordan

Jubran, Bassam
Ryerson University, Canada

Kakac, Sadik
University of Miami, USA

Khalil, Essam-Eddin
Cairo University, Egypt

Mutoh, Yoshiharu
Nagaoka University of Technology, Japan

Pant, Durbin
Iowa State University, USA

Riffat, Saffa
The University of Nottingham, U. K

Saghir, Ziad
Ryerson University, Canada

Sarkar, MD. Abdur Rashid
Bangladesh University of Engineering &
Technology, Bangladesh

Siginer, Dennis
Wichita State University, USA

Sopian, Kamaruzzaman
University Kebangsaan Malaysia, Malaysia

Tzou, Gow-Yi
Yung-Ta Institute of Technology and Commerce,
Taiwan

EDITORIAL BOARD SUPPORT TEAM

Language Editor

Dr. Qusai Al-Debyan

Publishing Layout

Eng. Mohannad Oqdeh

SUBMISSION ADDRESS:

Prof. **Nabil Anagreh**, Editor-in-Chief
Jordan Journal of Mechanical & Industrial Engineering,
Hashemite University,
PO Box 330127, Zarqa, 13133, Jordan
E-mail: jjmie@hu.edu.jo



Hashemite Kingdom of Jordan



Hashemite University

Jordan Journal of
Mechanical and Industrial Engineering

JJMIE

An International Peer-Reviewed Scientific Journal
Financed by Scientific Research Support Fund

<http://jjmie.hu.edu.jo/>

ISSN 1995-6665

Jordan Journal of Mechanical and Industrial Engineering (JJMIE)

JJMIE is a high-quality scientific journal devoted to fields of Mechanical and Industrial Engineering. It is published by The Jordanian Ministry of Higher Education and Scientific Research in corporation with the Hashemite University.

Introduction: The Editorial Board is very committed to build the Journal as one of the leading international journals in mechanical and industrial engineering sciences in the next few years. With the support of the Ministry of Higher Education and Scientific Research and Jordanian Universities, it is expected that a heavy resource to be channeled into the Journal to establish its international reputation. The Journal's reputation will be enhanced from arrangements with several organizers of international conferences in publishing selected best papers of the conference proceedings.

Aims and Scope: Jordan Journal of Mechanical and Industrial Engineering (JJMIE) is a refereed international journal to be of interest and use to all those concerned with research in various fields of, or closely related to, mechanical and industrial engineering disciplines. Jordan Journal of Mechanical and Industrial Engineering aims to provide a highly readable and valuable addition to the literature which will serve as an indispensable reference tool for years to come. The coverage of the journal includes all new theoretical and experimental findings in the fields of mechanical and industrial engineering or any closely related fields. The journal also encourages the submission of critical review articles covering advances in recent research of such fields as well as technical notes.

Guide for Authors

Manuscript Submission

High-quality submissions to this new journal are welcome now and manuscripts may be either submitted online or mail.

Online: For online submission upload one copy of the full paper including graphics and all figures at the online submission site, accessed via E-mail: jjmie@hu.edu.jo. The manuscript must be written in MS Word Format. All correspondence, including notification of the Editor's decision and requests for revision, takes place by e-mail and via the Author's homepage, removing the need for a hard-copy paper trail.

By Mail: Manuscripts (1 original and 3 copies) accompanied by a covering letter may be sent to the Editor-in-Chief. However, a copy of the original manuscript, including original figures, and the electronic files should be sent to the Editor-in-Chief. Authors should also submit electronic files on disk (one disk for text material and a separate disk for graphics), retaining a backup copy for reference and safety.

Note that contributions may be either submitted online or sent by mail. Please do NOT submit via both routes. This will cause confusion and may lead to delay in article publication. Online submission is preferred.

Submission address and contact:

Prof. **Nabil Anagreh**, Editor-in-Chief
Jordan Journal of Mechanical & Industrial Engineering,
Hashemite University,
PO Box 330127, Zarqa, 13115 , Jordan
E-mail: jjmie@hu.edu.jo

Types of contributions: Original research papers

Corresponding author: Clearly indicate who is responsible for correspondence at all stages of refereeing and publication, including post-publication. Ensure that telephone and fax numbers (with country and area code) are provided in addition to the e-mail address and the complete postal address. Full postal addresses must be given for all co-authors.

Original material: Submission of an article implies that the work described has not been published previously (except in the form of an abstract or as part of a published lecture or academic thesis), that it is not under consideration for publication elsewhere, that its publication is approved by all authors and that, if accepted, it will not be published elsewhere in the same form, in English or in any other language, without the written consent of the Publisher. Authors found to be deliberately contravening the submission guidelines on originality and exclusivity shall not be considered for future publication in this journal.

Supplying Final Accepted Text on Disk: If online submission is not possible: Once the paper has been accepted by the editor, an electronic version of the text should be submitted together with the final hardcopy of the manuscript. The electronic version must match the hardcopy exactly. We accept MS Word format only. Always keep a backup copy of the electronic file for reference and safety. Label the disk with your name. Electronic files can be stored on CD.

Notification: Authors will be notified of the acceptance of their paper by the editor. The Publisher will also send a notification of receipt of the paper in production.

Copyright: All authors must sign the Transfer of Copyright agreement before the article can be published. This transfer agreement enables Jordan Journal of Mechanical and Industrial Engineering to protect the copyrighted material for the authors, but does not relinquish the authors' proprietary rights. The copyright transfer covers the exclusive rights to reproduce and distribute the article, including reprints, photographic reproductions, microfilm or any other reproductions of similar nature and translations.

PDF Proofs: One set of page proofs in PDF format will be sent by e-mail to the corresponding author, to be checked for typesetting/editing. The corrections should be returned within 48 hours. No changes in, or additions to, the accepted (and subsequently edited) manuscript will be allowed at this stage. Proofreading is solely the author's responsibility. Any queries should be answered in full. Please correct factual errors only, or errors introduced by typesetting. Please note that once your paper has been proofed we publish the identical paper online as in print.

Author Benefits

Page charge: Publication in this journal is free of charge.

Free off-prints: Three journal issues of which the article appears in along with twenty-five off-prints will be supplied free of charge to the corresponding author. Corresponding authors will be given the choice to buy extra off-prints before printing of the article.

Manuscript Preparation:

General: Editors reserve the right to adjust style to certain standards of uniformity. Original manuscripts are discarded after publication unless the Publisher is asked to return original material after use. If online submission is not possible, an electronic copy of the manuscript on disk should accompany the final accepted hardcopy version. Please use MS Word for the text of your manuscript.

Structure: Follow this order when typing manuscripts: Title, Authors, Affiliations, Abstract, Keywords, Introduction, Main text, Conclusions, Acknowledgements, Appendix, References, Figure Captions, Figures and then Tables. For submission in hardcopy, do not import figures into the text - see Illustrations. For online submission, please supply figures imported into the text AND also separately as original graphics files. Collate acknowledgements in a separate section at the end of the article and do not include them on the title page, as a footnote to the title or otherwise.

Text Layout: Use double spacing and wide (3 cm) margins. Ensure that each new paragraph is clearly indicated. Present tables and figure legends on separate pages at the end of the manuscript. If possible, consult a recent issue of the journal to become familiar with layout and conventions. All footnotes (except for table and corresponding author footnotes) should be identified with superscript Arabic numbers. To conserve space, authors are requested to mark the less important parts of the paper (such as records of experimental results) for printing in smaller type. For long papers (more than 4000 words) sections which could be deleted without destroying either the sense or the continuity of the paper should be indicated as a guide for the editor. Nomenclature should conform to that most frequently used in the scientific field concerned. Number all pages consecutively; use 12 or 10 pt font size and standard fonts. If submitting in hardcopy, print the entire manuscript on one side of the paper only.

Corresponding author: Clearly indicate who is responsible for correspondence at all stages of refereeing and publication, including post-publication. The corresponding author should be identified with an asterisk and footnote. Ensure that telephone and fax numbers (with country and area code) are provided in addition to the e-mail address and the complete postal address. Full postal addresses must be given for all co-authors. Please consult a recent journal paper for style if possible.

Abstract: A self-contained abstract outlining in a single paragraph the aims, scope and conclusions of the paper must be supplied.

Keywords: Immediately after the abstract, provide a maximum of six keywords (avoid, for example, 'and', 'of'). Be sparing with abbreviations: only abbreviations firmly established in the field may be eligible.

Symbols: All Greek letters and unusual symbols should be identified by name in the margin, the first time they are used.

Units: Follow internationally accepted rules and conventions: use the international system of units (SI). If other quantities are mentioned, give their equivalent in SI.

Maths: Number consecutively any equations that have to be displayed separately from the text (if referred to explicitly in the text).

References: All publications cited in the text should be presented in a list of references following the text of the manuscript.

Text: Indicate references by number(s) in square brackets in line with the text. The actual authors can be referred to, but the reference number(s) must always be given.

List: Number the references (numbers in square brackets) in the list in the order in which they appear in the text.

Examples:

Reference to a journal publication:

- [1] M.S. Mohsen, B.A. Akash, "Evaluation of domestic solar water heating system in Jordan using analytic hierarchy process". *Energy Conversion & Management*, Vol. 38, No. 9, 1997, 1815-1822.

Reference to a book:

- [2] Strunk Jr W, White EB. *The elements of style*. 3rd ed. New York: Macmillan; 1979.

Reference to a conference proceeding:

- [3] B. Akash, S. Odeh, S. Nijmeh, "Modeling of solar-assisted double-tube evaporator heat pump system under local climate conditions". 5th Jordanian International Mechanical Engineering Conference, Amman, Jordan, 2004.

Reference to a chapter in an edited book:

- [4] Mettam GR, Adams LB. How to prepare an electronic version of your article. In: Jones BS, Smith RZ, editors. *Introduction to the electronic age*, New York: E-Publishing Inc; 1999, p. 281-304

Free Online Color: If, together with your accepted article, you submit usable color and black/white figures then the journal will ensure that these figures will appear in color on the journal website electronic version.

Tables: Tables should be numbered consecutively and given suitable captions and each table should begin on a new page. No vertical rules should be used. Tables should not unnecessarily duplicate results presented elsewhere in the manuscript (for example, in graphs). Footnotes to tables should be typed below the table and should be referred to by superscript lowercase letters.

EDITORIAL PREFACE

It is my great pleasure to publish Volume 7, Number 1, December 2013 of the *Jordan Journal of Mechanical and Industrial Engineering (JJMIE)*. *JJMIE* is a refereed, peer reviewed international journal issued by the Jordanian Ministry of Higher Education and Scientific Research in cooperation with the Hashemite University. *JJMIE* aims at providing a highly readable and valuable addition to the literature, which will serve as an indispensable reference tool for the years to come .

The journal covers a wide range of research and development concerning mechanical, industrial, material, mechatronics, and biomedical engineering. Through this publication, we hope to establish and provide an international platform for information exchange in the different fields mentioned above. The journal also encourages the submission of critical review articles, as well as technical notes, covering advances in the recent research pertaining to such fields.

This issue contains nine interesting research papers covering various aspects of solar energy, control, nanomaterial, composite material, quality management, and manufacturing: (i) performance study of on-grid thin-film photovoltaic solar station as a pilot project for architectural use; (ii) hourly solar radiation prediction based on nonlinear autoregressive exogenous (narx) neural network; (iii) development of a bond graph control maximum power point tracker for photovoltaic: theoretical and experimental; (iv) a comparative study of PZT-based & TiNi-shape memory alloy based MEMS microactuators; (v) crystallization behavior of iPP/LLDPE blend filled with Nano kaolin particles; (vi) studying the properties of polymer blends sheets for decorative purposes; (vii) investigating the applicability of EFQM and KAIIAE in Jordanian healthcare organizations: a case study; (viii) understanding the linkage between soft and hard total quality management: evidence from Malaysian manufacturing industries; (ix) prediction of surface roughness in electrical discharge machining of SKD 11 tool steel using recurrent Elman networks. The methodology employed in these research articles ranges from analytical and empirical models to experimental studies.

It is due to the dedicated efforts of our editors and reviewers that our journal is attracting high quality research papers from the authority in the field, and is becoming increasingly more popular amongst our engineer profession colleagues. It gives us immense pleasure to see the journal grow by leaps and bounds, and become stronger with each day passing by.

The Editorial Board is very committed to build the Journal as one of the leading international journals in mechanical, industrial, material, mechatronics, and biomedical engineering in the next few years. With the support of the Ministry of Higher Education and Scientific Research and Jordanian Universities, it is expected that valuable resources will be channeled into the Journal to establish its international reputation.

It is my great pleasure to thank the former Editorial Boards and Editors-in-Chief for founding *JJMIE*. I would like to thank all members of the recent editorial board, the international advisory board members, assistant editors, and the editorial board support team (language editor and publishing layout) for their continued support to *JJMIE* with their highly valuable advice. Additionally, I would like to thank the manuscript reviewers for providing valuable comments and suggestions to the authors that helped greatly in improving the quality of the papers. My sincere appreciation goes to all authors and readers of *JJMIE* for their excellent support and timely contribution to this journal. My great appreciation goes to the dean of Faculty of Engineering (Dr. Shaher Rababeh) and my colleagues at the Engineering Faculty of Hashemite University.

I would be delighted if the *JJMIE* could deliver valuable and interesting information to the worldwide community at the various fields of engineering. Your cooperation and contribution would be highly appreciated. More information about the *JJMIE* guidelines for preparing and submitting papers may be obtained from: www.jjmie.hu.edu.jo

Now, the *JJMIE* invites contributions from the entire international research community. The new journal will continue to deliver up-to-date research to a wide range of mechanical, industrial, material, mechatronics, and biomedical engineering professionals. The *JJMIE* will assure that rapid turnaround and publication of manuscripts will occur within three to six months after submission.

Prof. Nabil Anagreh
Editor-in-Chief
Hashemite University
Zarqa, Jordan, 2013

PAGES	PAPERS
1 - 9	Performance Study of On-Grid Thin-Film Photovoltaic Solar Station as a Pilot Project for Architectural Use <i>Bashar K. Hammad, Shaher M. Rababeh, Mohammad A. Al-Abed and Ahmed M. Al-Ghandoor</i>
11 - 18	Hourly Solar Radiation Prediction Based on Nonlinear Autoregressive Exogenous (Narx) Neural Network <i>Lubna. B. Mohammed, Mohammad. A. Hamdan, Eman A. Abdelhafez And Walid Shaheen</i>
19 - 26	Development of A Bond Graph Control Maximum Power Point Tracker For Photovoltaic: Theoretical And Experimental <i>BADOUD Abd Essalam and KHEMLICHE Mabrouk</i>
27 - 34	A Comparative Study of PZT-Based & TiNi- Shape Memory Alloy Based MEMS Microactuators <i>S. D. Nijmeh, M. S. Ashhab and R. F. Khasawneh</i>
35 - 39	Crystallization behavior of iPP/LLDPE blend filled with nano kaolin particles <i>Amin Al Robaidi , Nabil Anagreh, Mohammed A-l Addous and Sami Massadeh</i>
41 - 48	Studying the Properties of Polymer blends Sheets for Decorative Purposes <i>Abdullah M. Al-Huneidei and Issam S. Jalham</i>
49 - 55	Investigating the Applicability of EFQM and KAIIE in Jordanian Healthcare Organizations: A Case Study <i>Abdallah Abdallah, Ban M. Haddadin, Hiba M. Al-Atiyat, Leen J. Haddad and Samer L. Al-Sharif</i>
57 - 65	Understanding the Linkage between Soft and Hard Total Quality Management: Evidence from Malaysian Manufacturing Industries <i>Amjad Al-Khalili and Khairanum Subari</i>
67 - 71	Prediction of surface roughness in Electrical Discharge Machining of SKD 11 TOOL steel using Recurrent Elman Networks <i>R. DAS, M. K Pradhan and C Das</i>

Performance Study of On-Grid Thin-Film Photovoltaic Solar Station as a Pilot Project for Architectural Use

Bashar K. Hammad^{*,a}, Shaher M. Rababeh^b, Mohammad A. Al-Abed^c

and Ahmed M. Al-Ghandoor^d

^a *Mechatronics Engineering Department, the Hashemite University, Zarqa, Jordan*

^b *Architecture Engineering Department, the Hashemite University, Zarqa, Jordan*

^c *Biomedical Engineering Department, the Hashemite University, Zarqa, Jordan*

^d *Industrial Engineering Department, the Hashemite University, Zarqa, Jordan*

Abstract:

We present a full description of a pilot photovoltaic station with thin-film modules, a newly-introduced technology in the market of solar systems in Jordan. In order to take the issue of landscaping of outdoor spaces in a hot semi-arid environment, give the Hashemite University campus a unique identity, and improve its aesthetic image, this pilot station has been installed as a canopy covering for 4-car parking space. The system is tested for a two-month period to check its behavior in the Northeastern sector of Jordan environmental conditions and study the effect of local climate. The system is connected to the local grid via a solar inverter. Measurement and monitoring systems are utilized to acquire data necessary to analyze the system performance. We investigate the effect of the system location, modules and ambient temperatures, wind, and dust on the system efficiency. We show instantaneous and daily average data for several performance metrics. The preliminary results show that the efficiency of the system is within the normal range for this type of technology tested in other countries. Harsh environment of Jordan semi-arid region has adverse effects, where the efficiency of the system is reduced by about 10% due to accumulation of dust. However, a feasibility study is planned in the near future after obtaining sufficient data to evaluate the economic value of thin-film systems in Jordan.

© 2013 Jordan Journal of Mechanical and Industrial Engineering. All rights reserved

Keywords: Pilot Study; Thin-film; On-grid; Efficiency; Semi-arid environment; Dust; Landscape; Visual Impact.

1. Introduction

Two factors forced decision-makers in Jordan to think seriously of changing the reliance on traditional sources of energy into renewable sources; dependence on oil imported from outside and surge in its price. Solar energy, as one of the most important sources of renewable energy, obtains increasing attention in Jordan. Jordan is considered one of the sun-belt countries where the average annual solar radiation per day is 3.8 kWh/m² in winter and more than 8 kWh/m² in summer. In addition, the average sunshine duration is more than 300 days per year, and the yearly global solar radiation ranges from 1700 kWh/m² in Jordan valley and over 2250 kWh/m² for hill area [1].

It is important to mention that to the best of the authors' knowledge, all these PV systems, installed in Jordan for residential or commercial use, are of mono- or polycrystalline modules; there is no published data on the efficiency and functionality of thin-film PV system in semi-arid environment in Jordan. Although thin-film technologies were developed to reduce the cost of solar cells significantly [2; 3], the relatively low efficiency, compared to "traditional" PV technologies, makes it unattractive for consumers.

Razykov et al. [2] reviewed the progress made of mono- and poly-crystalline and thin-film photovoltaic manufacturing based on Si, semi-conductor and nano-technologies. They reported the efficiency of modules from several manufacturers ranging between 1.7% and 12.0%. However, research results showed that efficiencies up to 19-20%, for CIGS (Copper Indium Gallium Selenide), and 40%, for multi-junction III-V materials, can be achieved. In [4], Muñoz-García et al. analyzed different thin-film technologies to find the easiest method for obtaining the current-voltage (I-V) characteristics at standard conditions.

Thin-film PV technology utilized in a wide range of application, Yoon et al. [5] integrated transparent thin-film amorphous modules on the front windows of a building in Korea. After monitoring the system for 2 years, they reported that an electrical power of 580.5 kWh/kWp/year was generated.

Dust, humidity, and air speed are among the environmental factors that affect efficiency of PV systems. However, the study of Mekhilef et al. [6] is one of few studies on the effect of these three factors all together at the same time on the performance of PV cells.

However, Campus Master Plan for the Hashemite University (HU), as one contemporary building project

* Corresponding author. e-mail: bkhammad@hu.edu.jo.

constructed in a semi-arid zone, did not take into consideration the landscape issue of the outdoor spaces. Ill-planning for the outdoor spaces is clear where no efforts have been made to apply any passive design concepts. Adapting to the hot and arid climate in the HU campus, users like to stay at outdoor places, such as courtyards, streets and other open spaces in the summer time. However, the design of the university master plan does not include a decrease in solar exposure to maximize the frequency of acceptable thermal conditions resulting in exacerbating the urban heat effect. By recognizing how well HU campus outdoor spaces respond to the needs of faculty, students, and staff, one can recommend ways of improving the outdoor environment necessary to facilitate the work and learning experiences of different users within the campus and the desired student-faculty interaction.

For this purpose, the decision has been made to construct 5 MWp PV plants at HU. The proposal is to divide them into two forms; 4 MWp as a farm station on a hillside in the university, and 1 MWp PV system as distributed shelters for pedestrians and canopies for car parks. The users as local community were involved in the decision for this project and committed to the future care of the landscape elements. Project enhancements may cover sidewalk improvements, furnishings, lighting, and car parks. New elements should be properly integrated with and linked to existing streetscape elements and should contribute to creating a sense of place and university identity. In order to address the issues mentioned above and as a first step to give HU campus a unique identity, and to improve its aesthetic image, a pilot station has been installed as a canopy covering for 4-car parking space, (Figure 1). We installed a PV system in a shade-free location at the south side of the workshops of the Faculty of Engineering at HU (Figure 2). However, addressing this novel idea and strategy at HU will identify the PV plants as one of the technologies that would contribute and create more comfortable outdoor spaces for the inhabitants and their belongings. A discussion on how this procedure may be used and integrated into the administrative requirements of large and small scale PV plants developments is carried out.

The issue of visual impact seems to be the greatest. The visual impact, due to its subjective nature, is one of the main barriers that the wide adoption of solar panels could face [7]. The critical elements of the visual and aesthetic impact from the solar energy systems are the integration of their characteristics in the design, and the rational siting of the solar parks. The studies, concerning the procedures for assessing the territorial and landscape impacts of this type of systems, have recently seen a remarkable development [8; 9]. Landscape planning is setting the scale for a sustainable utilization. The main characteristics of a coherent landscape compose a state where all the functions and the processes are integral parts of the harmonious route in time and space. This coherence can break when building materials are used or when new structures are not related to the typical character of the region. Very often the integration can be solved by taking into account not only the visibility of the plant but also other aspects of the perception that are more difficult to measure, such as the shape and color of the artefacts. In this sense, the "clerestory concept" is implemented in the design of car-

parking canopy, (Figure 1) for supplying natural light and circulation of fresh air.

The thin-film technology is selected in this pilot project where a large shaded area is required, because it has a larger surface area per kWp of power generated compared to poly- and mono-crystalline technologies. Thin-film modules have a surface area of 16 m²/kWp, whereas it is 7 m²/kWp for monocrystalline modules and 8 m²/kWp for polycrystalline modules [10].



Figure 1. Solar PV parking installed at HU.

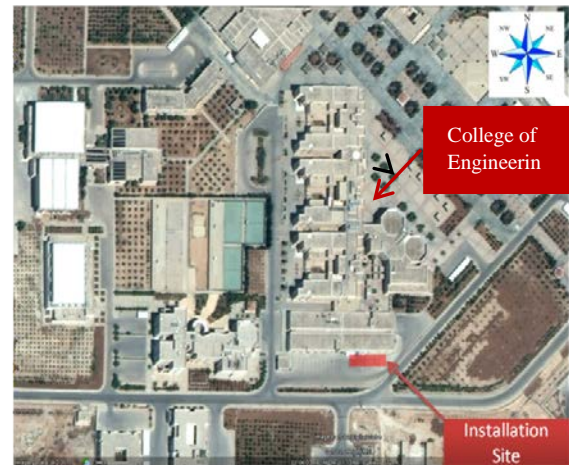


Figure 2. Aerial view of PV system at HU

The remainder of this paper is organized as follows: Section 2 describes the PV system, while Section 3 explains the measurement and monitoring system implemented to acquire and analyze data. Section 4 discusses some of the most important results obtained thus far, before we conclude some final remarks in Section 5.

2. Design and Setup

The system is oriented towards the exact south and is fixed at 30° from the horizontal (optimal inclination for maximum annual energy yield in Jordan). The system has the following features:

- 20 thin-film modules of 150 W (+/-5%) at the standard test conditions (STC). Technical specifications of each module are shown in Table 1.
- The system is composed of two strings connected in parallel. Each string has two parallel arrays and each array has 5 modules connected in series. By

implementing this design, a maximum current of 9.28 A and 323.5 V at STC are obtained, which are well below the maximum inputs to the solar inverter (Table 2).

- A steel/Aluminum frame to support the system.
- A Solar inverter, which a device that inverts DC power generated from the PV system into AC power synchronized with electricity available in local grid. Technical specifications of the inverter supplied with this system are shown in Table 2.

Table 1. Technical specifications of thin-film PV modules at Standard Test Conditions (STCs)

Parameter	Value
Open circuit voltage (V)	85.5
Short circuit current (A)	2.54
Maximum power voltage (V)	64.7
Maximum power current (A)	2.32
Power reduction (%/°C)	-0.28
Dimensions (mm)	1412×1112

Table 2. Technical specification of solar inverter

Parameter	Value
Maximum efficiency (%)	97.0
Maximum DC input power (W)	3200
Maximum DC input voltage (V)	550
Minimum DC input voltage (V)	125
Start Voltage(V)	150
Maximum input current (A)	17
Maximum AC apparent output power (VA)	3000
Maximum output current (A)	16
Power factor	1

3. Measurement Instruments And Data Logger

In this work, the system is equipped with the following sensors:

- Sensor box: it is used to measure solar radiation and modules and ambient temperatures. It provides data logger (described later) with continuous meteorological data. It is installed next to the PV system at the same orientation to measure total radiation without any need for further calculations. The solar radiation sensor consists of a PV cell type (amorphous silicon - aSi) with a measurement range between 0 and 1,500 W/m² and accuracy ± 8 % with a resolution of 1 W/m². The modules temperature sensor is attached underneath one of the modules far from the direct sun light. The module temperature sensor consists of a PT100 resistance and operating range between -20 °C and +110 °C and accuracy ± 0.5 °C with resolution of 0.1 °C
- Ambient temperature sensor: it consists of a PT 100 resistance and is connected to the sensor box described above. It is installed in a plastic enclosure and in the shade underneath system far from the direct sun light. Its operating range is -30 °C to +80 °C with a tolerance of ± 0.7 °C.

- Anemometer: it is installed at the top of system. It measures wind speed between 0.8 m/s to 40 m/s with 0.4 m resolution.
- A data logger is used for remote monitoring, diagnosis, and configuration of the PV system. It receives and stores simultaneously measured values and data from PV inverter and sensors. Data transmission takes place via the international wireless standard, Bluetooth, allowing remote inspection of the system at any time, detection of operational faults at early stages, and adjusting operating parameters from any location in the world as long as there is an internet connection. The data collected can be displayed daily, monthly, and yearly. It has a maximum communication range up to 100 m, an internal memory of 12.5 MB, and external memory (SD card) up to 2 GB.
- The shaded area (vertical projection), provided by the system as a whole, giving the system its architectural functionality as solar canopy, is about 10 m in length, and 5 m in depth, providing each car with about 12.5 m² of functional shade, that was not available for cars beforehand.

4. Results and Discussion

Sun path and ambient temperature vary from winter to summer and from day to day, and, consequently, affects the efficiency of PV modules. The Energy Efficiency is calculated simply as the output energy (electricity generated) divided by input energy (solar radiation). Mathematically, it is given by

$$\eta = \frac{\text{Output}}{\text{Input}} \% = \frac{\text{Power}}{\text{Direct Irradiance}} \%$$

$$= \frac{I \cdot V \cdot \text{power factor}}{(\frac{\text{Irradiance}}{\text{m}^2}) \cdot (\text{module area (m}^2\text{)}) \cdot \text{number of modules}} \%$$

where I and V are AC current and voltage, respectively, recorded by data logger, and assuming a power factor (PF) of 1 as an output of the inverter.

We ran the experiment on July 20th, 2012 for 60 days. Data for Five days (Days 22, 26, 41, 52, and 54) is missing or corrupt due to main power blackout (system is designed to shut down when main power is cut for safety purposes). We set the data logger to acquire measurements every five minutes. Figures 3 and 4 show the current and voltage, respectively, recorded during the period of the experiment supplied to the local grid (AC power). The maximum current (approximately 11 A) is below the limit of maximum output current (check Table 2 for inverter specification). In Figure 3, values for instantaneous current go from zero at the beginning of the day until they reach a maximum when the total radiation reaches its maximum for the day, Figure 5. However, the instantaneous voltage in Figure 4 jumps suddenly from zero to higher values when the voltage reaches a certain threshold set by the inverter. In addition, the value of maximum output voltage in Figure 4 is expected considering the arrangement of modules (parallel and series arrays and strings) and maximum power voltage of each module (check Table 1 for modules' specification). Figure 5 shows the total radiation incident on the system where the maximum solar radiation exceeds 1000 W/m² for the whole sixty days of

data collecting. This is expected during the summer season in Jordan. Comparing the behavior of current, voltage, and incident radiation, we notice that the output voltage is almost constant within a certain range and transition from ON state to OFF state is abrupt (inverter passes no voltage below a certain threshold), while the current goes from minimum value (zero or very small value) to a maximum gradually in a direct relationship with incident solar radiation. The values in Figures 3, 4, and 5 are used to calculate instantaneous efficiency for the whole system considering total surface area of the thin-film modules, Figures 6. It is clear that instantaneous efficiency rises abruptly (due to jump in voltage values, Figure 4) at the beginning of every day, then it decreases slightly before it increases considerably at the end of each day with a maximum instantaneous efficiency of 8–9.7%.

The average daily AC current, voltage, and incident solar radiation are shown in Figures 7, 8, and 9, respectively. The daily efficiency, Figure 10, agrees with reported values in several studies for other parts of the world, around 7%, [10, 11].

Due to the harsh environment at HU, its location near a major industrial and free-trade zone, and east of Jordan's main refinery, the modules were covered with accumulated dust, as pictured in Figure 11. After cleaning the system on Day 51 of the experiment, the daily efficiency increases from below 7% to above 7.5%, which translates to about

10% increase in the thin-film efficiency in converting solar radiation into AC power output per unit area. This increase in efficiency may be contributed to other factors other than dust such as cooling of modules. Further analysis is planned in the future.

Solar inverter efficiency (AC output power divided by DC input power) is calculated and shown in Figure 12. The inverter becomes switched on when voltage reaches a certain threshold and the instantaneous conversion efficiency jump to maximum of approximately 95%, which is below the maximum efficiency listed in tables of specifications for the inverter, Table 2. However the daily conversion efficiency is around 90%, Figure 13.

Increasing temperature has an adverse effect of the efficiency of the system (both for modules and inverter). Figure 14 shows variation of ambient and module temperatures for the 60 days of the experiment, and Figures 15 and 16 show the average daily ambient and module temperature, respectively, during the experiment.

The wind speed during the experiment, which was recorded and daily averaged, is shown in Figure 17. The values indicate that the wind speed is within the expected range in Jordan for this time of year.

The correlation between dust, wind, and ambient and modules temperature with the system efficiency will be the heart of the next study after acquiring sufficient data over all the seasons of the year.

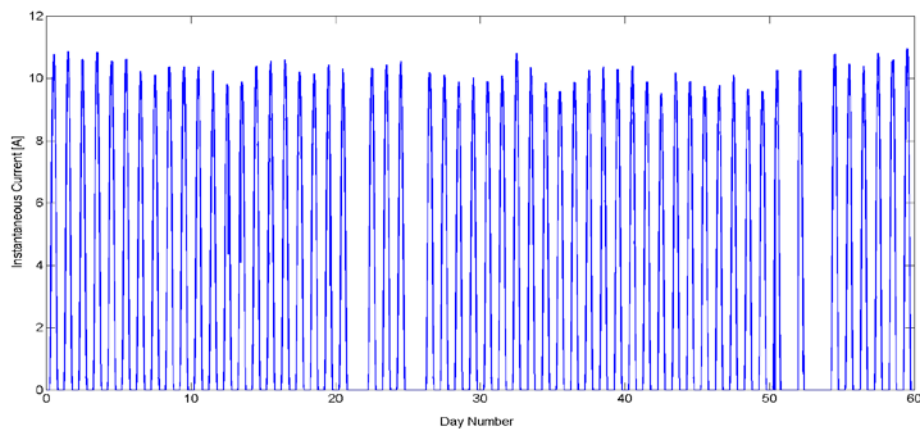


Figure 3. Instantaneous AC current supplied to the grid

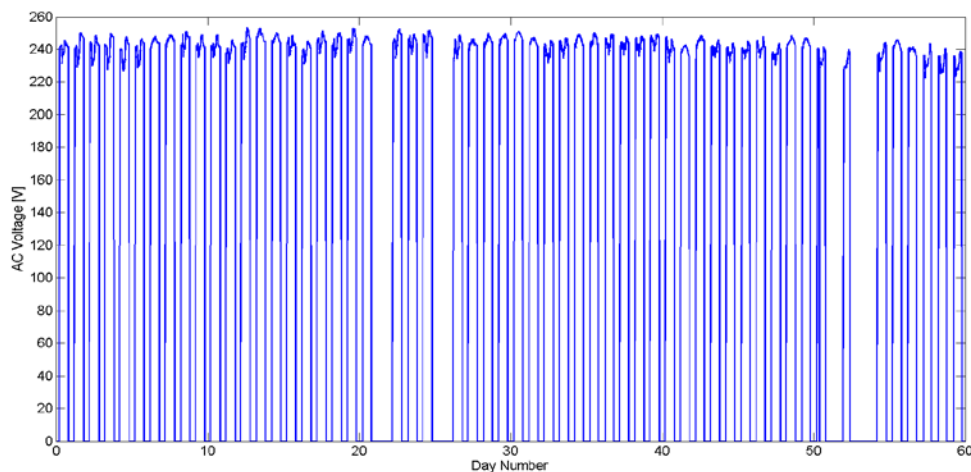


Figure 4. Instantaneous voltage supplied to the grid

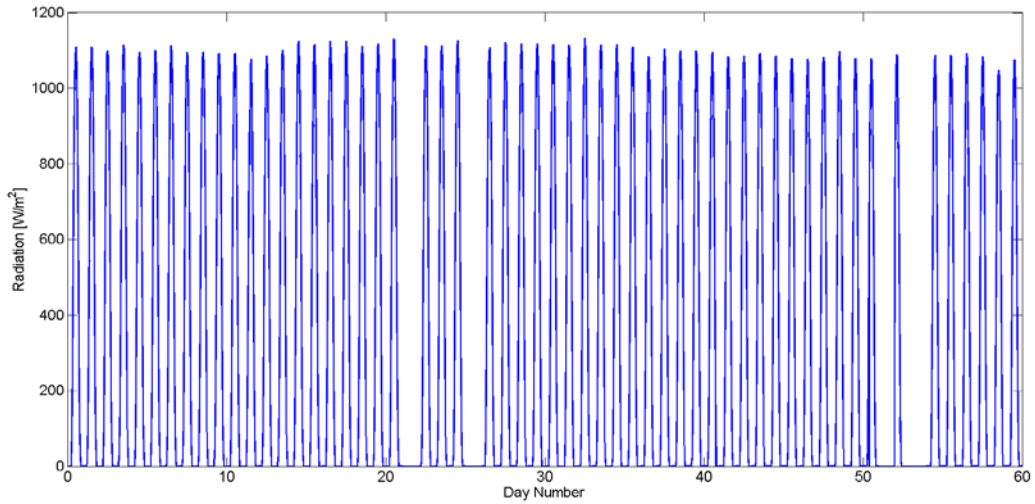


Figure 5. Instantaneous total solar radiation incident on system

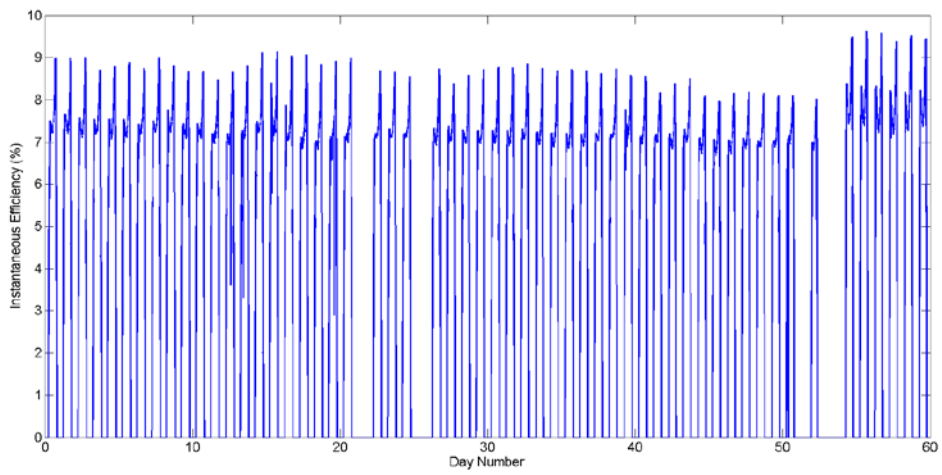


Figure 6. Instantaneous efficiency for the whole system

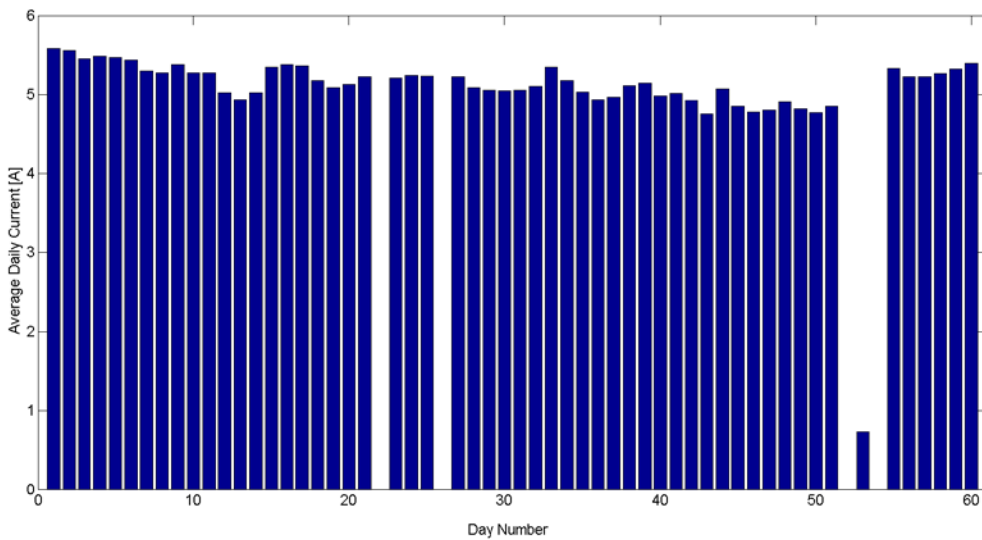


Figure 7. Average daily AC current supplied to the grid

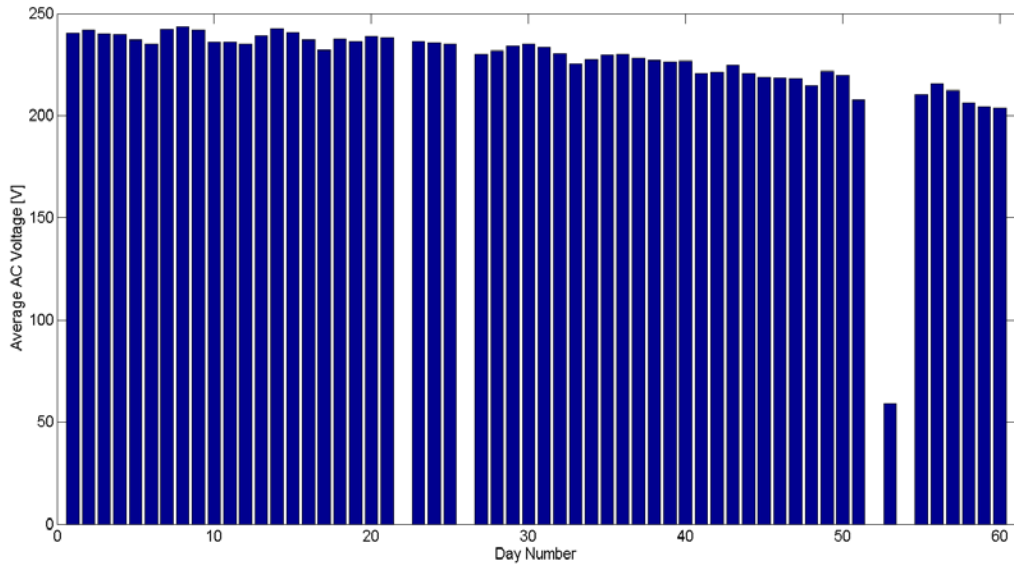


Figure 8. Average daily AC voltage supplied to the grid

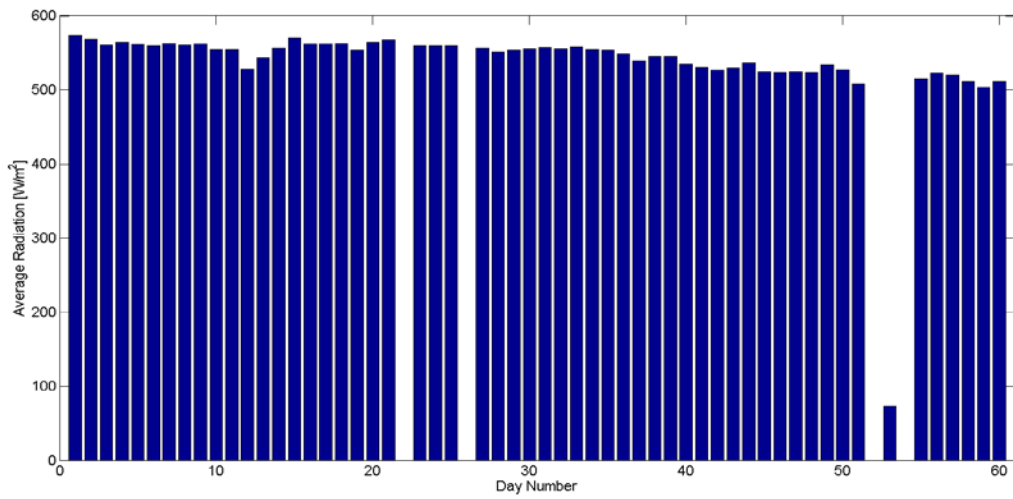


Figure 9. Average daily total solar radiation incident on system

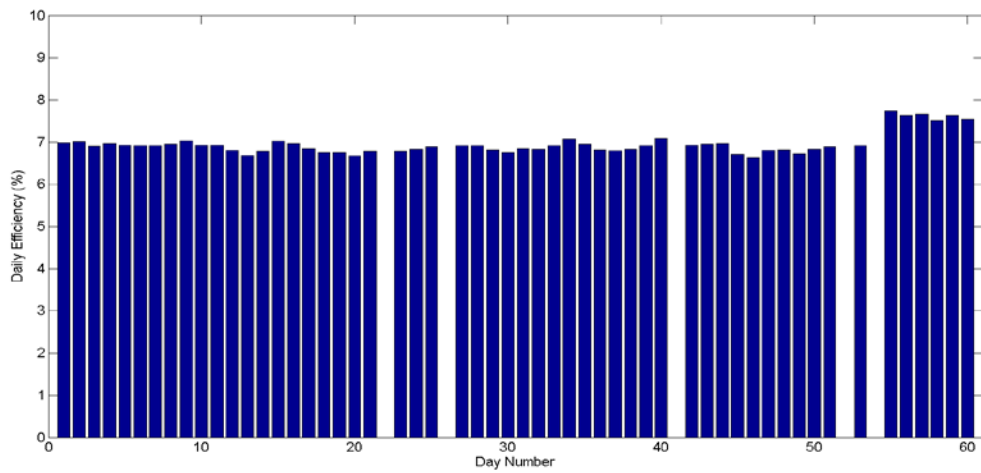


Figure 10. Daily efficiency for the whole system



Figure 11. System is covered with dust (picture taken after 45 days from running the system)

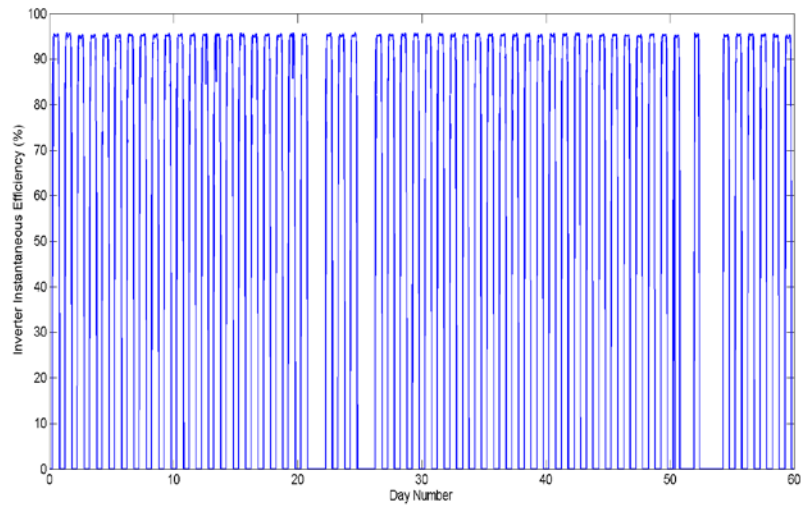


Figure 12. Instantaneous efficiency of the solar inverter

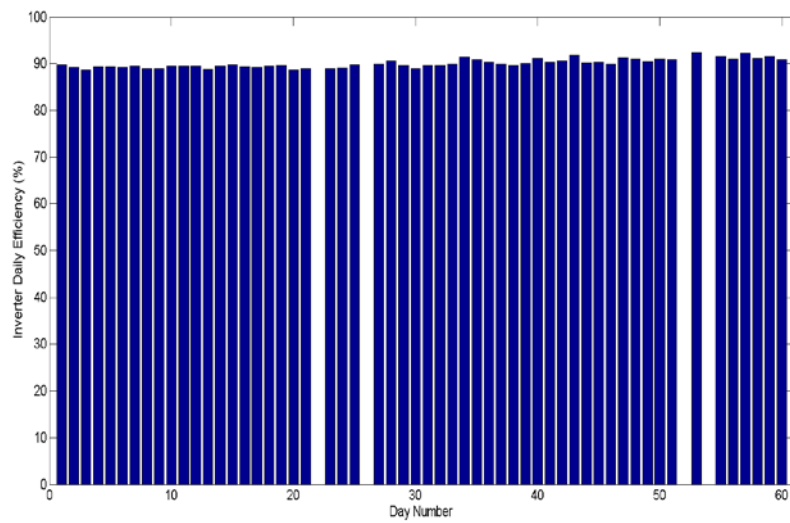


Figure 13: Daily efficiency of the solar inverter

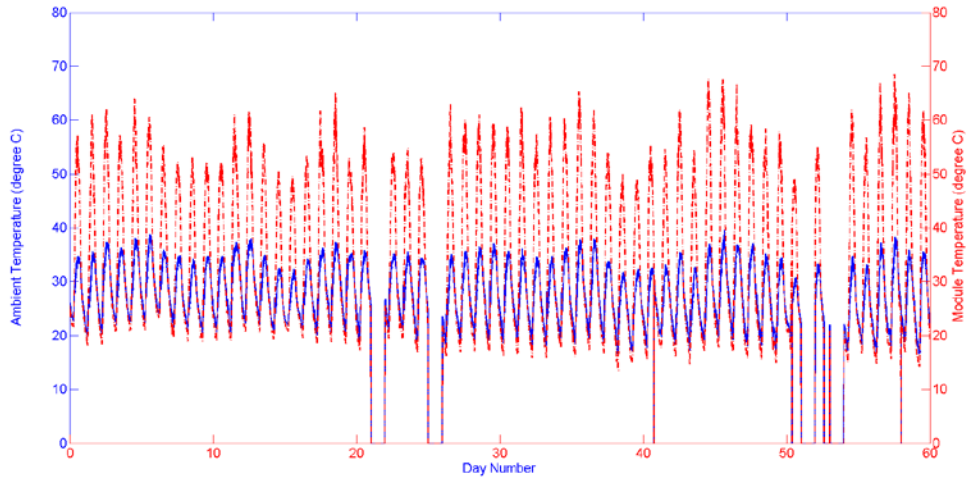


Figure 14. Variation of ambient (blue color) and module (red color) temperatures

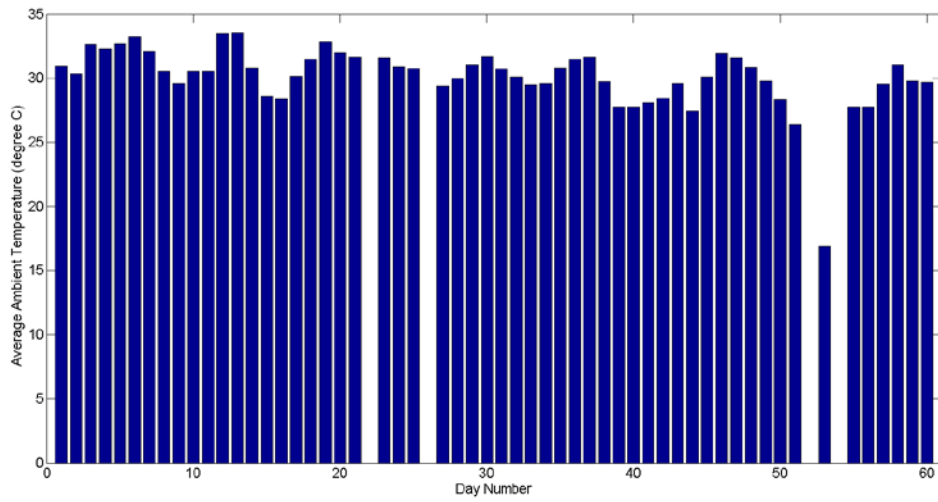


Figure 15. Average ambient temperature

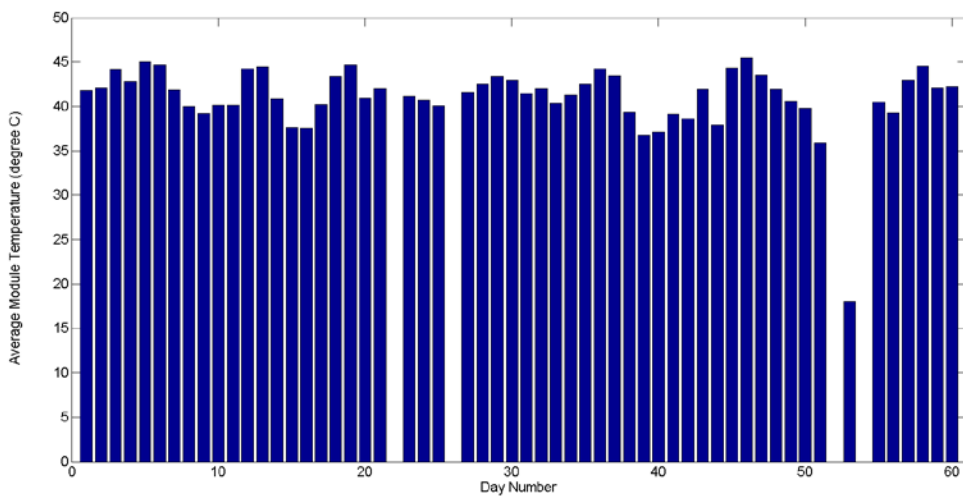


Figure 16. Average module temperature

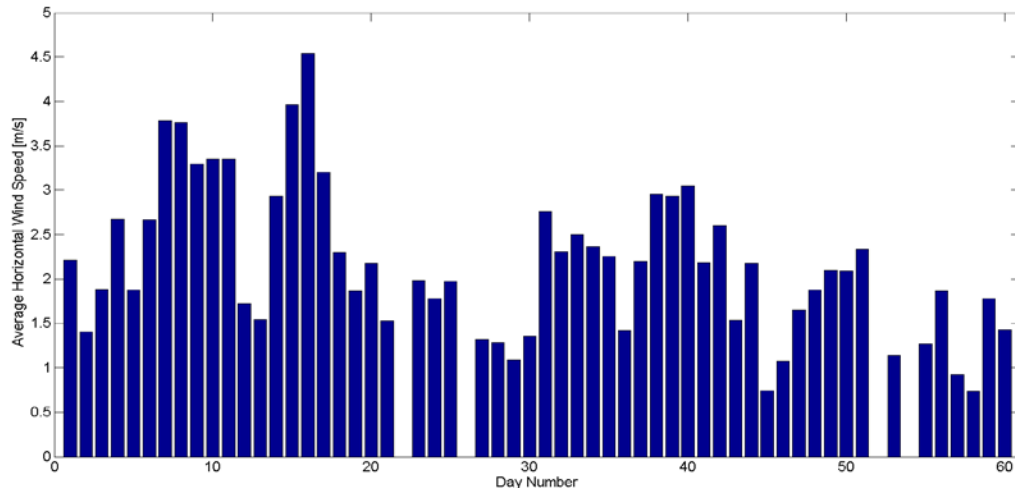


Figure 17. Average horizontal wind

5. Summary, conclusions, and Future Work

A thin-film PV system is installed and tested at the Hashemite University, Jordan. The system is fixed at near optimal orientation for the location selected and is connected to the local grid. The system constructed to function in part as a car parking that is utilized to increase thermal comfort in the harsh environment at the Hashemite University. We found that the instantaneous and average efficiencies are within the reported values from the manufacturer and other studies in different parts of the world. We plan in the near future to extend testing time to study the behavior of thin-film PV system over all seasons of the year. In doing so, we plan to carry out a feasibility study on the use of thin-film PV in Jordan.

The future installation and operation of PV plants as a step toward urban technology concept should be promoted in the Hashemite University by considering new criteria for the landscape integration of PV plants. The viewpoints from which the visual simulation of the PV plant should be taken are very important parameter. Other relevant parameters such as materials and color, land use, visual impact on the landscape, and glare should be considered to solve any future concerns of the users about the environmental, and landscape impacts of PV plants technology. At the university level, the future guidelines for the authorization of renewable energy plants should contain some new criteria for the landscape integration of PV plants and the visual simulations techniques.

Acknowledgments

The authors thank BTS s.r.o., Czech Republic, for supplying and installing the thin-film PV system at the Hashemite University.

References

- [1] Jordan Annual Climate Bulletin, JMD. Amman: Jordan Metrological Department, 2000.

- [2] T.M. Razykov, C.S. Ferekides, D. Morel, E. Stefanakos, H.S. Ullal, H.M. Upadhyaya, "Solar photovoltaic electricity: Current status and future prospects," *Solar Energy*, Vol. 85, pp. 1580–1608, 2011.
- [3] W. Hoffmann, T. Pellkofer, "Thin films in photovoltaic: Technology and perspectives," *Thin Solid Films*, Vol. 520, pp. 4094–4100, 2012.
- [4] M.A. Muñoz-García, O. Marin, M.C. Alonso-García, F. Chenlo, "Characterization of thin film PV modules under standard test conditions: Results of indoor and outdoor measurements and the effects of sunlight exposure," *Solar Energy*, Vol. 86, pp. 3049–3056, 2012.
- [5] J.-H. Yoon, J. Song, S.-J. Lee, "Practical application of building integrated photovoltaic (BIPV) system using transparent amorphous silicon thin-film PV module," *Solar Energy*, Vol. 85, pp. 723–733, 2011.
- [6] S. Mekhilef, R. Saidur, M. Kamalisarvestani, "Effect of dust, humidity and air velocity on efficiency of photovoltaic cells," *Renewable and Sustainable Energy Reviews*, Vol. 16, pp. 2920–2925, 2012.
- [7] J. Good, "The Aesthetics of Wind Energy," *Human Ecology Review*, Vol. 13, No. 1: 76-89, 2006.
- [8] A. Torres Sibille, V. Cloquell-Ballester, V. Cloquell-Ballester, M. Ramirez, "Aesthetic impact assessment of solar power plants: an objective and subjective approach," *Renewable and Sustainable Energy Reviews*, Vol. 13 (5), pp. 986–999, 2009.
- [9] R. Chiabrando, E. Fabrizio, G. Garnero, "The territorial and landscape impacts of photovoltaic systems: definition of impacts and assessment of the glare risk," *Renewable and Sustainable Energy Reviews*, Vol. 13 (8), pp. 2441–2451, 2009.
- [10] Lynn, Pual A. *Electricity from Sunlight: An Introduction to Photovoltaics*. 1st Ed, Wiley, 2010.
- [11] Nelson, Vaughn. *Introduction to Renewable Energy*. 1st Ed, CRC Press, 2011.

Hourly Solar Radiation Prediction Based on Nonlinear Autoregressive Exogenous (Narx) Neural Network

Lubna. B. Mohammed^{*,a}, Mohammad. A. Hamdan^a, Eman A. Abdelhafez^a

And Walid Shaheen^b

^a Al Zaytoonah University of Jordan, Jordan

^b National Center for Research & Development, Jordan

Abstract:

In this study, Nonlinear Autoregressive Exogenous (NARX) model was used to predict hourly solar radiation in Amman, Jordan. This model was constructed and tested using MATLAB software. The performance of NARX model was examined and compared with different training algorithms. Meteorological data for the years from 2004 to 2007 were used to train the Artificial Neural Network (ANN) while the data of the year 2008 were used to test it. The Marquardt–Levenberg learning algorithm with a minimum root mean squared error (RMSE) and maximum coefficient of determination (R) was found as the best in both training and validation period when applied in NARX model.

© 2013 Jordan Journal of Mechanical and Industrial Engineering. All rights reserved

Keywords: Solar Radiation Prediction; Nonlinear Autoregressive Exogenous; Neural Network.

1. Introduction

Solar radiation data are a fundamental input for solar energy applications. The data should be reliable and readily available for design, optimization and performance evaluation of solar technologies for any particular location. Unfortunately, for many developing countries, solar radiation measurements are not easily available. Therefore, it is necessary to develop methods to estimate the solar radiation on the basis of the more readily available meteorological data.

Many models have been developed to estimate the amount of global solar radiation on horizontal surfaces using various climatic parameters, such as sunshine duration, cloud cover, humidity, maximum and minimum ambient temperatures, wind speed, etc. Chakhchoukh [1] and Wu [2] used the metrological data of Nanchang station (China) from 1994 to 2005 to predict the daily global solar radiation from sunshine hours, air temperature, total precipitation and dew point. Z. Sen [3] proposed a nonlinear model for the estimation of global solar radiation from available sunshine duration data. This model is an Angstrom type model with a third parameter which appears as the power of the sunshine duration ratio that gives the nonlinear effects in solar radiation and sunshine duration relationship.

A simple model for estimating the monthly average of the daily global solar radiation data on horizontal surfaces was recently proposed by R. Perdomo, E. Banguero, and

G. Gordillo in [4]. The model is based on a trigonometric function, which has only one independent parameter, namely the day of the year. It was found that the model can be used for estimating monthly average of daily global radiation for 68 provinces of Turkey with a high accuracy. Janjai [5] proposed a model for calculating the monthly average hourly global radiation in the tropics with high aerosol load using satellite data. This model was employed to generate hourly solar radiation maps in Thailand.

In literature, Artificial Neural Networks (ANN) has been widely used as time series predictors. Many techniques have been developed in the general framework of time series prediction. These methods can be classified into two main categories: classical statistical methods, and intelligent based methods. Statistical methods (such as Fractional difference model, Structure model, Bayesian method, Threshold AR model, alterable variance model, Zhang [6] and Ji [7], and the Ratio-of-Medians Estimator (RME) method) are used for the estimation of the autoregressive moving-average (ARMA) parameter model and time series prediction [1] and [8-10]. Most time series prediction methods based on intelligent used Artificial Neural Network (ANN) technique, such as multilayer perceptrons with back propagation, recurrent neural networks, and a radial basis function (RBF) neural network [11-13].

Traditional statistical methods are very easy to understand and implement, but they are not tractable in complex time series with a fast alteration and complicated involvement Zhang [6]. ANNs are good for tasks involving incomplete data sets, fuzzy or incomplete information, and

* Corresponding author. e-mail: lubnabadri@gmail.com.

for highly complex and ill-defined problems. They can learn from examples, and are able to deal with non-linear problems Kalogirou [14].

As indicated above, several conventional models have been presented by researchers to predict global solar radiation (GSR) using different meteorological variables. However, using ANN has proved its efficiency as a prediction tool to predict factors through other input variables which have no specified relationship. Meteorological and climatological variables are most comprehensive and important factors for indicating the amount of solar radiation in a selected reign (Behrang [15], and Hrayshat [16]).

The main objective of this study is to investigate the ability of NARX model to predict the hourly solar radiation data in Amman, Jordan. NARX model, with different training algorithms, is examined and compared using MATLAB software.

2. Artificial Neural Network (ANN)

ANNs, commonly known as biologically inspired, highly sophisticated analytical techniques, are able to model extremely complex non-linear functions Chena [17]. In general, they are composed of three layers, which are an input layer, some hidden layers, and an output layer [18]. The advantages of the ANNs are speed, simplicity and ability to train past data to provide the necessary predictions. ANNs are used to solve complex functions in various applications such as control, data compression, forecasting, optimization, pattern recognition, classification, speech, vision Sözen [19].

To develop an ANN model, three steps must be followed. Firstly, the input is introduced with the desired output to the network together. Secondly, the network is trained to estimate the output in the training step. Finally, the testing step, in this step estimating output data are obtained by using the input data, which are not used in the training step. More details about these steps are found in Caner [18].

In this Study, Nonlinear Autoregressive Exogenous (NARX) neural network, shown in Figure (1), is used to investigate its ability to predict the hourly solar radiation data in Amman, Jordan, using different training algorithms based on the results obtained in Moghaddammia [20]. It was found that NARX model is the best network that can

be used to predict solar radiation. More details about this model is found in Moghaddammia [20]. The recorded hourly solar radiation for four years (from 2004 to 2007) were used as training data, while the data recorded in the year 2008 were used as target data. The input hourly solar data were provided by the National Center for Research and development, Energy Research Program in Amman, Jordan. They were obtained using a metrological station located in Amman. The performance of the model has been carried out using three global statistics: coefficient of determination (R^2), root mean squared error (RMSE) and mean bias error (MBE). More details about these parameters are found in Caner [18]. These three parameters are given by:

$$R^2 = 1 - \frac{\sum_j (t_j - o_j)^2}{\sum_j (o_j)^2} \quad (1)$$

$$RMSE = \sqrt{\frac{\sum_j (t_j - o_j)^2}{p}} \quad (2)$$

$$MBE = \frac{\sum_j (t_j - o_j)}{p} \quad (3)$$

Where:

t_j is the target value,

o_j is the output value and

p is the pattern

ANN network with neuron numbers (4, 20, 1) was constructed and tested by MATLAB software Beale [21]. Previously obtained experimental data of 8670 sample were used as the input of ANN network. Among this data, 40% were used for training, 30% for validation, and 30% for testing. The number of the hidden layer was selected as 20 following trail and error technique. Tangent sigmoid function was applied for the hidden layer, and linear transfer function is used in the output layer. Training parameters used in algorithms are shown in Table (1) with their values. The performance of all models have been carried out using three global statistics: coefficient of determination (R^2), root mean squared error (RMSE) and mean bias error (MBE).

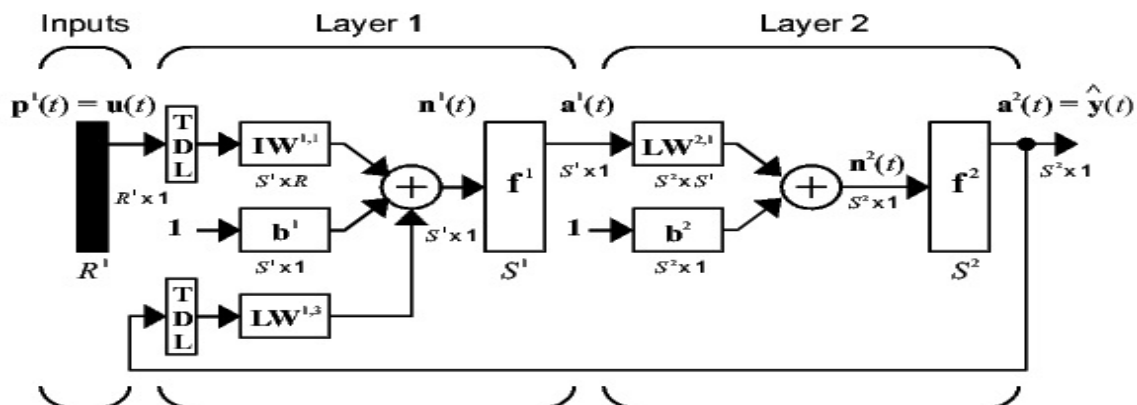


Figure 1. A typical neural network auto-regressive with exogenous inputs (Beale, Hagan, & Demuth, 2007).

Table 1. Training parameters.

Epochs between displays	1
Maximum number of epochs to train	800
Maximum time to train in seconds	inf
Performance goal	0
Maximum validation failures	15
Factor to use for memory/ speed Tradeoff	1
Minimum gradient error	$1*10^{-5}$
Initial μ	$1*10^{-3}$
μ decrease factor	0.1
μ increase factor	10
Maximum μ	$1*10^{10}$

3. Results and Discussion

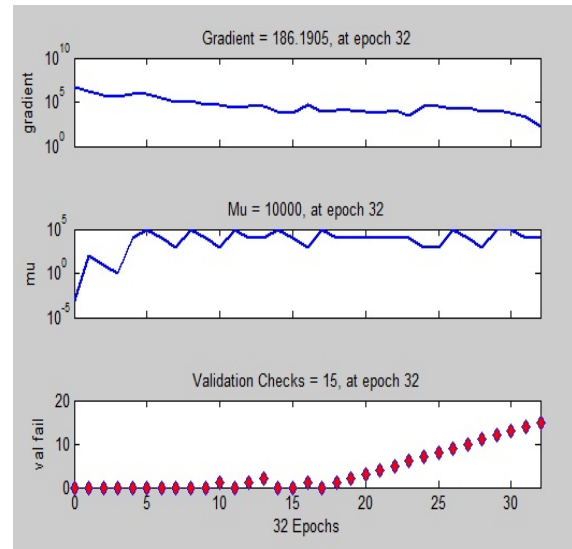
The data measured between January 1st 2004 and December 31st 2007 were used for training, testing, and validation of ANN. Once the ANN is trained, which means that all the weights and bias are set, it can be tested. The proposed network was trained using seven training algorithms: Levenberg-Marquardt (trainlm), Resilient Backpropagation (trainrp), Scaled Conjugate Gradient (trainscg), Conjugate Gradient with Powell/Beale Restarts (traincgb), Fletcher-Powell Conjugate Gradient (traincgf), Polak-Ribière Conjugate Gradient (traincgp), and One Step Secant (trainoss).

Variation of the gradient error, value of μ , and validation checks at each epoch results produced by the seven training algorithms based NARX network are shown in Figure (2). In Figure (3), the scatter plots of training, testing, and validation are shown. The mean square error at each epoch for the training algorithms is shown in Figure (4). As shown in Figures (2) and (4), the NARX network trained with Levenberg-Marquardt algorithm converges faster than other algorithms; where the training stopped after 32 epochs. The mean square error (MSE) of training period was found to be 42.8367 MJ/m²/hour, and RMSE of validation period was found to be 48.3991 MJ/m²/hour. Figure (3) shows quite close results of the scatter plot during training, validation, and testing of the experimental data using different training algorithms. For Levenberg-Marquardt algorithm, it was found that it has the highest values of R in training, validation, and testing are 0.99157, 0.98916 and 0.98935 respectively.

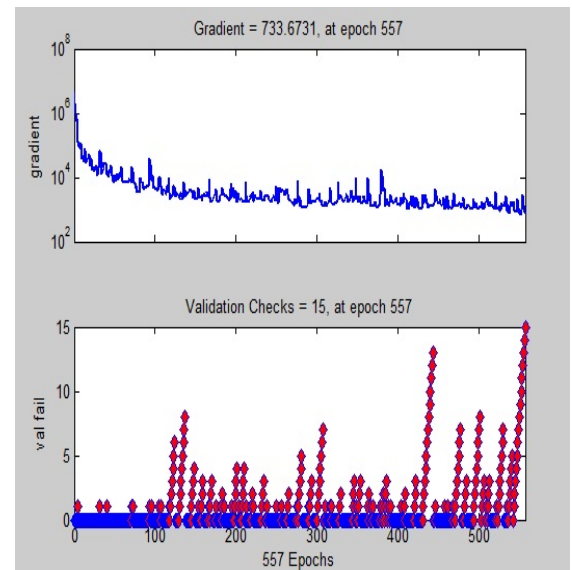
Figures (5) and (6) show a comparison of measured and predicted values using the proposed NARX network. This comparison was based on seven training algorithms taken data on summer day (6th of August 2008) and on winter day (16th of December 2008).

The comparative analysis of different training algorithms using some basic statistics (coefficient of determination (R^2), root mean squared error (RMSE) and mean bias error (MBE)) has been carried out and is shown in Table (2), where trainlm algorithm provided the best performance, i.e., the lowest RMSE and highest R^2 , for the training period and validation period. The results of the research indicate that the predictive capability of Scaled Conjugate Gradient (trainscg) algorithm is poor compared

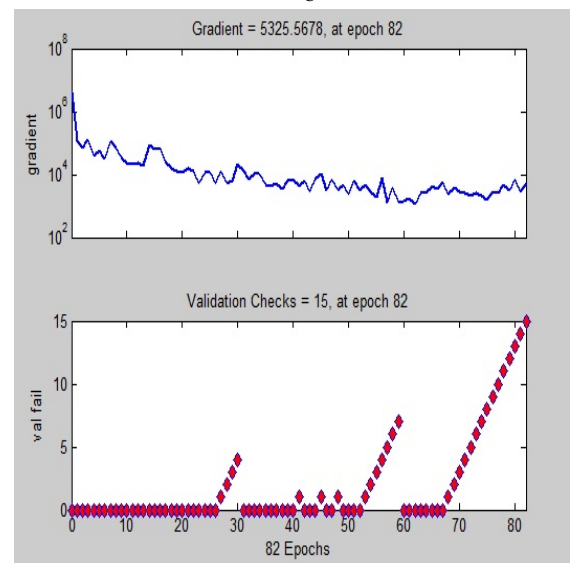
with other training algorithm in hourly solar radiation modelling.



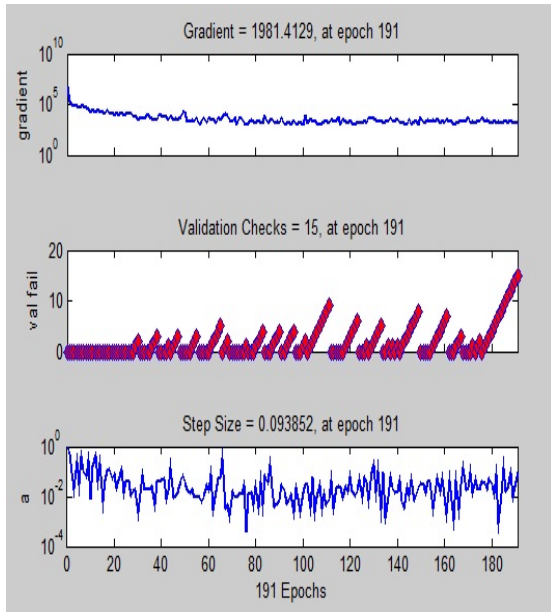
a



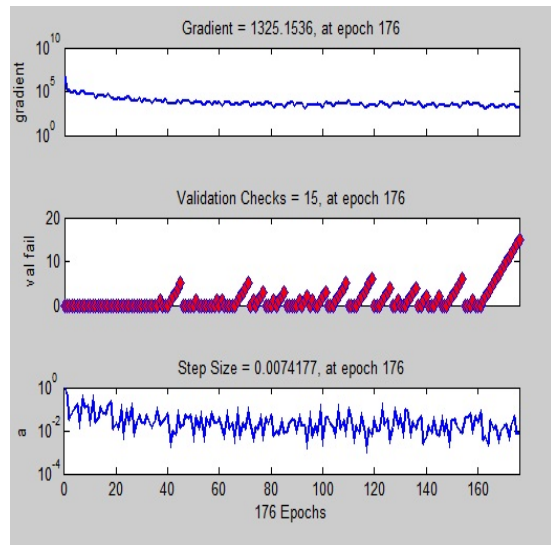
b



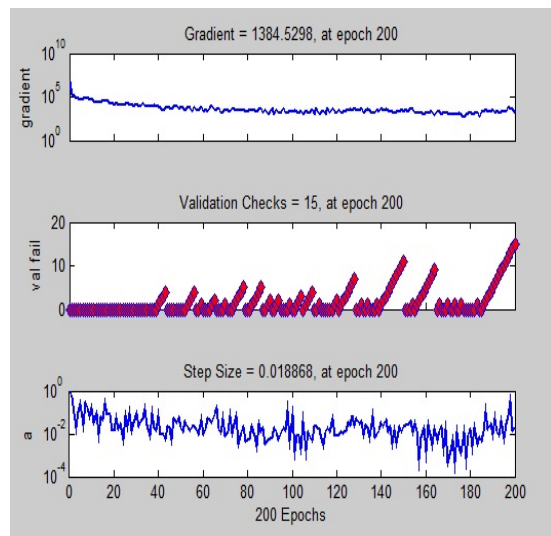
c



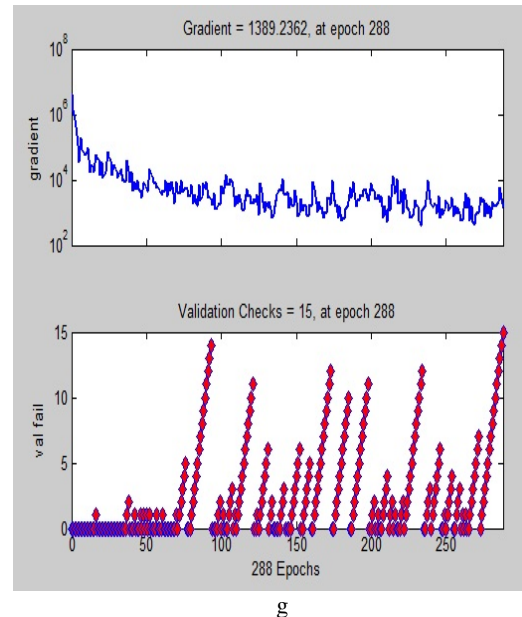
d



e

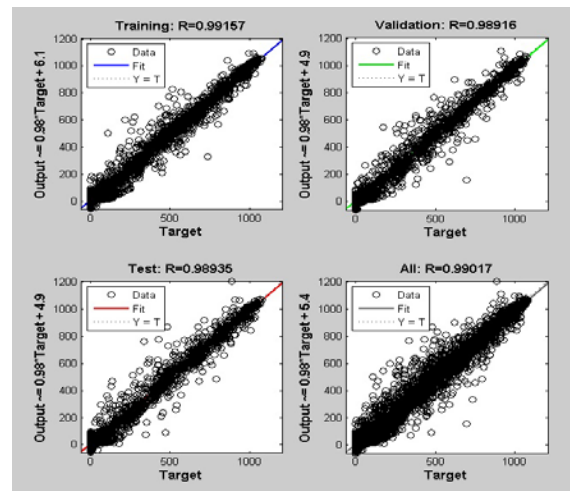


f

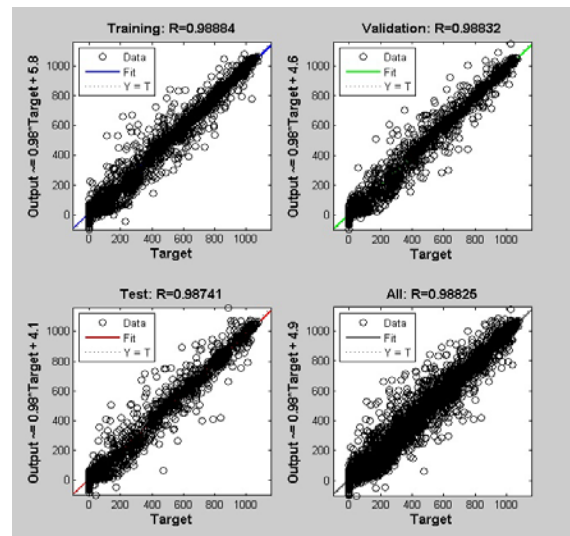


g

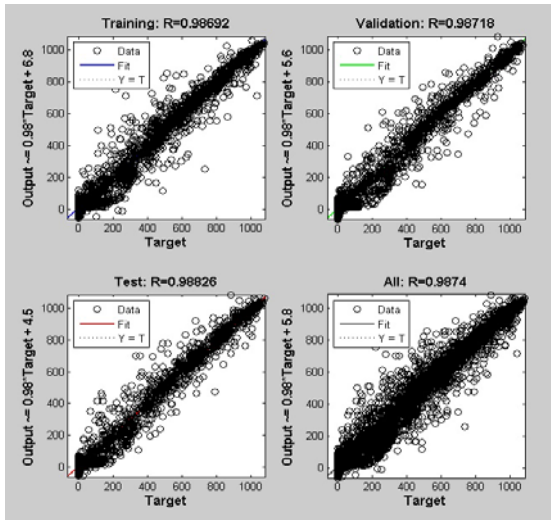
Figure 2. Comparison of variation of gradient error and validation checks using (a) trainlm, (b) trainrp, (c) trainsg, (d) traincgb, (e) traincgf, (f) traincgp, and (g) trainoss.



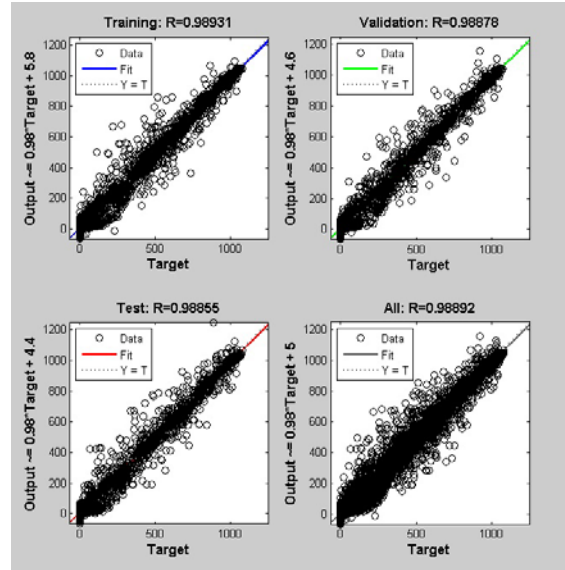
a



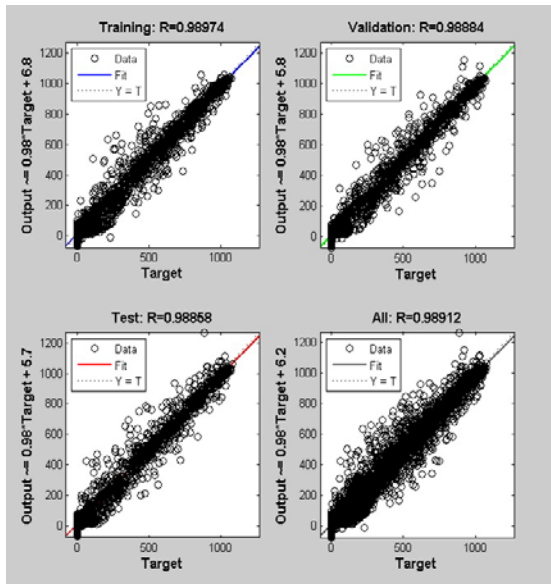
b



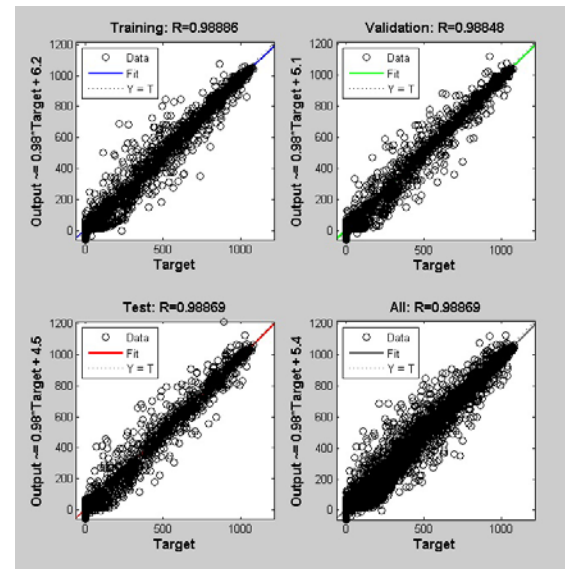
c



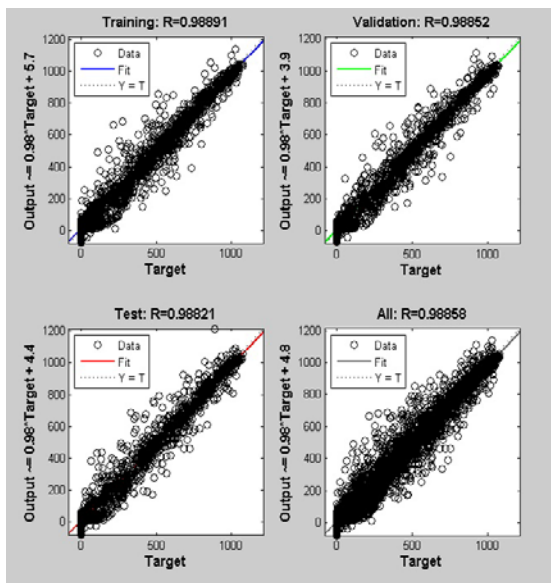
f



d

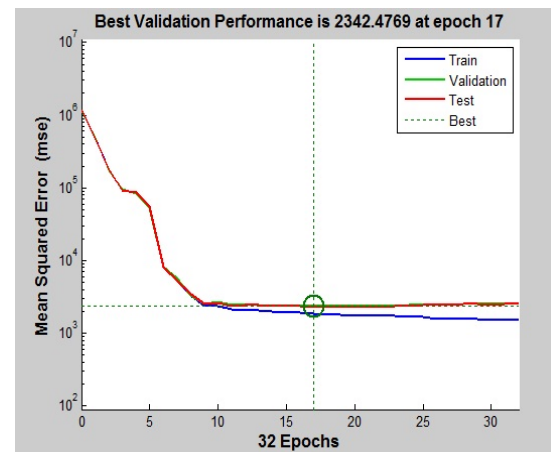


g

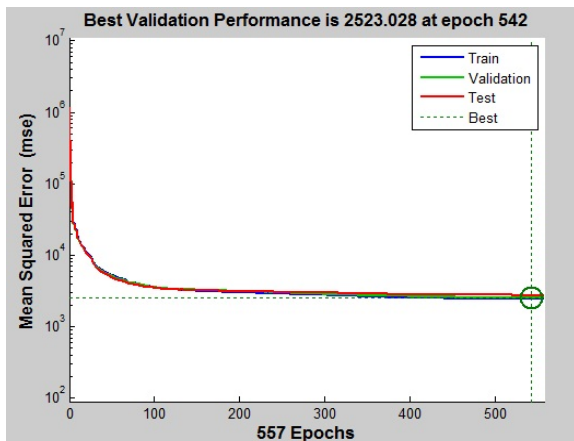


e

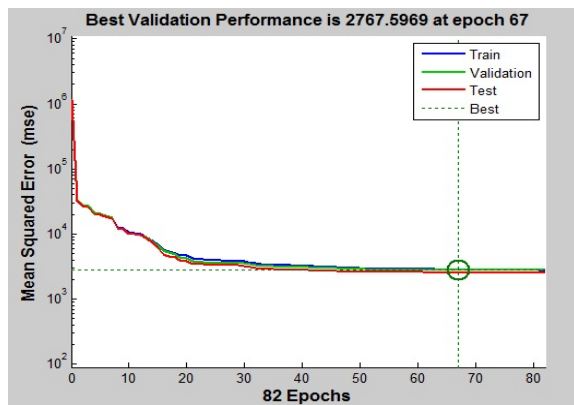
Figure 3. Comparison of scatter plots of the models used for solar radiation. (a) trainlm, (b) trainrp, (c) trainscg, (d) traincgb, (e) traincgf, (f) traincgp, and (g) trainoss.



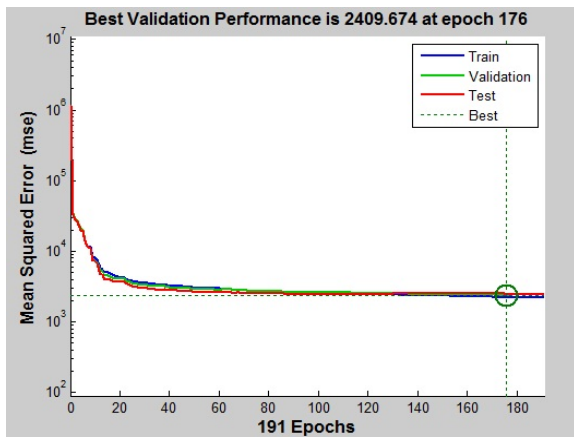
a



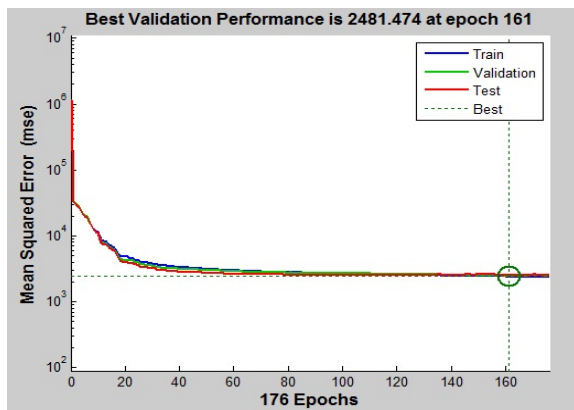
b



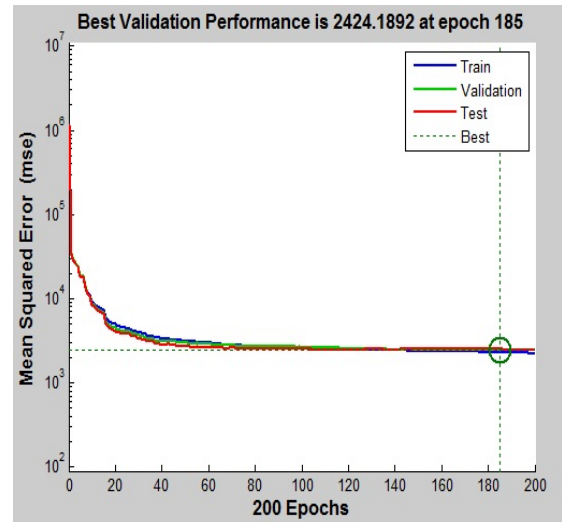
c



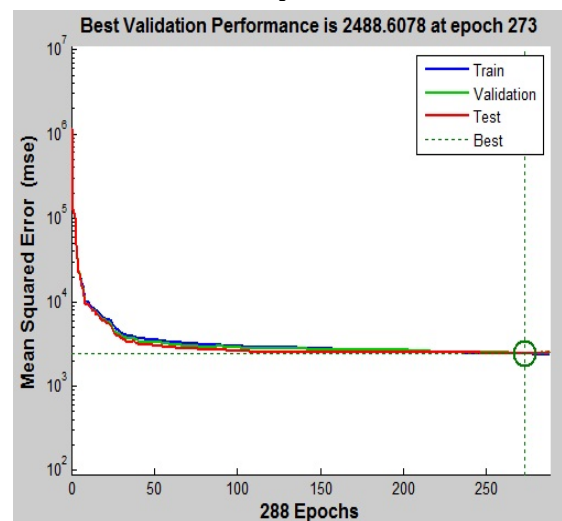
d



e



f



g

Figure 4. Comparison of Mean Square Error (MSE) training performance of the ANN for a given training dataset. (a) trainlm, (b) trainrp, (c) trainscg, (d) traincgb, (e) traincgf, (f) traincgp, and (g) trainoss.

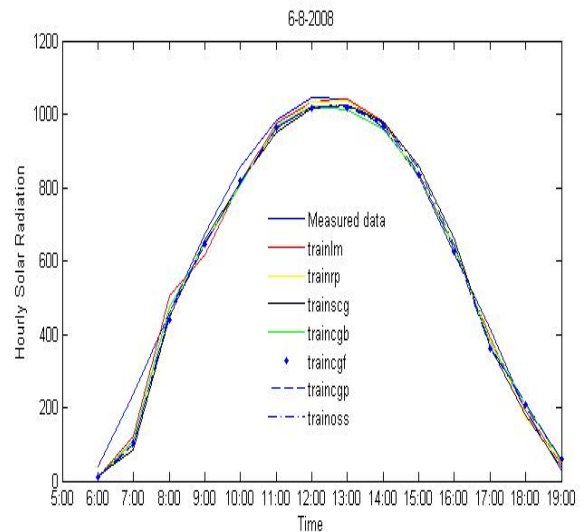


Figure 5. Comparison between measured and estimated hourly solar radiation at 6/8/2008.

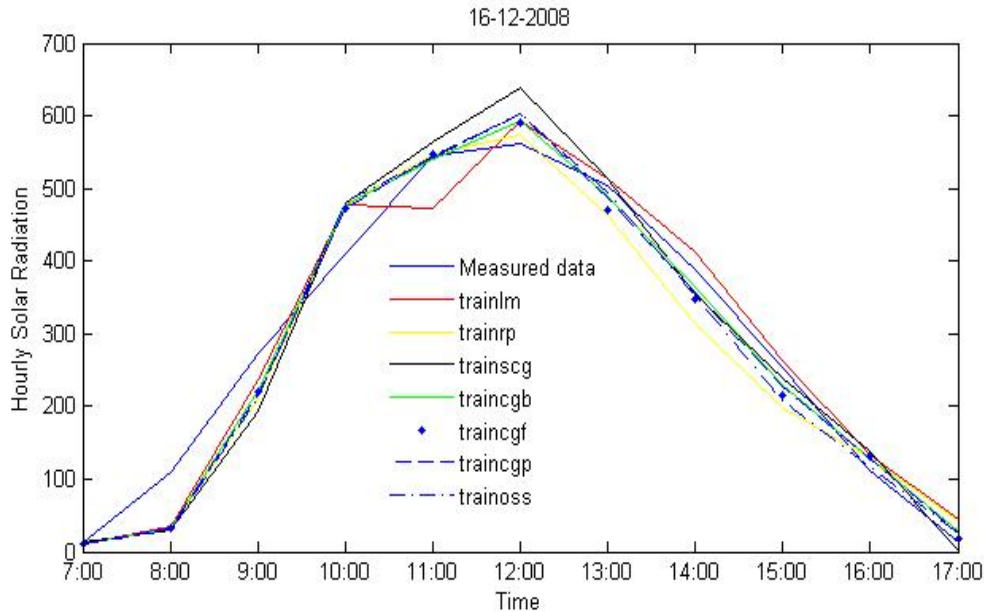


Figure 6. Comparison between measured and estimated hourly solar radiation at 16/12/2008.

Table 2. Comparison of performance of different training algorithms based on statistical criteria.

Algorithm	RMSE		MBE		R	
	Training	Validation	Training	Validation	Training	Validation
trainlm	42.8367	48.3991	25.5612	28.5317	0.99157	0.98916
trainrp	49.2078	50.2298	28.9444	30.6432	0.98884	0.98832
trainscg	53.2732	52.6080	31.3656	32.5375	0.98692	0.98718
traincgb	47.2268	49.0884	28.0998	29.7275	0.98974	0.98884
traincgp	49.0563	49.8144	29.5055	30.9015	0.98891	0.98852
traincgp	48.1758	49.2361	28.3929	29.9944	0.98931	0.98878
trainoss	49.1726	49.8859	28.7343	30.1949	0.98886	0.98848

4. Conclusion

In this study, an approach to estimating hourly solar radiation from meteorological data sets, based on NARX model using different training algorithms, was developed. The comparative analysis between the estimated data and measured data showed that NARX model has the ability to recognize the relationship between the input and output variables and predict hourly solar radiation accurately. The statistical error analysis shows the prediction accuracy based on NARX model.

Different training algorithms were compared to select the best suited algorithm. The Marquardt–Levenberg learning algorithm with a minimum root mean squared error (RMSE) and maximum coefficient of determination (R) was found as the best in both training and validation period when applied in NARX model. Based on our results, NARX network is recommended for hourly solar radiation prediction in Jordan and nearby regions.

References

- [1] Chakhchoukh, Y., Panciatici, P., Mili, L., Electric Load Forecasting Based on Statistical Robust Methods. IEEE Transactions on Power Systems. 26 (2011) 982 - 91.
- [2] Wu, G., Liu, Y., Wang, T. J., Methods and strategy for modeling daily global solar radiation with measured meteorological data : a case study in Nanchang station, China. Energy conversion and management. 48 (2007) 2447-52.
- [3] Sen, Z.. Simple nonlinear solar irradiation estimation model Renewable Energy. 32 (2007) 342–50.
- [4] Buluta, H., Büyükcalab, O., Simple model for the generation of daily global solar-radiation data in Turkey. Applied Energy. 84 (2007) 477-91.
- [5] Janjai, S., Pankaew, P., Laksanaboonsong, J., A model for calculating hourly global solar radiation from satellite data in the tropics. Applied Energy. 86 (2009) 1450-7.
- [6] Zhang, X.-Z., Xing, L.-N., The Multi-Rule & Real-Time Training Neural Network Model for Time Series Forecasting Problem. International Conference on Machine Learning and Cybernetics2006. pp. 3115- 8.
- [7] [Ji, W., Chan, C., Loh, J., Choo, F., Chen, L.H., Solar radiation prediction using statistical approaches. 7th International Conference on Information, Communications and Signal Processing, ICICS 20092009. pp. 1-5.
- [8] Chakhchoukh, Y., A New Robust Estimation Method for ARMA Models. IEEE Transactions on Signal Processing. 58 (2010) 3512- 22

- [9] Perdomo, R., Banguero, E., Gordillo, G., Statistical modeling for global solar radiation forecasting in Bogotá. 35th IEEE Photovoltaic Specialists Conference (PVSC)2010. pp. 002374 - 9
- [10] Shahidi, N., Rahnamaei, M., Sharifan, R. A., Nematollahi, A. R., Modeling and forecasting groundwater level fluctuations of Shiraz plain using advanced statistical models. International Conference on Environmental Engineering and Applications (ICEEA)2010. pp. 137- 41
- [11] Parras-Gutierrez, E., Rivas, V. M., Time series forecasting: Automatic determination of lags and radial basis neural networks for a changing horizon environment. The 2010 International Joint Conference on Neural Networks (IJCNN)2010. pp. 1-7.
- [12] Wang, D., Li, Y., A novel nonlinear RBF neural network ensemble model for financial time series forecasting. Third International Workshop on Advanced Computational Intelligence (IWACI)2010. pp. 86 - 90
- [13] Xinxia, L., Anbing, Z., Cuimei, S., Haifeng, W., Filtering and Multi-Scale RBF Prediction Model of Rainfall Based on EMD Method. 1st International Conference on Information Science and Engineering (ICISE)2009. pp. 3785 - 8.
- [14] Kalogirou, S. A.. Artificial Intelligence in Renewable Energy Applications in Buildings. Proceedings of the International Conference on the Integration of the Renewable Energy Systems (RES) into the Building Structures, Patra, Greece, 2005. pp. 112-26.
- [15] Behrang, M. A., Assareh, E., Ghanbarzadeh, A., Noghrehabadi, A. R., The potential of different artificial neural network (ANN) techniques in daily global solar radiation modeling based on meteorological data. Solar Energy. 84 (2010) 1468-80.
- [16] Hrayshat, E. S., Al-Soud, M. S.. Solar energy in Jordan: current state and prospects. Renewable and Sustainable Energy Reviews. 8 (2004) 193–200.
- [17] Chena, H., Zhanga, J., Xub, Y., Chenb, B., Zhanga, K.. Performance comparison of artificial neural network and logistic regression model for differentiating lung nodules on CT scans. Expert Systems with Applications. 39 (2012) 11503–9.
- [18] Caner, M., Gedik, E., Keçebas, A.. Investigation on thermal performance calculation of two type solar air collectors using artificial neural network. Expert Systems with Applications 38 (2011) 1668–74.
- [19] Sözen, A., Menlik, T., Ünvar, S., Determination of efficiency of flat-plate solar collectors using neural network approach. Expert Systems with Applications. 35 (2008) 1533-9.
- [20] Moghaddamnia, A., Remesan, R., Kashani, M. H., Mohammadi, M., Han, J. P. D., Comparison of LLR, MLP, Elman, NNARX and ANFIS Models—with a case study in solar radiation estimation Journal of Atmospheric and Solar-terrestrial Physics. 71 (2009) 975-82.
- [21] Beale, M. H., Hagan, M. T., Demuth, H. B., Neural Network Toolbox User's Guide. The MathWorks Inc. p. 420, 2007.

Development of A Bond Graph Control Maximum Power Point Tracker For Photovoltaic: Theoretical And Experimental

BADOUD Abd Essalam* and KHEMLICHE Mabrouk

Automatic laboratory of Setif, electrical engineering department, University of Ferhat Abbas Setif 1, Maabouda city, Algeria

Abstract:

Maximum power point tracking is important in solar power systems because it reduces the solar array cost by decreasing the number of solar panels needed to obtain the desired output power. Several different Maximum power point tracking (MPPT) methods have been proposed, but there has been no comprehensive experimental comparison between all the different algorithms and their overall maximum power point (MPP) tracking efficiencies under varying conditions (i.e., illumination, temperature, and load). In this paper, a new maximum power point tracking controller using bond graph approach (BG-MPPT) for a photovoltaic energy conversion system has been developed, consisting of a boost buck DC/DC converter, which is controlled by a bond graph algorithm. The main difference between the method used in the proposed MPPT system and the techniques used in the past is that the PV array output power is used to directly control the DC/DC converter, thus reducing the complexity of the system. The resulting system has high-efficiency, lower-cost, and can be easily modified to handle more energy sources. The experimental results show that the use of the proposed MPPT control increases the PV output power by as much as 15% compared to the case where the DC/DC converter duty cycle is set such that the PV array produces the maximum power at 1 kW/m² and 25°C.

© 2013 Jordan Journal of Mechanical and Industrial Engineering. All rights reserved

Keywords: Maximum Power Point Tracking; Buck-Boost Converter; Photovoltaic; Bond Graph.

1. Introduction

The use of renewable energy systems as an alternative way to produce electricity has been increasing over the past few years [1]. The need of a cleaner, more efficient, and cheaper method for generating electric power is helping this growth.

Among all the renewable energy systems, the photovoltaic (PV) energy is a solution among the promising energy options with advantages such as abundance, the absence of any pollution and the availability in large quantities in anywhere of the globe worldly [2].

Photovoltaic sources are used today in many applications such as battery charging, water pumping, home power supply, swimming-pool heating systems, satellite power systems, electric vehicles, hybrid systems military and space applications, refrigeration and vaccine storage, power plants and some applications where nonlinear power source is needed. They have the advantage of being maintenance and pollution-free but their installation cost is high and they require a dc/dc or dc/ac converter for load interface.

There are three major approaches for maximizing power extraction in solar systems. They are sun tracking, maximum power point tracking or both [3]. These methods need intelligent controllers (such as fuzzy logic controller

or conventional controller (such as PID controller). In the literature, many maximum power point tracking systems have been proposed and implemented ([4]; [5]). The fuzzy theory, based on fuzzy sets and fuzzy algorithms, provides a general method of expressing linguistic rules so that they may be processed quickly. The advantage of the fuzzy logic control is that it does not strictly need any mathematical model of the plant. It is based on plant operator experience, and it is very easy to apply. Hence, many complex systems can be controlled without knowing the exact mathematical model of the plant [6]. In addition, fuzzy logic simplifies dealing with nonlinearities in systems [7]. The advantage of using fuzzy logic control is that the linguistic system definition becomes the control algorithm.

Many tracking techniques and algorithms have been developed. The Perturbation and Observation method (P&O) ([8]; [9]; [10]), the Incremental Conductance method ([11]; [12]) as well as Fractional Open Circuit Voltage method ([13]) and Fractional Short Circuit Current method ([14]) are the most widely used. The P&O Method has been widely used because of its simple feedback structure and fewer measured parameters and easy to implement. The peak power tracker operates by periodically incrementing or decrementing the solar array voltage. If a given perturbation leads to an increase (or decrease) in array power, the subsequent perturbation is made in the same (or opposite) direction. In this manner,

* Corresponding author.e-mail: badoudabde@yahoo.fr.

the peak power tracker, continuously hunts or seek the peak power conditions. Most maximum power trackers are based on the perturb and observe approach, implemented by a hill-climbing [15] algorithm often on a microcontroller. However, this approach is quite complex, can be slow and thus can become ‘confused’ if the MPP moves abruptly.

In this work, the aim is to control the voltage of the solar panel in order to obtain the maximum power possible from a PV generator, whatever the solar insolation conditions. Since quite a few control schemes had already been used and had shown some defects, it was necessary to find and try some other methods to optimize the output, bond graph controller seemed to be a good idea. The controllers by bond graph can provide an order more effective than the traditional controllers for the nonlinear systems, because there is more flexibility.

This work is motivated by the need to optimize solar array performance in Setif’s climate, which is characterized by rapidly varying environmental conditions. The main objective of this paper is to present an improved BG-MPPT in order to increase the tracking response and consequently increase the tracking efficiency.

2. Proposed Method

Figure 1 shows the proposed scheme for the MPPT. This system use a PV array (s x p) composed of sin series cells and p in parallel cells. It is then connected to a DC-DC converter in order to increase or decrease the desired voltage. It is then connected directly to the load. The duty cycle of the converter is controlled by a bond graph controller. Measurement of the PV array voltage, Irradiance and Temperature on the PV array surface are taken in order to estimate the optimal voltage for the maximum power, and then a nonlinear MPPT algorithm takes this value to produce the signal for driving the switching element of the DC/DC converter.

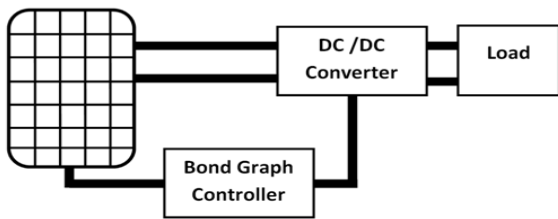


Figure 1. General scheme for the proposed method

3. Bond Graph Approach

Bond graph is an explicit graphical tool for capturing the structures among the physical systems and representing

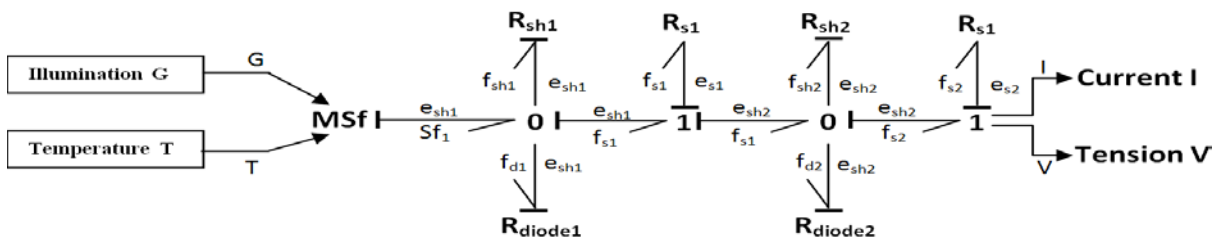


Figure 3. PV bond graph model with tow diodes

them as an energy network based on the exchange of power ([16-19]). Others ([20-22]) have extended the bond graph concept to represent Phenomena such as chemical kinetics and to extract causal models and control structures from the bond graph networks. Bond graph, a graphical modeling language, provides a model formalism that decomposes the system into subsystems that map to the physical connections [23]. The resulting subsystems are essentially physical fields including mechanics, electronics, hydraulics, and chemistry. The time granularity for these domains is usually distinct.

A bond graph consists of subsystems linked together by lines representing power bonds. Each process is described by a pair of variables, effort e and flow f. Besides the effort and flow variables, two other types of variables are very important in describing dynamic systems; these variables, sometimes called energy variables, are the generalized momentum p as time integral of effort and the generalized displacement q as time integral of flow ([24, 25]).

4. PV Module Modelling

The use of equivalent electric circuits makes it possible to model characteristics of a PV cell. The typical model of a solar cell is shown in figure 2.

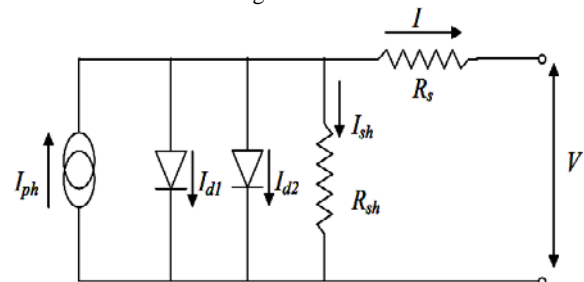


Figure 2. Equivalent circuit model of PV cell

A PV system directly converts sunlight into electricity. The basic device of a PV system is the photovoltaic cell; they may be grouped to form panels or arrays ([26]; [27]). This is the most classical model to be found in the literature [28], and it involves a current generator for modeling the incident luminous flux, two diodes for the cell polarization phenomena, and two resistors (Rs and Rsh) for the losses (figure 3).

The current provided by the cell is given by the relation (1)

$$I = I_{s1} \left[\exp \left\{ \frac{q(V - R_s I)}{AKT} \right\} - 1 \right] + I_{s2} \left[\exp \left\{ \frac{q(V - R_s I)}{AKT} \right\} - 1 \right] - I_{ph} + \frac{V - R_s I}{R_{sh}} \quad (1)$$

For the bond graph representation, the PV generator is then modeled by a flow source $S_f = I_{ph}$ in parallel with two resistors R_{sh1} and R_{sh2} , the whole followed by a serial resistance R_s ([29]; [30]). The PV diode bond graph representation is a non-linear resistor R_{diode} .

BP Solar BP SX 150S PV module is chosen for a Symbols simulation model. The module is made of 72 multi-crystalline silicon solar cells in series and provides 150W of nominal maximum power. Table 1 shows its electrical specification.

Table 1. Electrical Specification

Electrical Characteristics	Value
Maximum Power (P_{max})	150W
Voltage at P_{max} (V_{mp})	34.5V
Current at P_{max} (I_{mp})	4.35A
Open-circuit voltage (V_{oc})	43.5V
Short-circuit current (I_{sc})	4.75A
Temperature coefficient of I_{sc}	$0.065 \pm 0.015\% / ^\circ C$
Temperature coefficient of V_{oc}	$-160 \pm 20 \text{ mV} / ^\circ C$
Power temperature coefficient	$-0.5 \pm 0.05\% / ^\circ C$
NOCT	$47 \pm 2^\circ C$

In order to characterize the solar cell, we used the model presented to provide the values of the tension V , of the current I and of the generated power produces P .

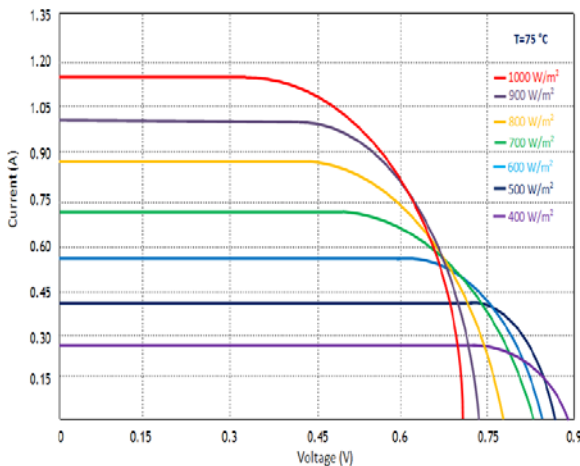


Figure 4. (I-V) characteristic for various illuminations.

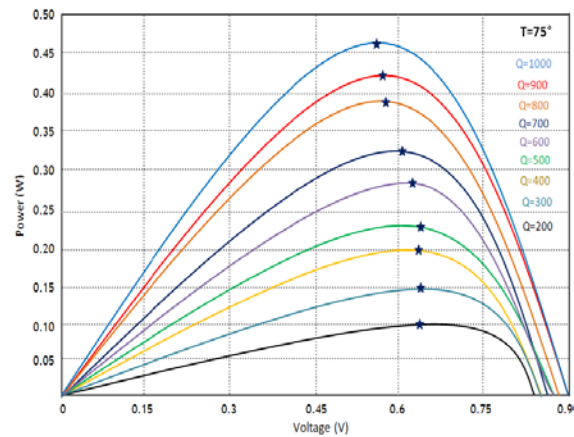


Figure 5. (P-V) characteristic for various illuminations

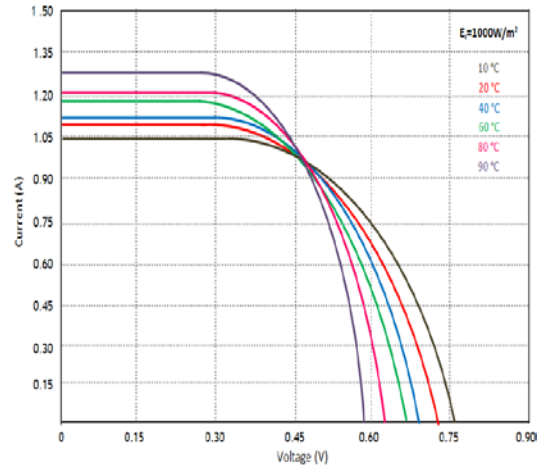


Figure 6. (I-V) characteristic for the various temperatures

If the temperature of the cell increases, the photo current I_{ph} also increases; this is mainly due to the reduction in the forbidden band dispatcher of material. This increase is about 0.1% by $^\circ C$ the forward current of the junction increases also, but much more quickly and involving a reduction in the open circuit tension of about 2mV by cell. The reduction in the provided power is estimated at approximately 0.5% by $^\circ C$ for a module.

5. Modeling of Dc-Dc Buck-Boost Converter

A buck-boost converter provides an output voltage that can be controlled above and below the input voltage level. The output voltage polarity is opposite to that of the input voltage.

Figure 7 shows the circuit diagram of a buck-boost converter. This converter either steps up or steps down the input DC voltage fed from the diode rectifier. The converter consists of a DC input voltage source V_s , inductor L , controlled switch S , filter capacitor C , diode D , and load resistance R .

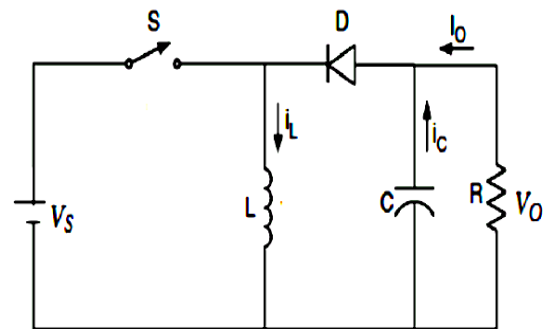


Figure 7. Circuit of Buck Boost Converter

There are two modes of operation of the converter. In Mode I, the switch is turned ON, the inductor current increases and the diode is in the OFF condition. In Mode II, the switch is turned OFF, the diode is turned ON and provides a path for the inductor current. The inductor current now decreases ([31,32]). In both the modes, the load current is assumed constant $i_o = I_o$.

The bond graph model of the buck-boost is thus given by the figure (8).

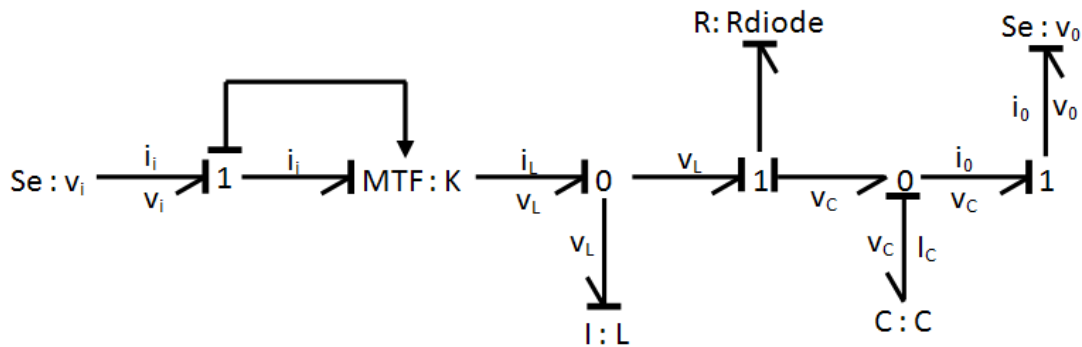


Figure 8. Bond graph model buck-boost converter

6. Perturbation And Observation (P&O)

The P&O algorithm is probably the most frequently used in practice, mainly due to its easy implementation [33]. Its operation is briefly explained as follows: assume that the PV array opera test a given point, which is outside the MPP. The PV array operational voltage is perturbed by a small DV, and then the change in the power (DP) is measured. If $DP > 0$, the operation point has approached the MPP, and therefore, the next perturbation must take place in the same direction as the previous one (same algebraic sign). If, on the contrary, $DP < 0$, the system has moved away from the MPP and, consequently, the next perturbation must be performed in the opposite direction. As stated before, the advantages of this algorithm are its

simplicity and easy implementation. However, it has limitations that reduce its tracking efficiency. When the light intensity decreases considerably, the P-V curve becomes very flat. This makes it difficult for the MPPT to locate the MPP, since the changes that take place in the power are small as regards perturbations occurred in the voltage.

Another disadvantage of the “P&O” algorithm is that it cannot determine when it has exactly reached the MPP. Thus, it remains oscillating around it, changing the sign of the perturbation for each DP measured. It has also been observed that this algorithm can show misbehaviour under fast changes in the radiation levels [34]. The flowchart of the P&O method is shown in figure (9).

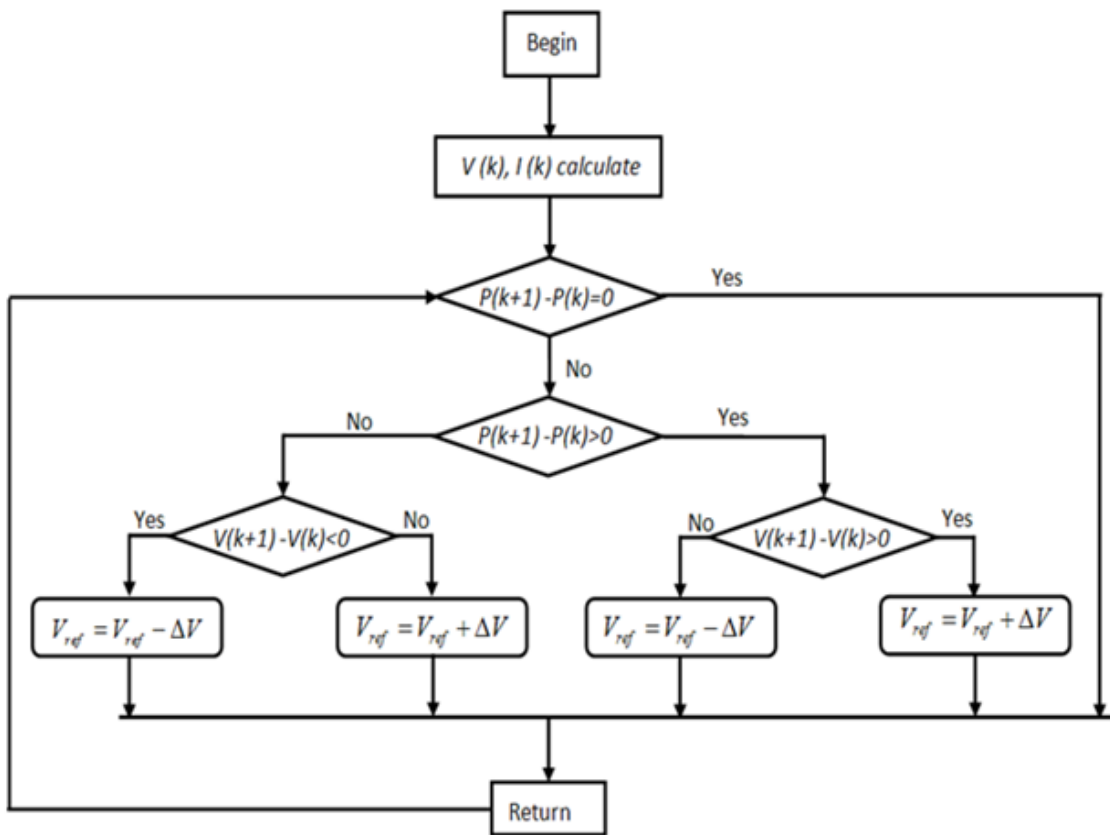


Figure 9. Flowchart of perturb and observe method

The P&O MPPT method can be implemented using a minimal amount of components; however, its speed is limited by the size and the period of the perturbation. The P&O method also has the problems of erroneous responses to quick changing conditions, and in steady state conditions will oscillate around the MPP causing losses. A more advanced technique for choosing direction can be employed by comparing the current power to the two previous power points which helps reduce errors.

7. Bond Graph Controller

The block diagram of the bond graph MPPT control is shown in figure (10). The proposed control consists of two loops, the maximum power point tracking loop is used to set a corresponding SE1 to the charger input, the regulating voltage loop is used to regulate the solar array output voltage according to SE1 which is set in the MPPT loop.

The controller senses the solar array current and voltage to calculate the solar array output power, power slope and SE1 (figure 10) for maximum power control.

The bond graph control requires that variable used in describing the control rules has to be expressed in elements of bond graph (elements R, I and C) with bond graph junction (0, 1 and TF). In this paper, the bond graph control MPPT method has two input variables, namely $\Delta P(k)$ and $\Delta U(k)$, at a sampling instant k.

The output variable is $\Delta U(k+1)$, which is voltage's increase of PV array at next sampling instant k+1. The variable $\Delta P(k)$ and $\Delta U(k)$ are expressed as follows:

$$\Delta P(k) = P(k) - P(k-1) \tag{1}$$

$$\Delta U(k) = U(k) - U(k-1) \tag{2}$$

Where $P(k)$ and $U(k)$ are the power and voltage of PV array, respectively. So, $\Delta P(k)$ and $\Delta U(k)$ are zero at the maximum power point of a PV array.

In figure (10), e25, SE1 and e6 are respectively the converter switching duty ratio, the demanded cell voltage and the actual cell voltage in the jth MPPT controller cycle, where $j = k, k+1$.

The MPPT controller calculates the new cell voltage set point based on the converter switching duty ratios and the measured cell voltages in the past and at present. The lead compensator (e27) forces the cell voltage to follow the demanded cell voltage signal. In the practical design of the control software, the threshold ϵ , which is a small positive number close to zero, is used to determine whether the MPP has been reached and e26 is used as a positive increment in the demanded cell voltage.

The variable δ_j can be defined as:

$$\delta 1 = e_2 + e_4 + e_5 - e_3 \tag{3}$$

$$\delta 2 = e_{31} - e_{28} \tag{4}$$

$$\delta 3 = e_{31} + (e_2 + e_4 + e_5 - e_3) \frac{\delta 2}{\delta 1} \tag{5}$$

When $|\delta 1| > \epsilon$, the MPPT controller can be simplified as:

$$SE_1(k+1) = SE_1(k) + e_{20}, \delta 3 > \epsilon 3 \tag{6}$$

$$SE_1(k+1) = SE_1(k), |\delta 3| > \epsilon 3 \tag{7}$$

$$SE_1(k+1) = SE_1(k) - e_{20}, \delta 3 < -\epsilon 3 \tag{8}$$

When $|\delta 1| < \epsilon 1$, the MPPT controller can be simplified as:

$$SE_1(k+1) = SE_1(k) + e_{20}, \delta 2 > \epsilon 2 \tag{9}$$

$$SE_1(k+1) = SE_1(k), |\delta 2| < \epsilon 2 \tag{10}$$

$$SE_1(k+1) = SE_1(k) - e_{20}, \delta 2 < -\epsilon 2 \tag{11}$$

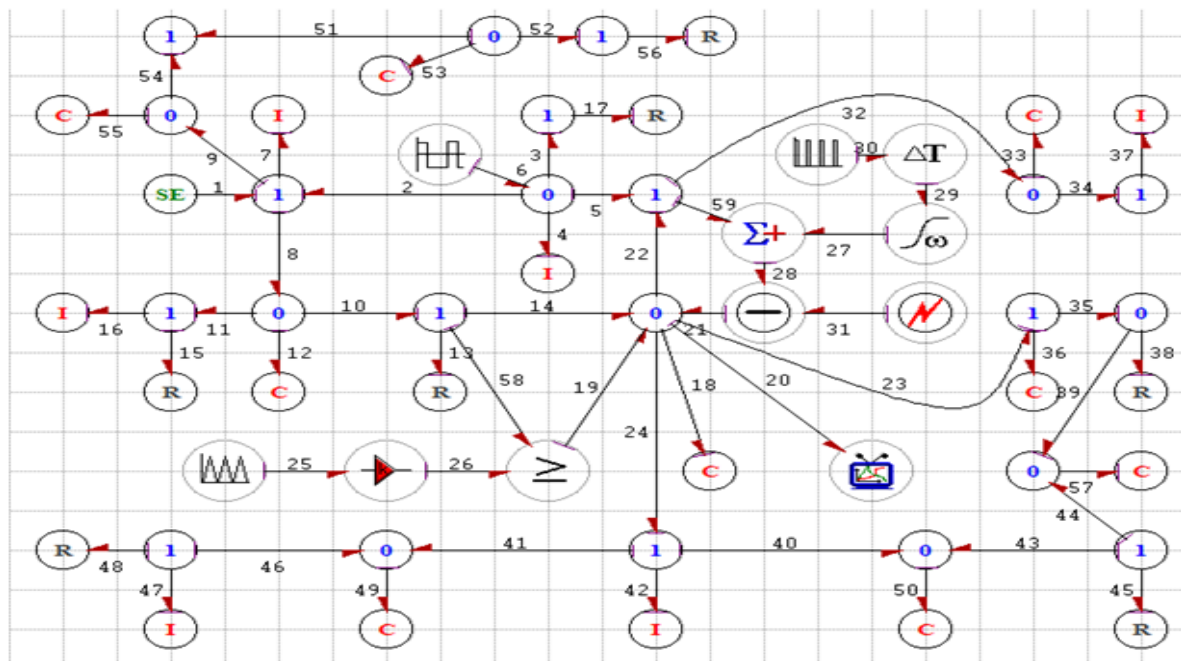


Figure 10. Bond graph MPPT control.

8. Experimental Results

A prototype MPPT system (figure 11) has been developed using the described method and tested in the laboratory

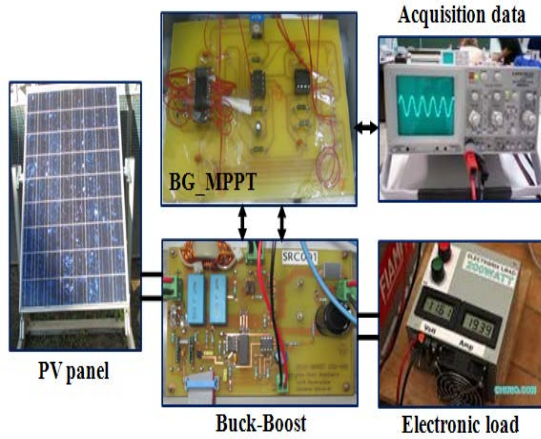


Figure 11. PV Global view of the prototype.

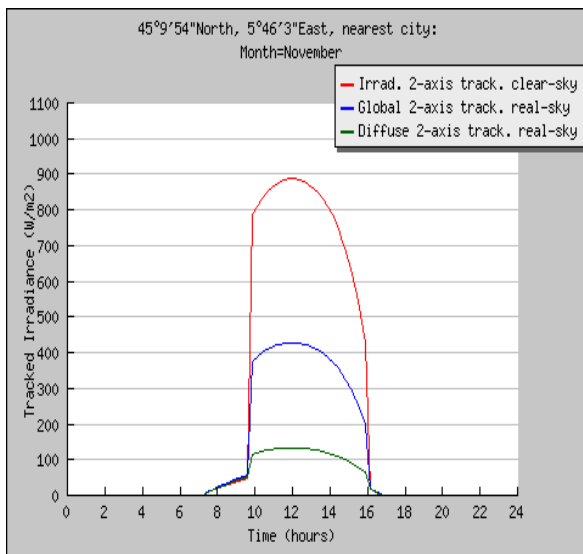


Figure 12. Characteristics of the site.

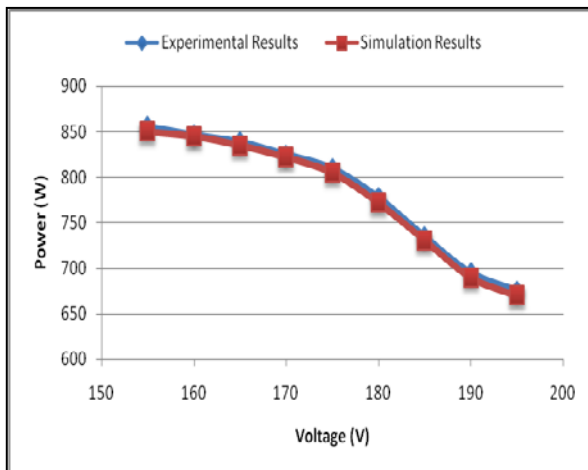


Figure 13. Variation of power according to the voltage.

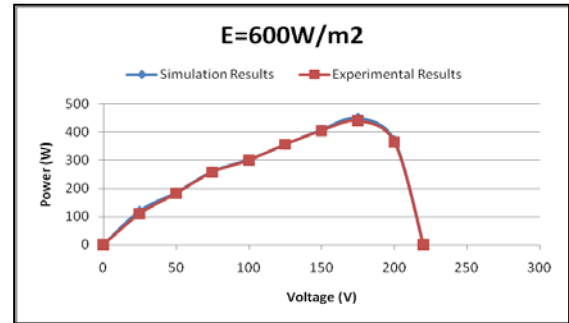
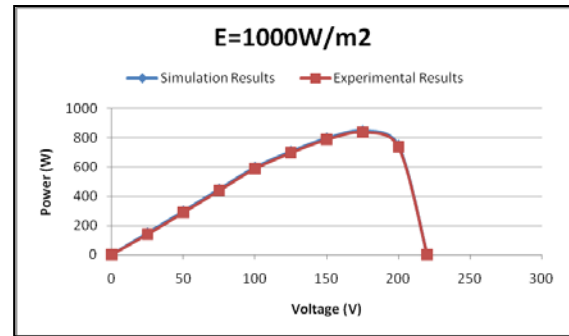


Figure 14. PV power of MPPT method under step changing irradiance.

The response time of the maximum PV power tracking, due to a step irradiance input, reflects the tracking speed of the bond graph MPPT method (shown in figure (13) and figure (14)) and present the PV power of MPPT method under step changing irradiance.

9. Comparative study

The proposed algorithm was validated by means of simulations performed with the Symbols code in two different situations, the former assuming the presence of the proposed control system and the latter its absence.

The simulation results of the PV system using a BG-MPPT and P&O algorithm are discussed in this section. Figure (15) compares the obtained P-V characteristics of the PV module from using the P&O algorithm and the proposed BG-MPPT algorithm.

From the figure, it is shown that by using the proposed algorithm, the location of the maximum power point (MPP) of the PV module is the nearest to the theoretical power as compared to the P&O algorithm.

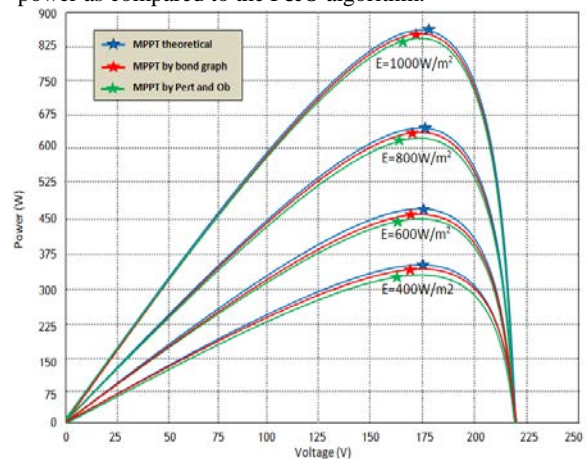


Figure 15. Comparing P-V characteristics.

To evaluate the performance of the proposed system, a comparison between the P&O algorithm and the proposed BG-MPPT algorithm is carried out for a set of solar radiation and the results are plotted in figure (16). From this figure, it is noted that the power of the proposed algorithm is higher than the classical P&O algorithm.

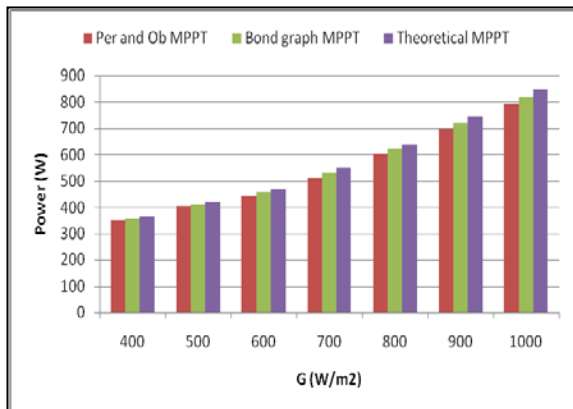


Figure 16. Comparing PV module powers.

In terms of efficiency, the efficiency of classical P&O algorithm is calculated by dividing the obtained power by the theoretical maximum power of PV module, while the efficiency of the proposed algorithm BG-MPPT is obtained by dividing the predicted power by the theoretical maximum power of PV module. According to the results, the tracking efficiency of proposed algorithm is not less than 92% as compared to using the P&O algorithm as shown in figure (17).

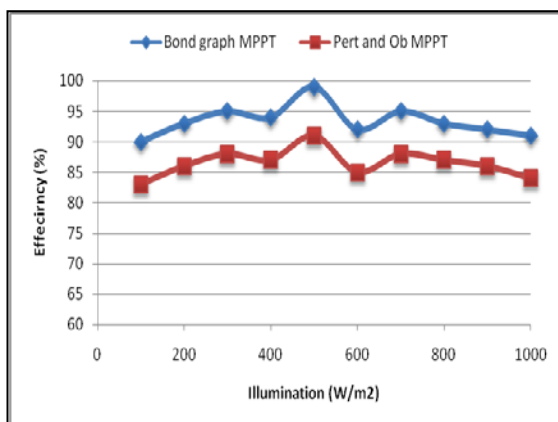


Figure 17. Comparing efficiency of PV system.

From the previous figures, the bond graph method is most effective among all the other methods. The second method is slower (speed point of view), given the number of iterations required to reach the MPP (180 iterations) and for slow changes in illumination, but with power losses due to the oscillation around the MPP, these losses may be even more important when weather conditions fluctuate rapidly (as a day cloud).

Such weather conditions are a problem for the search of MPP whatever the algorithm used, in fact, so that it can be effective, it is necessary that the static converter operates in steady state before new disturbances are made like bond graph method. In terms of speed the latter technique is faster, given the number of iterations required to reach the MPP (152 iterations).

10. Conclusions

This paper proposed the maximum power point tracker, using bond graph control, is developed to increase the energy generation efficiency of the solar cells. The proposed method involves implementing a maximum power point tracker controlled by bond graph controller and using buck boost converter to keep the PV output power at the maximum point all the time. This controller is tested using Symbols program, and the results were compared with a perturbation and observation controller applied on the same system. The comparison shows that the bond graph controller is better in response and does not depend on knowing any parameter of PV panel. The information required for bond graph control is only generating power; therefore, the hardware is simple and the cost of this system is inexpensive.

A general approach on modelling photovoltaic modules is presented. The proposed BG-MPPT is based on a DC/DC converter control with an original algorithm. The theoretical evaluations of the MPPT advantages, based on the proposed model, suggest that the power gain, obtained by MPP tracking, is higher than 27%.

The experimental results were compared with the simulated ones, for the same conditions and panel parameters. This comparison reveals that the differences between experimental data and simulated characteristics were less than 1%.

References

- [1] J. Lyons and V. Vlatkovic, "Power electronics and alternative energy generation, Power Electronics Specialists Conference, PESC 04.2004 IEEE 35th Annual, vol. 1, June 2004, pp. 16–21 Vol. 1.
- [2] T. Mrabti, M. El Ouariachi, R. Malek, Ka. Kassmi, B. Tidhaf, F. Bagui, F. Olivie and K. Kassmi, "Design, realization and optimization of a photovoltaic system equipped with analog maximum power point tracking (MPPT) command and detection circuit of the dysfunction and convergence the system (CDCS)", International Journal of the Physical Sciences Vol. 6(35), 23 December, 2011, pp. 7865 - 7888,
- [3] K. K. Tse, M. T. Ho, H. Chung, and S. Y. Hui, "A Novel Maximum Power Point Tracker for PV Panels Using Switching Frequency Modulation". IEEE transactions on power electronics, vol. 17, n°. 6, 2002, PP. 980-989.
- [4] M.A.S Masoum and M.Sarvi, Design, simulation and construction of a new fuzzy-based maximum power point tracker for photovoltaic applications, AUPEC'02 -- Monash University -- Melbourne Sept 29 - Oct 2, 2002.
- [5] C.Y. Won, D.H.Kim, S.C.Kim, W.S.Kim, H.S.Kim, A New Maximum Power Point Tracker of Photovoltaic Arrays using Fuzzy Controller, Proceedings of the IEEE Power Elec. Specialist Temp Conference, 1994, pp.396-403,
- [6] Castro, J.L., "Fuzzy logic controllers are universal approximators", IEEE transactions on system, man, and cybernetics, Vol. 25, No. 4, 1995, PP. 629-635.
- [7] Wang, L.X., Stable adaptive fuzzy control of nonlinear systems". IEEE Trans. Fuzzy systems, 1(2). 1993. PP.146-154.
- [8] Femia, N., G. Petrone, G. Spagnuolo and M. Vitelli, Optimizing sampling rate of P&O MPPT technique. IEEE

- 35th Annual Power Electronics Specialists conference, PESC, 04(3). Aachen, Germany, PESC.2004. PP. 1945-1949.
- [9] Femia, N., G. Petrone, G. Spagnuolo and M. Vitelli, "Optimization of Perturb and Observe Maximum power point tracking method". IEEE Trans. on Power Electronics, 20(4), 2005. PP. 963-973.
- [10] Abu Tariq, M.S, Jamil Asghar. Development of microcontroller-based maximum power point tracker for a photovoltaic panel. IEEE Power India Conference, POWERI.2006, PP. 1-8.
- [11] Menniti, D., A. Burgio, N. Sorrentino, A. Pinnarelli, G. Brusco, An incremental conductance method with variable step size for MPPT: Design and implementation. 10th International Conference on Electrical Power Quality and Utilisation, EPQU.2009.
- [12] Fangrui, Liu, Shanxu Duan, Fei Liu, Liu. Bangyin and Yong Kang, Variable step size inc MPPT method for PV systems. IEEE Transactions on Industrial Electronics, 55(7). 2008.
- [13] Esram, T., P.L. Chapman, "Comparison of Photovoltaic Array Maximum Power Point Tracking Techniques". IEEE Transactions on Energy Conversion, 22(2). 2007. PP. 439-449.
- [14] Noguchi, T., S. Togashi and R. Nakamoto, "Short-current pulse-based maximum-power-point tracking method for multiple photovoltaic and converter module system". IEEE Trans. Ind. Electron. 2002, 49(1): 217-223.
- [15] Xiao, W. and W. Dunford, A modiWed adaptive hill climbing mppt method for photovoltaic power systems," IEEE 35th Annual Power Electronics Specialists Conference, PESC 04. 2004.
- [16] G. D-Tanguy, "les bond graphs", Hermess, NJ: 2000, pp. 377.
- [17] P.C. Breedveld and G. Dauphin-Tanguy, cds., Bond Graph for Engineers, North-Holland, Amsterdam, 1992.
- [18] J. Thoma, Introduction to bond graphs and their applications, Pergamon Press, 1975.
- [19] Paynter, H.M. Analysis and design of engineering systems. Cambridge, MA: MIT Press. 1961.
- [20] Bouamama, B., Busson, F., Dauphin-Tanguy, G., & Staroswiecki, M. Analysis of structural properties of thermodynamic bond graph models. In Proceeding of the 4th IFAC : Fault Detection Supervision and Safety for Technical Processes, vol. 2 IFAC, Budapest, Hungary, 2000. pp.1068–1073.
- [21] Dauphin-Tanguy, G., Rahmani, A., & Sueur, C.a. Bond graph aided design of Controlled systems. Simulation Practice and Theory, 7, 1999. PP. 493–513.
- [22] Gawthrop, P., & Bevan, G. Bond graph modeling — A tutorial introduction for Control engineers. IEEE Control System Magazine, 27(2), 2007. PP. 24–45.
- [23] Karnopp, D., & Rosenberg, R. Analysis and simulation of multiport systems: The Bond graph approach to physical system dynamics. Cambridge, MA: MIT Press. 1968.
- [24] D. Karnopp, R. Rosenberg, System Dynamics: A Unified Approach, John Wiley, NewYork, 1974.
- [25] J. Thoma, Introduction to Bond Graphs and Their Applications, Pergamon Press, Oxford, 1975.
- [26] S. Gomathy, S. Saravanan, S. Thangavel, Design and implementation of Maximum Power Point Tracking (MPPT) Algorithm for a Standalone PV System, International Journal of Scientific & Engineering Research Volume 3, Issue 3, March -2012, pp. 1-7
- [27] M. Gradella Villalva, Jonas Rafael Gazoli, and Ernesto Ruppert Filho, Comprehensive Approach to Modeling and Simulation of Photovoltaic Arrays, IEEE Transactions on Power Electronics, Vol. 24, No. 5, May 2009. pp. 1198 – 1208
- [28] S. Jain and V. Agarwal, "A single-stage grid connected inverter topology for solar PV systems with maximum power point tracking," IEEE Trans. Power Electron., vol. 22, no. 5, Sep. 2007, pp. 1928–1940.
- [29] Badoud A, Khemliche M, Grid-Connected modeling, Control and Simulation of Single-phase two-Level Photovoltaic Power Generation System Coupled to a Permanent Magnet Synchronous Motor, 7th international workshop on systems, signal processing and their applications WOSSPA, IEEE 2011, pp. 1-7.
- [30] Mezghanni, D. et al., Bond graph modeling of a photovoltaic system feeding an induction motor-pump. Simulation Modelling Practice and Theory 15(10), 2007. pp. 1224–1238.
- [31] Mohammad H. Rashid, 2007. Power Electronics Handbook, Academic Press.
- [32] T. Porselvi, Ranganath Muthu, Design of Buck-Boost Converter for Wind Energy Conversion System, European Journal of Scientific Research Vol.83 No.3, 2012, pp.397-407.
- [33] Kim, Y., Jo, H., Kim, D. A new peak power tracker for cost effective photovoltaic power systems. IEEE Proceedings 3(1), 1996. pp. 1673–1678.
- [34] Kawamura, T., Harada K., Ishihara Y., Todaka T., Oshiro T., Nakamura H., Imataki M., 1997. Analysis of MPPT characteristics in photovoltaic power systems. Solar energy materials and solar cells. In: Proceedings of the 9th International Photovoltaic Science and Engineering Conference, PVSEC-9, vol. 47, no. 14, 1996, pp.155–165.
- [35] Tafticht T., Agbossou K., Doumbia M. L., Chériti A., An improved maximum power point tracking method for photovoltaic systems", Renewable Energy 33, 2008, pp. 1508–1516.

A Comparative Study of PZT-Based & TiNi- Shape Memory Alloy Based MEMS Microactuators

S. D. Nijmeh^{*, a}, M. S. Ashhab^a and R. F. Khasawneh^b

^a Mechanical Engineering Department, The Hashemite University, Zarqa, 13115, Jordan

^b Industrial Engineering Department, Al-Balqa Applied University, Al Salt, 19117, Jordan

Abstract:

In this paper, we are interested in drawing a comparison between PZT & TiNi shape memory alloy (SMA) thin films using microelectromechanical systems (MEMS). Also, we present a new hybrid heterogeneous structure. Different characteristics are investigated in this comparative study. Based on the comparison made, it was shown that TiNi-SMA based microactuators can serve higher flow rates in fluid systems and at low operating voltages in comparison with that provided by PZT-Based microactuators. Another concluded result indicates that the fast response and the high operating frequencies are provided by PZT-based microactuators, but displacement is relatively small, whereas TiNi-SMA has a slow response frequency and a large force-displacement. By combining TiNi and PZT films, we proposed in our paper a new hybrid heterogeneous structure that can utilize the unique properties of the individual bulk materials and present large displacement and multiple responses.

© 2013 Jordan Journal of Mechanical and Industrial Engineering. All rights reserved

Keywords : PZT films; TiNi films; MEMS; Piezoelectric Thin Films; Shape Memory Alloy(SMA); Composite; Smart Material.

1. Introduction

Microelectromechanical systems (MEMS) are the core of the technology of miniature chip device, which integrates mechanical elements, sensors, actuators and electronics. MEMS are components between 1 to 100 micrometers in size, and MEMS devices range in size from 20 micrometers to a millimeter. MEMS were used in 1980s in USA, but they were commercially used in the early 1990s in automotive industry [1].

Over the last decade, this field has been growing daily with a motivation to make smaller and smaller MEMS. They are not only smaller, but also cheaper and more functional with fast response times. A weather station that measures temperature, humidity and barometric pressure can be built on a single chip. Conditions inside living bodies can be monitored, using implanted sensors and tiny submarines that can travel through the bloodstream. Different commercially applications of MEMS are found in automotive, military, telecommunications and aerospace industries. MEMS devices act as impact sensors in the accelerometers of automobile airbags. They also act as micronozzles in commercial inkjet printers [1].

MEMS microstructures are manufactured either through surface micromachining in which successive layers of material are deposited on a surface and then etched to shape or through bulk micromachining where the

substrate itself is etched to produce a final product. Different challenges are found in designing MEMS devices, such as finding skilled engineers with an adequate knowledge of micromechanical systems, materials and target manufacturing processes. Another challenge is transferring data between separate electronic and mechanical design teams who handle system and component-level development. Efforts are extending to optimize performance and improve the reliability of MEMS.

The world has gone through two material ages: the plastic age and the composite age, and a new area has developed in between, which is called smart materials. Smart materials are materials that receive, transmit, or process a stimulus and respond by producing a useful effect that may include a signal upon which the materials act. The action of receiving and responding to stimuli to produce a useful effect must be reversible [1]. Although a few materials that possess these capabilities are available so far, there are some materials that have multi-functions, such as shape memory alloys and piezoelectric materials [2].

SMA possesses the unique ability to recover their shape against strong deformations. They, particularly, exhibit an extremely interesting mechanical behavior as a function of temperature; they get deformed at low temperature since they will stay deformed until heated above some threshold temperature when they spontaneously return to the original

* Corresponding author.e-mail: drnijmeh@hu.edu.jo.

shape, with a mechanism involving large mechanical strengths [3]. SMA has been seen as a plighting and high performance material in MEMS applications, since standard lithography techniques can be used to pattern in batch process. Also, thin film SMA has a very small amount of thermal mass, thus the response time is reduced and speed of operation is increased significantly.

Piezoelectric materials are very important functions. Multiphase piezoelectric composites were developed for their synergetic effect between the piezoelectric activity of monolithic ceramics and the low density of nonpiezoelectric polymeric materials. One of the developed classes is the smart tagged composites. These piezoelectric composites are PZT-5A particles that are embedded into an unsaturated polyester polymer matrix and are used for structural health monitoring [1].

Section Two deals with literature review and available applications. Material characteristics of PZT and TiNi-SMA thin films are presented in Section Three, followed by aspects of comparison in Section Four concerning preparation and fabrication techniques in 4-1, operating conditions in 4-2, applications of TiNi-SMA and PZT based MEMS in subsection 4-3, and finally obstacles and challenges in Section Five. The proposed new hybrid heterostructure is presented in Section Six. Finally, conclusions and recommendations are summarized in Sections Seven.

2. Literature Review and Available Applications

Yongqing Fu. et al. in [4] discussed preparation, characterization, considerations, residual stress and adhesion, frequency improvement fatigue and stability, and modeling of behavior as well as composite thin films. A comparison of TiNi-SMA microactuation was made with other microactuation methods (High performance) TiNi-based films were deposited at a relatively high temperature (about 400°C). An AFM based in-situ testing method have been used to characterize phase transformation behavior of the deposited films. They concluded that TiNi actuators at micro-scale, out-performs other actuation mechanisms in work/volume ratio, large deflection and force but with a relatively low frequency (less than 100 Hz) and efficiency as well as non-linear behavior.

Yongqing Fu et al. in [5] designed and fabricated new types of TiNi thin film based microactuators, such as microgrippers, microvalves and micromirror using MEMS techniques. TiNi films were etched at room temperature using HF:HNO₃:H₂O (1:1:20). AZ 9620 positive photoresist with thickness of 10 µm was used as a mask. They concluded that miniature TiNi actuated devices based on sputtered TiNi films are ready for huge manufacturing market and for medical microdevices implantable into the human body.

A. Camposo, N. Puccini et al. in [3] combined TiNi-SMA with pulsed laser deposition (PLD) to produce films with shape memory effect onto Si-based substrates. PLD deposition technique was performed using Si/SiO₂ (450nm) wafers and Si₃N₄ triangular cantilevers at a rate of the order of 0.3-0.4A per laser shot. Temperature of substrate was 520-600°C with a 20-40min in situ high-vacuum annealing at the same temperature, followed by

free cooling to room temperature. TiNi pellet (51:49) was used as a target. Deposited samples were analyzed using an ad hoc setup, employing a temperature controlled Peltier stage and a tilt/twist measurement system based on an optical lever method. The attainment of shape memory effect was demonstrated to confirm PLD as a new technique for deposition of SMA films. MEMS prototypes with a wide range of possible applications can be fabricated by PLD in a simple, clean and congruent process.

Shuren Zhang, Jingsong Liu and Chengtao Yang in [6] investigated the growth mechanism of grains and the size effect on the coercive field. ULVAC Ferroelectric thin film deposition system was used to fabricate PZT on Pt/Ti/SiO₂/Si (100) structured substrates, then these films were annealed using ULVAC-RIKO Rapid Thermal Annealing (RTA) system, with a heating rate of 50°C/s. A two-step-warm-up method was designed to obtain different grain sizes. Lateral grain size was measured using scanning force microscopy (SPM), film crystal phase was identified using Bede DI multi-function X-Ray diffractometer (XRD), and the electrical properties were measured using the Radiant Precision LC Materials Analyzer. It was demonstrated that PZT thin films with different grain sizes were fabricated by controlling the nucleation process time and growth process time. Electrical properties and polarization has a great dependence on grain size, which was found to be 70nm as a critical value for the domain structure transition.

D.F.L.Jenkins, W.W.Clegg et al. in [7] optimized d₃₁ coefficient to maximize actuation efficiency. d₃₁ coefficient was measured for different PZT thin films and their effectiveness as microactuators was compared and evaluated. PZT thin films, with a (Zr/Ti) ratio equal to (54/46) were deposited on Si substrate at room temperature or the substrate temperature between 500-550°C by R.F. magnetron sputtering. Two thermal treatments have been used: conventional and rapid thermal process. It was shown that PZT films were extremely effective as micro-actuators and were able to operate efficiently over a wide bandwidth. d₃₁ coefficient was found to be -12, -1.3 and -0.05 for the 110, 100 and 111 films, respectively, and was significantly increased by poling at elevated temperatures of around 120°C. Actuation was increased by application of D.C. bias field, with up to 5.9µm of actuation being possible for a 110 film being driven with 10V a.c. with 5V D.C. bias voltage.

P. Delobelle et al. in [8] used nanoindentation technique to measure the transverse biaxial elastic modulus and hardness of piezoelectric ceramic films (PZT), and the true biaxial elastic modulus to describe the mechanical properties of these films having various grain size. Morphotropic PZT films Zr/Ti=54/46 were deposited by RF magnetron sputtering from cold pressed powder targets. Substrates were platinumized silicon. Post-deposition annealing was applied to samples in a conventional furnace in air at 625°C. Thicknesses of synthesized films in the range 0.3 to 2.0µm with varying grain diameters in the range 0.1 to 4.0µm. Nanoindenter was used for measuring the transverse elastic modulus and hardness. They concluded that there exists a relation between grain size and elastic behavior; hardness measurement also

confirmed that these sputtered films possess a hard mechanical behavior.

Romain Herdier, M. Detalle et al. in [9] compared the electric, ferroelectric and piezoelectric properties of two different PMN-PT composition, along with those of PZT of the same thickness. PMN-PT and PZT thin films have been grown by R.F. magnetron sputtering on Pt(111)/TiO_x/SiO₂/Si substrates. Titanium oxide and platinum bottom electrode were deposited with thicknesses of 15 and 120nm, respectively. The thickness of the PMN-PT and PZT films were 800nm. X-ray diffraction analysis was performed using a Siemens D5000 diffractometer. Piezoelectric coefficient was determined using a homemade Laser Doppler vibrometry. They concluded that 0.7PMN-0.3PT and PZT are good candidates for MEMS actuators, but PZT is superior and simpler to grow compared to PMN-PT. An important advantage for PZT material is the possibility to introduce dopants and improve the piezoelectric properties of PZT.

Sibei Xiong et al. in [10] evaluated the piezoelectric coefficient e_{31} of PZT thin film by measuring the tip displacement of PZT-coated cantilevers of the dimensions 50mm long, 4mm wide and 0.3mm thick. Micro-machined ultrasonic sensors, in which PZT-coated membrane functioned as sensing element, were fabricated and their properties were characterized. Pb(Zr_{0.52}Ti_{0.48})O₃(PZT) piezoelectric thin films with thickness of 0.7-2.2 μ m were prepared on Pt/Ti-coated SiO₂/Si(0.5 μ m) substrates by the sol-gel method. Fabrication procedures are reported in details in the paper, and piezoelectric coefficient was measured by observing the actual deflection of PZT-coated cantilevers under applied voltage. It was concluded that the effective piezoelectric transverse coefficient e_{31} of PZT thin film was -12.5+0.3c/m². The prepared PZT films demonstrated excellent piezoelectric properties and had been applied in MEMS ultrasonic sensors. The sensitivity of the micro-sensors reached 500 μ v/Pa.

S. Srinivasan, J. Hiller and B. Kabius in [11] integrated and demonstrated low voltage piezoactuated hybrid of PZT and UNCD films as a high performance platform for advanced MEMS/NEMS devices. Material integration involves growth of 1 μ m thick Ultra nanocrystalline diamond (UNCD) layer on si(100) substrate, fabrication of UNCD cantilevers, growth of a 10nm thick TaAl barrier layer on the UNCD film, growth of 180nm thick Pt layer on top of the TaAl barrier, growth of 70 nm thick PbZn_{0.47} Ti_{0.53} O₃ piezoelectric layer via sputter deposition at 600°C in 100 mTorr of oxygen and growth of the top 50 nm thick Pt layer to complete the capacitor like structure needed for piezo actuation via voltage application between the top and bottom Pt electrode layers. X-ray diffraction analysis showed preferential (001) orientation and this PZT layer yielded capacitors with well-saturated polarization in the 5-97 range. Another conclusion is that PZT/UNCD cantilevers can be fabricated using industrial processes, involving photolithography in conjunction with reactive ion etching in oxygen plasmas to produce large arrays of PZT/UNCD structures for high performance MEMS/NEMS piezoactuated devices.

F. Dauchy, R.A. Dorey in [12] described the fabrication and structuring of multilayer thick film piezoelectric structures (PZT) using composite sol-gel techniques and wet etching. PZT films of 10 and 40 μ m thick are produced

by repeated layering and infiltration with embedded thin (100nm thick) metal electrodes. Signal and multilayer structures were demonstrated. A crack free surface finish of a 28- μ m- thick film reveals the adaptability of spin coating technique to fabricate thick films. Wet etching technology revealed the possibility of great adaptability to pattern and shape innovative devices such as bars 10 μ m wide of 21 μ m PZT thick film. Byung -Moon Jin, SE-Hwan Bae and others in 2005[13] tested PZT/PZ multi-layered films and measured fatigue effects of PZT/PZ series and normal PZT films by applying AC 10 volts. Sol-gel technique was used to fabricate PZ/PZT multi-layered thin films. Different kinds of films with 250nm thick for each by using PZ and PZT precursors. Substrates for these were the same as Pt/Ti/sio₂/si. Piezoelectric Loops were measured by a standardized ferroelectric Tester System +10 volt saw type pulse and the pulse period of 1.000*10-3second were used for measurement. It was found that the best fatigue effect is in the sample that is made by 3PZT layers after 3PZ layers. The values of switch polarization and switch remnant polarization in this sample are reduced within the 10% of the initial values up to 108 cycles and this film is a good candidate for FeRAM application. A. Kumar, M. R. Alam and others in 1999 [14] synthesized and characterized TiNi films from crystallographic point of view by using X-ray diffractometer (XRD) and atomic force microscope (AFM) techniques. A deposition process was carried out in the "Materials Research Laboratory" at the university of south Alabama. A buffer Layer of BaTiO₃ was deposited at 600°C in 100m Torr oxygen environment. After depositing approximately 4000Å of BaTiO₃ at 10Hz repetition rate, TiNi films of nearly 600Å were deposited on the top of the buffer layer in the presence of 15m Torr nitrogen environment at various deposition temperatures (50,300,500°C). For TiNi/PZT films on si(100) substrates, first a PZT buffer layer was deposited at 600°C in a 200m Torr oxygen environment with the same previous deposition conditions. Also TiNi films were deposited on si(100) substrates without any buffer layer at various deposition temperatures in presence of 15m Torr nitrogen atmosphere. X-ray diffractometer was used to characterize these films, and AFM analysis was done by a digital Nanoscope. TiNi deposited films at lower temperatures have amorphous type structure but films at higher temperatures have crystalline quality thin films. Also buffer layers of BaTiO₃ and PZT have improved the crystalline of TiNi films deposited at higher temperatures. The TiNi/BaTiO₃ film was less uniform than TiNi/PZT film due to the differences in grain structure, and TiNi/PZT film has smaller diameter columns than the TiNi/BaTiO₃ film due to differences in deposition parameters.

All the above studies were concerned with deposition and analysis of single or double layered thin films for MEMS applications. Researchers studied PZT thin films and analyzed their mechanical behavior; others studied TiNi-SMA films. Others studied the possibility of integration of PZT an UNCD film to provide high performance platform for advanced MEMS devices. Another study described fabrication and structuring of multi-layer thick film piezoelectric structure using composite sol-gel techniques and wet etching ones. PZ and PZT multi-layered thin films were also testified.

Microactuators based on $\text{PbZr}_{1-x}\text{Ti}_x\text{O}_3$ (PZT) and TiNi-SMA are compared using MEMS. Operating frequencies pressures, pumping rates, design and fabrication are all studied and investigated. Also, a new hybrid heterostructure of TiNi and PZT films is proposed having superior static and dynamic properties.

3. Material Characteristics

Piezoelectric and Shape memory materials in thin film form can provide reasonable displacements that are suitable for microactuators, and, therefore, they were developed for MEMS applications [17]. Piezoelectric materials can be defined by dividing the word into piezo and electric. Piezo is from the Greek word piezoin, which means "to press tightly or squeeze," when combined into piezoelectric it means "squeeze electrically." Piezoelectric phenomenon was discovered by Jacques Curie and Pierre Curie in 1880 [17].

Lead zirconate titanate (PZT), $\text{PbZr}_x(\text{Ti}_{1-x})\text{O}_3$; $0 < x < 1$ are polar dielectric which exhibits a high degree of piezoelectric activity. Sol-gel PZT structures were crack free and had good crystallinity [16], and being widely used in MEMS actuators. When a piezoelectric material is subjected to a mechanical stress, an electric charge is generated across the material. Piezoelectric materials are also pyroelectric. As they undergo temperature change, an electric charge is generated. When temperature is increased, a voltage develops with the same orientation of polarization voltage, whereas a positive orientation to the polarization voltage is produced when temperature is decreased. In Rigaku RINT2000X-ray diffractometer (XRD), typical peaks were observed associated with perovskite-type PZT phase, and preferential (100), (110) and (111) orientations were dominant in the PZT. Dielectric constant and dielectric loss value were measured with a HIOKI 3532 LCR hitester. Dielectric constant and loss were over 300 and 0.03, respectively [16].

Shape memory materials possess different and desirable properties such as large power-density, scalable character, hence the ability to recover large transformation stress and strain upon heating and cooling, because of the molecular rearrangement of the metal that it constitutes of, high damping capacity, super elasticity, good chemical resistance and biocompatibility. Shape memory alloys can be patterned with standard lithography techniques and fabricated in batch process. They have a very small amount of thermal stress to heat or cool, consequently response time is reduced and the speed of operation is increased significantly [4].

Nickel-titanium alloys Ni/Ti(49/51) are the most widely used shape memory material, known as Nitinol after the laboratory where this material was first observed (Nickel Titanium Naval Ordinance Laboratory). As this alloy is cooled below a critical temperature, the crystalline structure enters into the Martensitic phase. During this stage, the material can be easily deformed through large strains with a little change in stress. As the temperature is increased above the critical temperature, it drives the molecular rearrangement of the alloy, and Martensite is now transformed into the cubic Austenite phase, accordingly the material regains its high strength and modulus and behaves normally. As a result, the material

shrinks during the change from the Martensitic to the Austenitic phase. This behavior (shape memory effect) is considered a unique property of shape memory alloys. Different kinds of shape memory effect can be reported but the most common memory effects are the one-way shape memory and the two-way shape memory. With the one-way effect, cooling from high temp. does not cause a macroscopic shape change, but with the two-way shape memory effect the material remembers two different shapes: one at low temperatures, and one at the high temperature shape, even without the application of an external force. Such behavior is attributed to training, in which a shape memory can learn to behave on a certain way. Under normal conditions, a shape memory alloy remembers its high temperature shape, but upon heating to recover the high temp. shape, immediately forgets the low temperature shape. However, it can be trained to remember to leave some reminders of the deformed low temperature condition in the high temp. phase. Pseudo-Elastic behavior is another unique property for shape memory alloys when the alloy is completely composed of Austenite. Unlike the shape memory effect, pseudo-elasticity occurs without a change in temperature. The load on SMA is increased until the Austenite becomes transformed into Martensite simply due to the loading. The loading is absorbed by the softer Martensite, but as soon as the loading is decreased the Martensite begins to transform back to Austenite and the material returns back to its original shape.

4. 4. Aspects of Comparison

4.1. Preparation & Fabrication Techniques

TiNi thin films are prepared using Laser ablation, plasma spray and flash evaporation, but with some problems such as non-uniformity in composition and film thickness, low deposition rate, non-batch processing and incompatibility with MEMS process. To overcome these difficulties, an alternative method mostly used is sputtering. However, transformation temperatures, shape memory behaviors and super elasticity of sputtered TiNi films are sensitive to sputtering conditions, metallurgical factors and the application conditions, this sensitivity provides flexibility in engineering a combination of properties for different applications. TiNi films were deposited either at room or high temperatures. Sputtering at room temperature necessitate post-sputtering annealing (higher than 450°C) to generate films of crystalline structure with shape memory effect. Films deposited at high temp. (about 400°C) were crystallized in crystalline form, so there was no need for post-annealing. Localized laser annealing was used for TiNi films [4] due to its precision in selection of the areas to be annealed as small as micrometer, non-contact and efficiency, free of restrictions on design and processing, ease in integration in MEMS processes and ease in cutting of the final structure using the laser beam.

PZT thin films can be prepared using different techniques, but these techniques are not practical because they need highly specialized equipment and have low compatibility with conventional IC/MEMS processes. Sol-gel technique was used as an alternative technique, which only requires simple and low temp. process. PZT precursor

solution 0.8M with molar ratio of Pb:Zr:Ti=1.2:0.53:0.47 of high concentration, high boiling point and low carbon content, based on the acetic acid-based method with "inverted mixing order(IMO)" of alkoxides, was prepared. Fabrication processes include the following:

First, wafer was preheated with the wet gel then Vacuum deposition of Pt(100nm)/Ti(30nm) bottom layers on a silicon wafer (thickness: 250 μ m). A layer of SU-8 25 of thickness 50 μ m was patterned to form circular apertures with 40 μ m, 80 μ m and 180 μ m diameters, respectively. Second, PZT solution was dispensed on the SU-8 layer, filtered with 0.2 μ m syringe filter. The wafer is dried in a sealed container at room temp. to gelatinize the sol. Third, PZT wet gel is prebaked at 140 °C prior to lapping. Fourth, the wafer is lapped using a urethane foam pad. Isopropyl alcohol was used as solvent and lubricant. Fifth the gel is fired on a hotplate at 350 $^{\circ}$ C for 10 min. The gel transforms into amorphous solid of PZT and SU-8 layer Separates from the PZT structures. Then the wafer was heat treated. At last, annealing is applied at 600 $^{\circ}$ C for 20 min [16].

4.2. Operating Conditions

The actuation mechanism of TiNi films is as straightforward as that for PZT-based microactuation. TiNi SMA-based microactuation operates at low voltages, which allows easier integration with electronic devices, and high output pressures which are required to overcome flow resistance associated with complicated flow paths. TiNi SMA-actuated microvalve that is capable of operating pressures of 200KPa under an operating voltage of 3.5V has been reported [18]. A large pumping volume per stroke can be achieved due to the high recoverable strain of TiNi SMAS that is generated by the ferroelastic deformation that occur in the low temperature Martensitic phase. The low operating frequencies reduce the flow rate of TiNi micropumps and microvalves below the expected values, and are limited by the necessary cooling of the microactuation and is in the range of tens of Hz or lower. Patterned TiNi films have been developed to reduce thermal mass, however, the power consumption is still in the range of hundreds of milliwatts [17].

PZT-based actuation operates at high frequencies due to the large actuation forces; stresses of up to 100MPa and operating frequencies of up to 10KHz have been reported, which provided high operating pressures and pumping rates up to 100KPa[19] and 2300 μ l/min[20], respectively. PZT actuators can be operated at their primary natural frequencies and multi-layered piezoelectric components can be used to avoid high voltages since some tens of volts are usually required for actuation. It was demonstrated that although operating at high voltages, the power consumption of PZT-based microactuators was not excessive.

4.3. Applications of TiNi-SMA & PZT Based MEMS

Shape memory alloys are used in many fields, in bio-engineering as mending bones and opening the clogged arteries. Other applications such as in antiscalding protection, coffee pot thermostat, fire security and protection systems, eyeglass frames and super elastic glasses. Most applications of TiNi films in MEMS are focused on micro-actuators, such as microgrippers, springs, micropumps and microvalves. Several

requirements for microgrippers such as large gripping force, sufficient opening distance for assembling works, in which TiNi films are promising. Two types of TiNi film based microgripper designs are available. The popular design is out-of-plane bending mode with two integrated TiNi/Si cantilever with opposite actuation directions as shown in Figure1 below.



Figure 1. the popular design of TiNi film based microgripper

The other type, shown in Figure2, is the patterned TiNi electrodes on silicon cantilevers. The cantilever bends up when the electrodes are electrically heated, due to the shape memory effects of TiNi films, consequently generating gripping force.

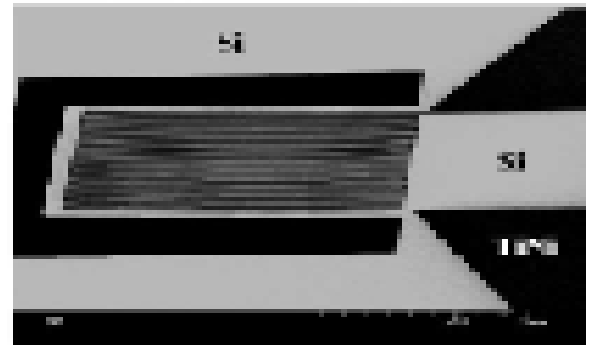


Figure 2. the patterned TiNi electrodes on silicon cantilevers

Both gripper designs need further bending process to combine two cantilevers to form gripping movement. A novel micro-wrapper was fabricated using freestanding TiNi films with out-of-plane movement as shown in Figure (3) [4].

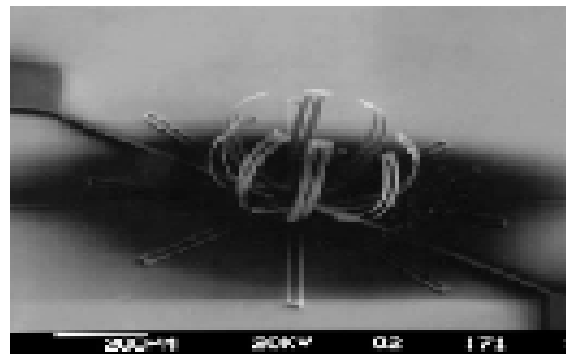


Figure 3. A novel micro-wrapper using freestanding TiNi films

It can be used in invasive surgery to remove anomalies such as tumors. The overall dimension of the micro-wrapper arms is 100 μ m. A small current passes through it to maintain the flat shape, whenever the current is removed, the small arms close to form a cage.

Piezoelectric materials were first applied in Sonar Devices then in piezoelectric filters, piezo buzzers, transducers and lighters. There are different applications of TiNi films in MEMS such as being used in Cantilever fabrication. PZT films were prepared using the sol-gel method. The precursor solution of PZT (52/48) was supplied by the Mitsubishi Materials Corporation. PZT films were then prepared on Pt/Ti-coated SiO₂/silicon wafers by multiple spin-coating and annealing. Each layer was fabricated by spin coating the solution precursor on the lower electrodes and was pyrolyzed at 350°C for 10min. After the fabrication of every four single layers, the PZT thin films were thermally annealed at 650°C for 10min using the RTA furnace in flowing oxygen. Heating rate in RTA was 8°C/s. As film thickness of single coating is about 58nm, 12single layers were coated to form 0.7- μ m-thick PZT films.

The size of the cantilever was 50mm long, 4mm wide and 0.3mm thick. Fabrication process can be described as follows:

Pt(100nm)/Ti(10nm) bottom electrode layer was deposited on SiO₂/Si substrates at RT by RF-sputtering. Pt/Ti bottom electrode layer was patterned by ion milling technology. PZT thin film was deposited by sol-gel method. Piezoelectric PZT thin film was patterned using wet-etching method to form contact holes. The etchant for PZT was a diluted solution of HF & HNO₃. Au/Cr films deposited by evaporation, and patterned to form the top electrode by lift-off, at last the Si wafers were diced into 50*4*0.3mm³. Figure 4 shows a photograph of the prepared PZT cantilever and the measurement setup.

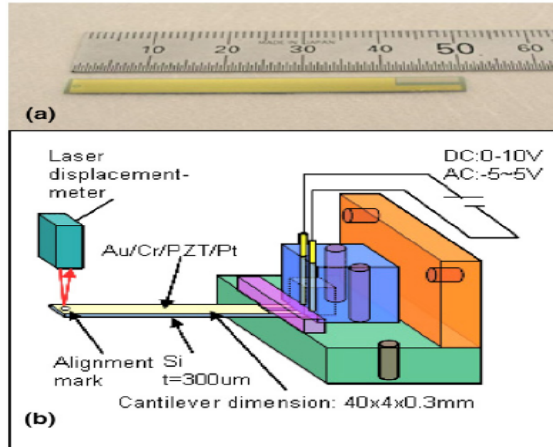


Figure 4. a) The prepared PZT cantilever, b) and the measurement setup of the microactuator.

One end of the cantilever was clamped by a plastic vise and the other end was left free. Piezoelectric vibration was generated by applying a sine wave voltage between the top and bottom electrode, and the tip displacement was measured using a laser displacement meters. The laser spot position was adjusted precisely to coincide with the alignment mark near the free end of the cantilever. Elastic contact of the bottom and top electrode was obtained using a pair of needles through the plastic vise.

Another application is the PZT microactuator. Its fabrication includes micromachining of the silicon diaphragm, depositions of PZT thin film with its electrode layers. Diaphragms were fabricated by wet etching of

silicon. Oxide layer (500nm) was grown followed by LPCVD deposition of (100nm) silicon nitride.

Nitride layer was patterned by RIE with a positive photoresist layer as a mask and the oxide layer was patterned in 6:1 BOE using the same photoresist mask layer. Etching of silicon was performed in 45% KOH solution. Three or four stages of etching were carried out to obtain 10-15 μ m thickness range. Then the nitride layer was stripped in hot phosphoric acid. The oxide layer was etched in 10: 1 BOE to 200nm thickness. At last, diaphragms of uniform thickness were obtained.

For the bottom electrode layer, Pt and Ta layers (100 and 10nm) were deposited using e-beam evaporation and patterned using the lift-off method. PZT film(118/52/48) in 10% PZT-E solution was deposited on the bottom electrode layer using the sol-gel technique. Five layers were applied, then the film was patterned using a positive photoresist for masking. The patterned PZT layer was annealed at 650°C for 90min in a RTA furnace. These procedures were repeated until a 600nm-thick PZT thin film was obtained. Finally, metal films of Cr and Ag were deposited using e-beam evaporation and patterned using the lift-off technique to form the top electrode layer.

5. Obstacles and Challenges

Functional materials such as PbZr_{1-x}Ti_xO₃(PZT) and TiNi shape memory alloy (SMAs) in thin film form can provide reasonable displacements that are suitable for microactuators, and have, therefore, been developed for MEMS applications. The main advantages of these materials are their high work density and ease of implementation, due to their relatively straightforward actuation mechanisms.

One of the major obstacles to commercializing PZT-based microactuation for MEMS is the lack of serviceable deposition techniques compatible with Si processing. Physical vapor depositions are not appropriate. Screen-printing and sol-gel deposition techniques have been reported. In contrast, Si compatible deposition and microfabrication techniques for TiNi films were developed in the past decade. However, they have not received much attention in the MEMS technology as is the case with other microactuator technologies.

Different challenges are found in designing MEMS devices, such as finding skilled engineers with an adequate knowledge of micromechanical systems, materials and target manufacturing processes and transferring data between separate electronic and mechanical design teams who handle system and component-level development. On the other hand, measuring the mechanical properties of these films is a difficult task because these films are clamped by their substrates, thus nanoindentation technique was chosen to characterize transverse mechanical properties of the films[21]. Biaxial elastic modulus and hardness were measured for PZT thin film using this advanced technique. Also, it does not require any complex modeling in order to extract the parameter values. However, few measurements, relating to mechanical characterization of ferroelectric films such as PZT, are published.

One of the main problems of particular concern is to elaborate novel interfacial technology to connect dissimilar components. To accomplish a multi-layered interface which provides durability, mechanical stability, dynamical coupling, chemical and physical compatibility, will be the key. The next problem is understanding and modeling the potential emergent properties of the complex systems with the non-linear integration effects of the components, and specifically understanding the phase transformation characteristics under constraints exerted by coupled components via the interface. Phase stability, degradation and transformation hysteresis under certain circumstances have not been understood very well yet.

6. The New Hybrid Structure

Multi-layer, composite or functionally graded TiNi-based, films can be designed in order to improve the properties of TiNi films. Different designs were modeled for the functionally graded TiNi thin films. One of them was through the gradual change in composition (Ti/Ni ratio), crystalline structures, and residual stress through film thickness and transformation temperatures. Material properties could change from pseudo-elastic to shape memory, and integration of both characteristics reveals a two-way reversible actuation, since residual stress variations in thickness will enable biasing force to be built inside the thin film.

Functionally graded TiNi films can be prepared by changing the target powers during deposition. Another way is to change the target temperature during sputtering. To optimize functionally graded TiNi thin films for MEMS application, it is necessary to characterize, model and control the variations in composition, thermomechanical properties and residual stress in these films. Another design includes materials and functions other than TiNi films. Functionally graded TiN/TiNi layer was deposited to achieve this objective (4), in which an adherent and hard TiN layer (300nm) on TiNi film (3.5 μ m) formed a good passivation layer, and improved the overall hardness, load bearing capacity and tribological properties without sacrificing the shape memory effect of the TiNi film. TiN layer is able to restore elastic strain energy during heating and to reset the martensite phase on subsequent cooling, forming a two-way SMA effect. As a result a functionally graded Ti/TiNi/Ti/Si graded layer was proposed to improve biocompatibility and adhesion of TiNi films.

A new functionally graded design is proposed in this paper which includes the combination of TiNi films with piezoelectric (PZT) thin films. It was found that the response time of PZT films is fast while the displacement is relatively small, while TiNi film has a large force-displacement, with slow response frequency. Upon coupling both of these a new hybrid heterostructure is generated in order to tune the static and dynamic properties of TiNi films, which produce a larger displacement than conventional piezoelectric thin films, and improve dynamic response compared with that of single layer TiNi films. TiNi films can be prepared by sputtering and PZT film by sol-gel methods. Either one of these films can be the bottom layer.

To integrate and hybridize such materials lead to composite materials with intrinsic mechanisms for sensing, control and response. A hybrid structure with embedded sensors or actuators and controlled by an external processor is named an adaptive structure rather than an intelligent material. The sensing, actuating and information-processing capabilities of an intelligent material stem from its intrinsic composition and microstructure. These structures can provide massive actuation stress, tolerable strain, high speeds and reasonable efficiency. One of the major problems encountered is to develop novel interfacial technology to bind dissimilar components. Also understanding the phase transformation characteristics for SMA-based composites exerted by coupled components via the interface. Detailed informations will be presented and validated in a future work. Amazing results will overtake the vested interest of workers and researchers in this field.

7. Conclusions and Recommendations

TiNi-SMA thin films were able to operate at low frequencies and generate a large force displacement, whereas PZT thin films were able to operate at high operating frequencies and generate a relatively small displacement. Low power consumption was attained using PZT films compared to that using TiNi-SMA which was in the range of hundreds of milliwatts although patterned TiNi films have been developed to reduce thermal mass. Also TiNi films were capable to operate at low voltage and high flow rates, while PZT-thin films operated at high operating voltages and low strains produced.

Different preparation and fabrication methods were optimized for both microactuation techniques. Sputtering technique was used to fabricate TiNi thin films to achieve high uniformity in composition, film thickness, high deposition rate and batch processing and compatibility with MEMS process. Sol-gel technique was optimized to fabricate PZT thin film, which only requires simple and low temperature process.

Different applications for both films were discussed and they seem to be promising for more accurate and complex applications in the future. Different difficulties were encountered, such as lack of a robust deposition technique compatible with Si processing for PZT thin films. In contrast, different Si compatible deposition and microfabrication techniques have been developed for TiNi-SMA thin films.

New hybrid heterostructure is proposed to tune the static and dynamic properties of TiNi thin films, which generate a larger displacement than conventional piezoelectric (PZT) thin films, and have an improved dynamic response compared with that of single layer TiNi films. It is promising to fabricate nano-scale SMA thin film structures, since shape memory effect still occur in films of nanometer grains. Physical actuation techniques at nano-scale may be achieved using these structures.

It is also recommended that TiNi and PZT films be coupled experimentally, to create a new hybrid heterogeneous structure composite. This new hybrid can tune the static and dynamic properties of TiNi thin films, which produce larger displacement than conventional piezoelectric thin films, and have an improved dynamic

response compared with that of single layer TiNi films. Sputtering technique is proposed to prepare TiNi film and sol-gel method to prepare PZT thin film. Fabrication processing, adhesion, dynamic coupling of dissimilar components can all be considered for this new hybrid.

References

- [1] James A. Harvey, *Mechanical Engineers Handbook: Materials and Mechanical Design*, John Wiley & Sons, Inc., 2006.
- [2] Z.G. Wei, C.Y. Tang, W.B. Lee, "Design and fabrication of intelligent composites based on shape memory alloys", *Journal of Materials Processing Technology*, 69, (1997), 68-74.
- [3] A. Camposo, N. Puccini, F. Fusco, M. Allegrini, E. Arimondo, A. Tuissi, "Laser Deposition of Shape-Memory alloy for MEMS applications", *Science Direct, Applied Surface Science*, 208-209, (2003), 518-521.
- [4] Yongqing Fu, Hejun Du, Weimin Huang, Sam Zhang, Min Hu, "TiNi-Based thin films in MEMS applications: a review", *Science Direct, Sensors and Actuators, A* 112, (2004), 395-408.
- [5] Yongqing FU, HEJUN DU, WEIMIN HUANG and MIN HU, "TiNi Film Based Shape Memory Alloy And Microactuators", *International Journal of Computational Engineering Science*, Vol. 4, No. 2, (2003), 221-225.
- [6] Shuren Zhang, Jingsong Liu, and Chengtao Yang, "Growth and Characterization of PZT Films with Different Grain Sizes", *Integrated Ferroelectrics*, 84: 99-105, (2006).
- [7] D.F.L. Jenkins; W.W. Clegg; G. Velu; E. Cattani; D. Remiens^b, "The Characterization of PZT films of differing orientations for MEM Applications", *Ferroelectrics*, 224:1, 259-266, (1999).
- [8] P. Delobelle; E. Fribourg-Blanc; O. Guillon and their friends, "Determination by Indentation Method of Sputtered PZT Films Mechanical Parameters for Si-MEMS applications", *Integrated Ferroelectrics*, 69:1, 213-221, (2005).
- [9] Romain Herdier, M. Detalle, David Jenkins, Caroline Soyer, Denis Remiens, "Piezoelectric thin films for MEMS applications-A comparative study of PZT, 0.7PMN-0.3PT and 0.9MN-0.1PT thin films grown on Si by r.f. magnetron sputtering", *Sensors and Actuators A: Physical*, 148, (2008), 122-128.
- [10] Sibeï Xiong, Hiroshi Kawada, Hiroshi Yamanaka, Tomoaki Matsushima, "Piezoelectric properties of PZT films prepared by the sol-gel method and their application in MEMS", *Science Direct, Thin Solid Films*, 516, (2008), 5309-5312.
- [11] S. Srinivasan, J. Hiller, and B. Kabius, "Piezoelectric/ultrananocrystalline diamond heterostructures for high-performance multifunctional micro/nanoelectromechanical systems", *Applied Physics Letters*, 90, 134101, (2007).
- [12] F. Daychy . R. A. Dorey, "Patterned crack-free PZT thick films for micro-electromechanical system applications", *Int j Adv. Manuf Technol*, (2007), 33:86-94.
- [13] BYUNG-MOON JIN, SE-HWAN BAE, KIE-BEOM JEON, AND ILL- WON KIM, "A Study of Fatigue Effect in PZ/PZT Multilayered Thin Films Prepared by Sol-Gel Technique", *Ferroelectrics*, 328:15-19, (2005).
- [14] A. Kumar, M.R. Alam, J.J. Weimer, L. Sanderson, "Synthesis and Characterization of Laser ablated TiNi films", *Applied Physics A, Materials Science & Processing*, 69, S917-S920, (1999).
- [15] D. Xu, L. Wang, G. Ding, Y. Zhou, A. Yu, and B. Cai, *Sensors and Actuators A*, 93, 87, (2001).
- [16] Nobuyuki Futai, Kiyoshi Matsumoto and Isao Shimoyama, "FABRICATION OF HIGH-ASPECT-RATIO PZT THICK FILM STRUCTURE USING SOL-GEL TECHNIQUE AND SU-8 PHOTORESIST", *Department of Mechano-Informatics*, 113-8656, (2008).
- [17] Bo-Kuai Lai; H. Kahn; S.M. Phillips; A. H. Heuer, "A Comparison of PZT-Based and TiNi Shape Memory Alloy-Based MEMS Microactuators", *Ferroelectrics*, 306:1, 221-226, (2004).
- [18] E. Makino, T. Mitsuya, and T. Shibata, *Sensors and Actuators A*, 88(3), 256, (2001).
- [19] R. Linnemann, P. Woias, C.D. Senfft and J. A. Ditterich, *Proc. MEMS 98 (IEEE, 1998)*, P. 532.
- [20] A. Olsson, G. Stemme, and E. Stemme, *Sensors and Actuators A* 47(1-3), 549 (1995).
- [21] Akihiro Yamano and Hiromitsu Kozuka, "Single-step sol-gel deposition and dielectric properties of 0.4µm thick, (001) oriented Pb (Zr, Ti)O₃ thin films", *JSol-Gel Sci Technol*, (2008), 47:316-325.
- [22] Mandar Deshpande, Laxman Saggere, "PZT thin films for low voltage actuation: Fabrication and characterization of the transverse piezoelectric coefficient", *Science Direct, Sensors and Actuators A*, 135, (2007), 690-699.

Crystallization behavior of iPP/LLDPE blend filled with nano kaolin particles

Amin Al Robaidi ^{*,a}, Nabil Anagreh^a, Mohammed A-I Addous^b
and Sami Massadeh^a

^a Materials Engineering Dept.- Al-Balqa Applied University, Al-Salt Jordan.

^b Faculty of Engineering – German Jordan University

Abstract:

The crystallization kinetics of isotactic polypropylene (iPP/LLDPE) blends, and iPP composite containing nano kaolin particles has been investigated. The addition of nano kaolin and LLDPE to iPP affects both its nucleation and spherulitic growth rate. With the addition of the nano filler particles, significant increase in the nucleation and maximum growth rate were observed. To improve the dispersion in the matrix, the filler particles were treated with silane. An experimentally determined value for the Avrami exponent was calculated. The Scanning electron microscopy indicates that the nano particles cause a finer dispersion of the LLDPE component in the iPP matrix. Due to the presence of nano size filler, additional heterogeneous nucleation of the iPP nuclei occurs through the enhancement of the interface area.

© 2013 Jordan Journal of Mechanical and Industrial Engineering. All rights reserved

Keywords: Nano Particles; LLDPE; iPP; Compatibilizer; Dispersion; Kaolin; Melt Blending

1. Introduction

The extent of crystallization and the morphology formed during polymer processing are critical for the determination of the resulting physical properties of the polymer products, thus influence their end-use values. Almost all the crystallized polymers are partly crystalline and partly amorphous. This specific semi-crystalline structure allows the adjustment of polymer products physical properties according to the application requirements. Formation of ordered solid phase, such as crystals, typically starts with nucleation, in which a seed, or a tiny embryo of the new phase, is formed. Nucleation occurs during a first order phase transition, in which a new phase is generated from an old phase that has higher free energy. Crystal growth, the overlapping process accompanying nucleation, is the successive deposition of polymer chains on the nucleus of the aligned polymer chains (Mandelkern 2004).

Understanding the mechanism of nucleation and crystal growth is critical for manufacturing process and determination of the final product properties, such as crystal size distribution, thermal stability and mechanical properties. Blending two thermodynamically immiscible polymers to create a material with desirable properties is an attractive alternative to synthesizing new polymers. A common example is rubber toughening. A small amount of rubbery polymer is dispersed into a glassy polymer in the

melt state and the resulting material is often much tougher and has a higher impact strength, when compared to the bulk glassy polymer (J. Yang, B.J. McCoy and G. Madras 2005). The microstructure of the blend often determines its physical properties. It is well-known that the impact resistance of thermoplastics can be improved by blending it with filler and elastomers (Bucknall, 1977; Galli et al., 1984; Kolarik et al., 1986a; Al Robaidi, 2001). For polypropylene, a variety of rubbers are suitable for this purpose, but it turns out that a second thermoplastic, polyethylene also increases the impact resistance of polypropylene at low temperatures (Al Robaidi, 2001; Kolarik et al., 1986b; Yang et al., 1984; Flaris and Stachurski, 1992). Unfortunately, this desirable mechanical behavior is often accompanied by a decrease in other properties, such as elastic modulus and stiffness. A way to overcome this disadvantage is to melt-blend the polymers with a compatibilizer and fillers. Compatibilizers act at the interface between the two components (Barensten and Heikens, 1973) and it is expected that the modification of the interface influence both the nucleation and the crystallization kinetics. It is the aim of this study to demonstrate that the interface of a compatibilized thermoplastic blend alters the nucleation of the matrix and consequently alters its morphology.

* Corresponding author. e-mail: arobaidi@yahoo.de.

2. Experimental Procedures

2.1. Materials and Sample Preparation

The starting materials were isotactic polypropylene (iPP, $\rho=0.905 \text{ g/cm}^3$). Linear Low Density Polyethylene (LLDPE, $\rho = 0.919 \text{ g/cm}^3$) and a kaolin as a nano filler. All these polymers are standard commercial grade materials with a typical additives present. The kaolin particles applied were prepared on a nano mill in the range averaging 50-80nm in diameter. To improve the dispersion and the compatibility of the filler in the matrix the particles were coated with 2.5% weight silane.

The materials were melt-blended in a brabender plastograph. Six samples were investigated: pure iPP and five blends as listed in table 1.

Table 1. Polymer characterization data

Material	Concentration
iPP	100 reference
iPP + LLDPE	80%/20%
iPP + LLDPE + coated Kaolin	70%/20%/10
iPP + coated kaolin	90%/10%
iPP + coated kaolin	80%/20%
iPP + coated Kaolin	70%/30%

The Polypropylene and LLDPE starting materials were characterized using gel permeation chromatography (GPC) and differential scanning calorimeter (DSC) to determine the melting points, molecular number, weights and distribution respectively. These results are summarized in Table 2. Samples thereof for Charpy impact tests were prepared by injection molding. The tests were carried out on a Ceast Impact Tester at a temperature of 20°C.

Table 2. Polymer characterization data

Material	Tm[°C]	Mn	Mn/M
iPP	161.4	64.300	4.2
LLDPE	123.5	37.300	3.7

2.2. Nucleation Kinetics Measurements

For the observations in the optical microscope (Leitz Metallux II), the samples were pressed to a thickness of approximately 100 μm , placed between glass slides, and put in the hot-stage microscope. Here, they were heated to 200°C for five minutes and then cooled to the isothermal crystallization temperature. Crossed polarizers were used and the crystallization was monitored on a video screen and recorded. From the recording, the growth of the spherulites as well as the number of nuclei as a function of time was determined. Isothermal crystallization temperatures were chosen between 130°C and 139°C.

3. Results And Discussion

For an isothermal experiment, the observed number of nuclei in a given volume as a function of time is:

$$N_{(t)} = M[1 - \exp(-vt)] \quad (1)$$

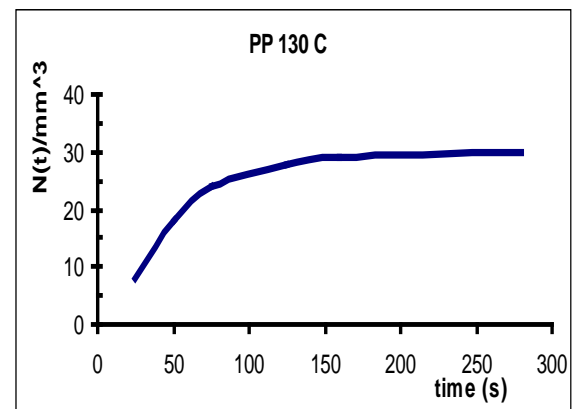
Where

v = the probability of nuclei development per unit time

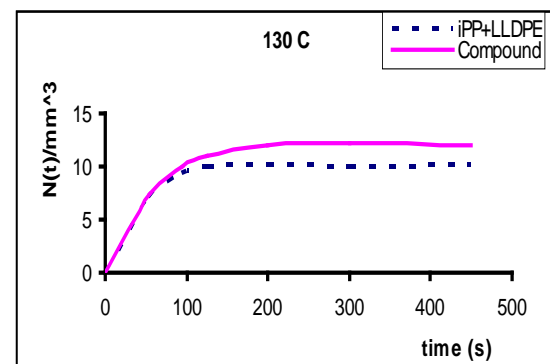
M = the nucleation density (Mandelkern, 2004; Aggarwal *et al.*, 1966; Icenogle, 1985)

$N(t)$ = a characteristic function for the nucleation behavior of the sample investigated

Representative data, $N(t)$ for the tested samples, iPP, iPP+LLDPE and the iPP+ 20% kaolin composite samples are shown in Figure 1.



a



b

Figure 1. Development of the number of nuclei as a function of time for (a) iPP and (b) the blend 80% iPP/20% LLDPE.

Differentiation of equation (1) yields the nucleation frequency per unit of untransformed volume at time t :

$$N_{(t)} = vM \exp(-vt) \quad (2)$$

The temperature-dependence of the nucleation density can be described by a cumulative Gauss-function ($\text{erf}(T)$):

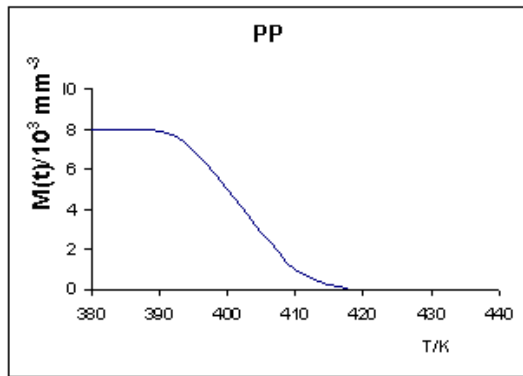
$$M(T) = M_0 \frac{1}{\sqrt{2\pi}\sigma} \int_{-\infty}^{T_c} \exp\left(-\frac{(T-\bar{T})^2}{2\sigma^2}\right) dT \quad (3)$$

Where M_0 is the total nucleation density and σ is the variance. \bar{T} is the temperature of the distribution maximum. Figure 2 shows $M(T)$ for the two selected samples PP and iPP+LLDPE. The values for the nucleation density are listed in

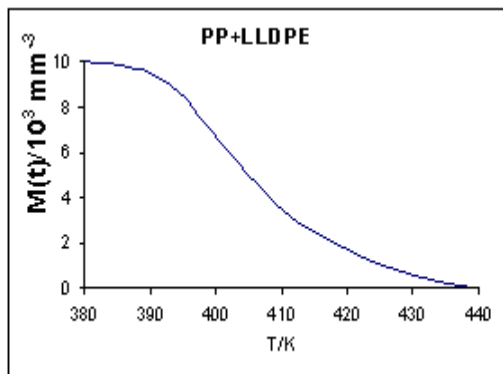
Table 3. Results from nucleation and crystallization kinetics for sample listed in table 1

Sample	Nucleation density M/mm^3	C_3 $10^5/k^2$	G_0 $10^6/mm/s$	G_{max} mm/s	T_{max} $^{\circ}K$	$\sigma\sigma_e$ $10^2 erg^2/cm^4$	Avrami number m
iPP	375	4.51	56.4	.33	341	12.7	2.3
iPP + LLDPE	542	3.83	90.3	.49	346	14.9	2.2
iPP+LLDPE+Kaolin	1005	4.01	12	.60	344	12.2	1.6
iPP + kaolin	517	4.39	121	.64	342	12.4	1.5
iPP + 20% Kaolin	657	3.95	118.5	.67	341	12.8	1.43
iPP + 30% Kaolin	1215	4.43	127	.72	343	14.1	1.37

We see that for the iPP+LLDPE, M is higher than for neat polypropylene. This is probably due to the interface of the second component, which causes the nucleation rate to increase by additional heterogeneous nucleation at the surfaces of the LLDPE occlusions. The area of this interface would then govern the amount of the heterogeneous part of the nucleation; a higher dispersion of the LLDPE and the kaolin should yield more heterogeneous nucleation. This assumption, however, cannot be verified by discussing the nucleation density alone.



a



b

Figure 2. Nucleation density as a function of temperature for (a) iPP and (b) the blend 80iPP/20LLDPE.

A good indication of the type of nucleation is the Avrami exponent, which is discussed later. The radial spherulite growth rates of neat iPP and iPP +nano kaolin compound were measured over time. Figure 3 shows the representative data concerning the change in spherulite

radius as a function of time at 130 °C. In all samples, the spherulite diameters increased linearly with time at all crystallization temperatures, indicating that growth rate was independent of the size of the spherulites. If non crystallizable species are excluded from growing spherulites, they will build up on the crystallization growth front and consequently hinder the transport of crystallizable species from the melt to the growing edge. This phenomenon will give rise to a deviation from linear spherulite growth after the spherulite reaches a certain diameter. Since no such deviation from linearity in spherulite growth was observed in the nano composites (Figure 3), it can be concluded that the kaolin particles are not excluded during spherulite growth.

Again, we assume that this behavior is connected with the change in the type of nucleation.

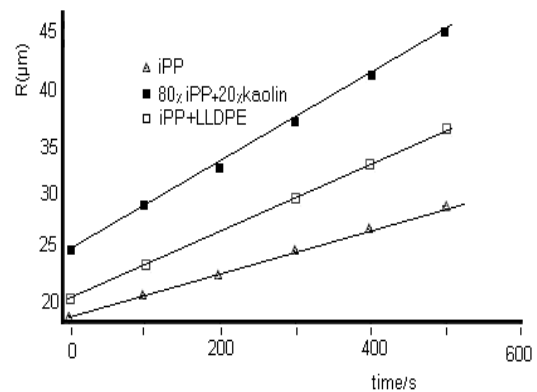


Figure 3. Spherulitic radius as a function of time for (a) iPP; iPP+LLDPE and nano kaolin filled compound.

Within the temperature range investigated, the radius of growing spherulite is expressed as a linear function of time as listed in equation (4) below:

$$r(t) = r_0 + Gt \tag{4}$$

Where r_0 is the radius of the spherulite at the beginning of the experiment and G is the growing rate. The temperature dependency of the growth rate is calculated from¹²⁻¹⁴.

$$G(T_c) = G_0 \exp(-C_1 C_2 / (C_2 + T_c - T_g)) \exp(-C_3 / T_c (T_m - T_c)) \tag{5}$$

Where T_g is the glass transition temperature, T_m is the melting temperature and G_0 , C_1 , C_2 and C_3 are constants. G_0 and C_3 are determined by plotting

In $G + C_1 C_2 / (C_2 + T_c - T_g)$ versus $1 / T_c (T_m - T_c)$. The values obtained from such a plot are listed in Table 3. From equation (5) the maximum growth rate G_{max} can be determined. The calculated values for G_{max} are also listed in Table 3.

We see that G_{max} increases for the sample containing 20% LLDPE from 0.33 mm/s to 0.49 mm/s. This is obviously the influence of the interface, where the nuclei generated by a thermal nucleation that find conditions suitable for undisturbed growth. We expect that G_{max} increase further for the samples containing kaolin. This is indeed the case. G_{max} increases to 0.60 mm/s for the sample containing 10% kaolin up to .72 to samples containing 30% kaolin. Consequently, a different spherulitic distribution is built up which affects the mechanical properties. Figure 4 represent the Charpy impact values for the different formulation investigated. In fact, the sample containing kaolin nano fillers yields the highest impact result; which increases from 0.8 kJ/m² for iPP to 1.2 kJ/m² for the iPP/LLDPE blend, increased further to 1.3 kJ/m² for the sample containing 10% kaolin up to 1.9 kJ/m² for the sample contain 20% kaolin. The kaolin molecules in the domains are crosslinked to the matrix by the silanol end groups; thus improving the toughness and impact energy.

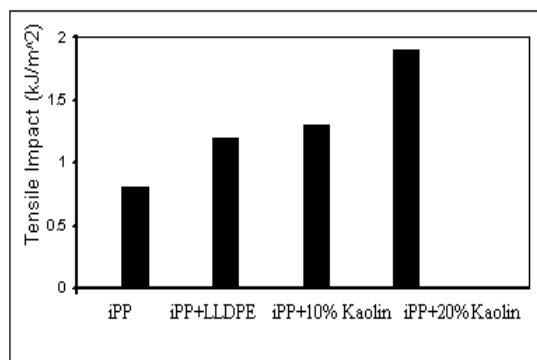


Figure 4. Charpy Impact for sample prepared in table 1

The crystallinity as a function of time in a growing spherulite can be described by the Avrami equation (Avrami, 1941; Mandelkern, 2004):

$$X_c(t) = 1 - \exp(-kt^m) \quad (6)$$

Where $X_c(t)$ is the volume crystallinity at time t , k is a characteristic constant, and m is the Avrami exponent describing the type of crystallization. In our experiment, m has been obtained by determining the volume of the spherulites through the calculation of their cross-sectional areas. Measuring the crystallization half time, $t_{c,1/2}$ can be calculated from can be calculated from (Wenig and Fiedel, 1991):

$$m = \frac{\log\left(\frac{3 \ln 2}{4 \pi G^3 N}\right)}{\log t_{c,1/2}} \quad (7)$$

The Avrami exponents are listed in Table 3. We find that m increases slightly for the samples containing LLDPE. For the blends, containing kaolin we find a sharp drop in the value of m . This indicates that the type of nucleation is indeed changing upon the addition of LLDPE and kaolin to polypropylene. It is in good agreement with

our concept of increasing heterogeneous nucleation, that the sample with the highest maximum growth rate and the highest Charpy impact value exhibits the lowest Avrami exponent.

It is obvious that the addition of kaolin leads to a finer dispersion of the LLDPE occlusions (see figure 5), creating a higher interface area, which in turn increases the secondary nucleation rate.

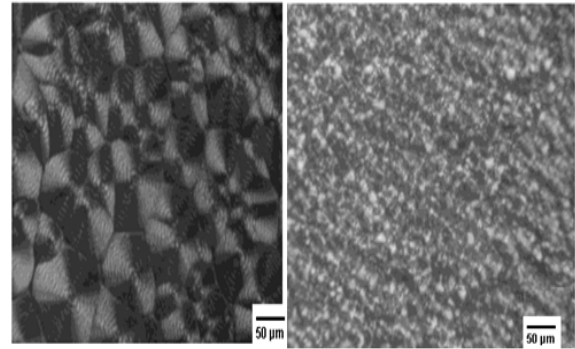


Figure 5. Spherulite structure

The lamellar crystallization itself remains un–changed. This can be demonstrated by calculating the interfacial free energy, σ_e , which can be de–rived from the temperature dependence of the growth rates:

$$\sigma_e = \Delta G \Delta H_m \rho_c \Delta T / 4 b_0 T_m \quad (8)$$

where σ and σ_e are the specific free interfacial energies for the surface and end area of the crystal lamella respectively and b_0 is the thickness of the secondary nucleus (thickness of a monolayer of chains). Values for σ_e are listed in Table 3. Except for the iPP/LLDPE blend, where σ_e is 14.9 erg²/cm⁴, we find the value between 12.1 and 12.7 erg²/cm⁴ for the other blends. As a result of the chang–ing kinetic conditions, the morphology of the iPP matrix should be affected, which is one of the con–ditions to increase the impact resistance. As additional investigations¹⁷ show, this is indeed the case. Calculations of interface distribution func–tions of these blends demonstrate that among other morphological parameters, the lamellar thickness is lowered when a kaolin is added to the iPP blend. It is significant to note that the blend containing kaolin yields the highest impact value and has the smallest lamellar thickness.

4. Conclusion

The crystallization behavior of Iso-tactic polypropylene blended with LLDPE and kaolin particles was investigated. The result obtained and presented in this paper has shown that the crystallization kinetics of miscible polymer blends is influences by filler type and copolymer, used. Adding a second polymer influences the crystallization mainly through thermodynamics and kinetics (equilibrium solubility and deposition mechanism). These effects are incorporated by varying the initial values of ingredients concentration and growth rate coefficient. Because of the chang–ing kinetic conditions, the morphology of the iPP matrix was affected, which is one of the con–ditions to increase the impact resistance. It is significant to note that the impact resistance was increased for the samples containing coated silane kaolin.

A finer dispersion of the filler was achieved, which is responsible for impact increase. The lamellar crystallization itself did not change. This was demonstrated by calculating the interfacial free energy σ_e . We find that the avrami exponent m increases slightly for the sample containing LLDPE, but decreasing significantly when kaolin is added, which indicates that the type of nucleation is changing.

References

- [1] L. Mandelkern, *Crystallization of Polymers*, 2nd edition, McGraw Hill, New York, 2004
- [2] J. Yang, B.J. McCoy and G. Madras, *J. Chem. Phys. B*, 109, 18550(2005)
- [3] J. Yang, B. J. McCoy and G. Madras, *J. phys. chem. B*, 110, 15198 (2006)
- [4] P. Charoenphol and P. Supaphol, *J. Appl. Polym. Sci.*, 95, 245(2005)
- [5] H. Chiu, *J. Polym. Res.*, 9, 169 (2002).
- [6] J. Hsu, B. Nandan, M. Chen, F. Chiu and H. Chen, *Polymer*, 46, 11837 (2005).
- [7] C. P. Bucknall., 1977. *Toughened Plastics*, Applied Science Publishers Ltd., London.
- [8] Jianing Zhang and M. Muthukumar, *J. Chem. Phys.* 126, 234904 (2007)
- [9] Yueh-Lin Loo, Richard A. Register, and Anthony J. Ryan, *Phys. Rev. Lett.* 84, 4120 (2000)
- [10] Nasir, N.F.M., N.M. Zain, M.G. Raha and N.A. Kadri, 2005. Characterization of chitosan-poly (ethylene oxide) blends as haemodialysis membrane. *Am. J. Applied Sci.*, 2: 1578-1583.
- [11] Susilawati and A. Doyan, 2009. Dose response and optical properties of dyed poly vinyl alcohol-trichloroacetic acid polymeric blends irradiated with gamma-rays *Am. J. Applied Sci.*, 6: 2071-2077.
- [12] Omar, W. and H. Al-Itawi, 2007. Removal of Pb+2 Ions from aqueous solutions by adsorption on kaolinite clay. *Am. J. Applied Sci.*, 4: 502-507.
- [13] AL-Shameri, A.A. and L.X. Rong, 2009. Characterization and evaluation of algaof kaolin deposits of yemen for industrial application. *Am. J. Eng. Applied Sci.*, 2: 292-296.
- [14] Saleh, M. and Z. Ali, 2007. Othman analysis of hierarchical diff-EDF schedulability over heterogeneous real-time packet networks. *J. Comput. Sci.*, 3: 673-684.
- [15] Nehra, N., R.B. Patel and V.K. Bhat, 2007. A framework for distributed dynamic load balancing in heterogeneous cluster. *J. Comput. Sci.*, 3: 14-24.
- [16] Louvros, S., 2007. Handover outage time optimization in heterogeneous networks. *J. Comput. Sci.*, 3: 860-862.
- [17] El-Sayed, H.M., 2009. Effect of partial orientation in [100] direction on the magnetic properties of co-ferrite prepared from nano particles. *Am. J. Applied Sci.*, 6: 43-47.
- [18] Al Jaafari, A.I., 2010. Controlling the morphology of nano-hybrid materials. *Am. J. Applied Sci.*, 7: 171-177.
- [19] Shahriari, E., W. Mahmood, M. Yunus, K. Naghavi and E. Saion, 2010. The optical nonlinearity of au and ag nanoparticle prepared by the γ -radiation method. *Am. J. Eng. Applied Sci.*, 3: 260-264.
- [20] Mouheddin, S. and B.T. Jamel, 2009. Indoor characterisation using high-resolution signal processing based on five-port techniques for signal input multiple output systems. *Am. J. Eng. Applied Sci.*, 2: 365-371.
- [21] A. Al Robaidi, *J of Polymers and the environment* vol. 9. no.1 ,2001 .

Studying the Properties of Polymer blends Sheets for Decorative Purposes

Abdullah M. Al-Huneidei^a, Issam S. Jalham^{*,b}

^aHead of Materials and Metallography lab, Royal Scientific Society, Amman-Jordan,

^b Professor in the Industrial Engineering Dept, University of Jordan, Amman 11942 Jordan

Abstract:

Polymeric sheets with different mixing compositions of bakelite and polystyrene were manufactured using the hot pressing method. Microstructure examination, water absorption, impact strength, wear resistance and infrared thermography tests were performed. It was found that there was a homogenous distribution of the bakelite particles in polystyrene and a good bonding was observed between them. Water absorption test showed that the water absorption percent increases with the increase of bakelite material in the blend. Impact test results did not show significant changes.

Wear resistance test was carried out at different forces: (5, 10 and 20 N) and different velocities (150, 250 and 350 rpm). It was found that the wear increases with increasing the applied forces and velocities although, wear resistance shows an improvement with increasing of bakelite content.

In infrared thermography test was also conducted. It was found that the relative temperature change increases with the increase of bakelite content.

Wear resistance and water absorption of the manufactured sheets were compared to the same properties of commercial ceramic tiles (used for decorations) at the same testing conditions. It was found that the water absorption test results for the manufactured sheets are much better than the results of the ceramic tiles test. Moreover, wear resistance test results for the ceramic tiles were close to those of the manufactured sheets when the percent of the bakelite in the blend was 20%, but for higher percentages of bakelite, the wear resistance of the manufactured sheets was better than the tiles.

© 2013 Jordan Journal of Mechanical and Industrial Engineering. All rights reserved

Keywords: Wear; Thermography; Decoration; Absorption; Infrared.

1. Introduction

Polymer blends and composites have become a central part of polymer science and engineering because people could make composites that have properties substantially unattainable with homo-polymers. Such properties include greater toughness, higher strength, better ductility, better absorption properties, and more homogeneous microstructure. Researchers continue work in this field. For example investigators in [1,2,3] studied the mechanical properties of composite materials. They concluded that characteristics of composite materials depend mainly on their manufacturing process and the reinforcement type, percentage, size, and shape. Others [4,5,6] studied the effect of processing on certain composite properties such as stiffness and compression strength. Their studies led to formulate mathematical models to predict the mentioned properties. While Mousa and Karger-Kocsis [7] studied the behavior of styrene / Butadiene rubber organoclay nanocomposites and found that the tensile strength was improved by increasing

nanosilicate. Moreover, Robinson et al. [8] reported that the mechanical properties of polymer matrix composites reinforced with silica were superior to their unreinforced polymer matrix and their strength increased by increasing the reinforcement content. More information about the improvement of the strength of polymers and their composites can be found in the works of Jalham [9], and Sahnoune, et al. [10].

The wear and friction properties of polyamide 66/high density polyethylene blends was studied by Chen, et al. (2004). They produced Polyamide 66 (PA66)/high density polyethylene (HDPE) blends, having miscible structure by compatibilization of HDPE grafted with maleic anhydride (HDPE-g-MAH) and investigated their Mechanical and tribological properties. It was found that the polymer blends greatly improved the mechanical properties of PA66 and HDPE. Blending HDPE with PA66 significantly decreased the friction coefficient of PA66; the friction coefficients of blends with different compositions were almost the same and approximately equal to that of pure HDPE; the blends with 80 vol % PA66 exhibited the best wear resistance.

* Corresponding author. e-mail: jalham@ju.edu.jo.

Chen, et al. [11] continued the investigation of friction and wear mechanisms of PA66/PPS blend reinforced with carbon fiber (CF). It was found that CF reinforcement greatly increases the mechanical properties of PA66/PPS blend. The friction coefficient of the sample decreases with the increase of CF content. When CF content is lower (below 30%), the wear resistance is deteriorated by the addition of CF. However, the loading of higher than 30% CF significantly improves the tribological properties of the blend.

Jalham [12] studied The influence of process and materials variables on the surface properties of polystyrene matrix reinforced with silica sand. He concluded that the introduction of the SiO₂ hard particles significantly increases the abrasive wear resistance of polystyrene. The higher each of the process variables (load, velocity, and time), the higher the dimensionless wear rate and the less the difference between the highest and the lowest wear rate when going to a higher volume fraction content and a higher particle size. While the higher each of the material variables (reinforcement content and particle size), the less the wear rate for fixed process conditions. It was also found that abrasive wear of SiO₂ reinforced polymers occurred by three wear mechanisms: microploughing, microcutting, and microcracking

Moreover, a number of studies on polymer matrix composites subjected to sliding and abrasive wear indicate that wear resistance depends on the detailed properties of the material as well as the external wear conditions such as applied pressure and contact velocity [13,14,15]. Furthermore, fiber addition to polymers doesn't necessarily improve their wear resistance [16]. It is worth mentioning that the performance of polymer matrix composite materials is different when subjected to different modes of wear. For example, the wear behavior of polyetherimide composites in adhesive and fretting wear modes is different from their behavior in abrasive and erosive wear modes [17].

The impact strength of polymers and their composites was also studied. Wantinee, et al. [18] studied the impact resistance of selected Immiscible Polymer Blends. Immiscible polymer blends were prepared by melt extrusion using a single screw extruder in the systems PS/HDPE and PS/PP to assess the effect of composition and morphology on tensile Young's modulus and impact resistance. Results of this work showed that the PS/HDPE system has poor impact resistance although the 20% PS in PP blend possessed an impact strength that was 127% greater than the proportional value for this composition. Thermal and mechanical properties of poly (butylene/terephthalate) epoxy blends was investigated by Zhang, et al. [19]. They concluded that the presence of epoxy resin influenced the mechanical properties of the PBT/epoxy and the completely miscibility of epoxy resin was beneficial to the improvement of the impact performance of the PBT/epoxy blends. In addition, the modification of the PBT/epoxy blends were achieved at epoxy resin contents from 1 to 7%. The maximum increase of the notched Izod impact strength ($\approx 20\%$) of the PBT/epoxy blends was obtained at 1 wt % epoxy resin content.

The above mentioned studies concentrated on two fields; the first studied thermoplastic or thermoset polymer matrix only, which was reinforced with silica sand

particles of different concentrations and different particle sizes. The main performed test on them was the compressive strength test and rarely the wear properties; the second concentrated on studying the properties of the blends of two thermoplastic materials, thermoplastic and elastomeric materials and a reinforced matrix of them.

This work differs from the previous studies in using a combination of polystyrene (thermoplastic material) and Bakelite (thermoset material) of different mixing percentages. To use this product for decorative purpose water absorption, wear, impact, and infrared thermography tests will be performed.

2. Materials, Equipment and Experimental Procedure

2.1. Materials

The main materials, which were used in this investigation, are:

1. Bakelite (the trade name of thermosetting phenol-formaldehyde), which was supplied by Buehler Company.
2. General purpose polystyrene (Granular solid and colorless). This material is a thermoplastic material, which was supplied by Sabic Company
3. Commercial Ceramic Tiles, which are made primarily of clay mixed with various minerals and water. These tiles were brought from the Jordanian market.

2.2. Equipment

The main equipment used in this project are:

1. Laboratory Balance. It is of shimadzu type and used to weigh the specimens with accuracy of 0.01 mg.
2. Plasti Corder BRABENDER (Figures 1a and b). It is used to make the blend by mixing the polystyrene and bakelite materials with each other at controlled temperature and torque.
3. Hydraulic Press Machine. This machine is of carver type (CARVER, Model 389.4PR1A07) and was used to press the mixture which was prepared by the brabender mixer at controlled temperature and force in order to manufacture the polymeric sheets. Figure 2 shows the used hot press machine.
4. Water Absorption Testing Equipment (Figure 3). This machine is of GFL type and was used to conduct the water absorption test for the specimens.
5. Impact Testing Machine. This machine is of CEAST type and was used to perform the impact test for the specimens.
6. Wear Testing Machine. This machine is of METASERV type and was used to perform the wear test for the specimens.
7. Optical Microscope (MEIJI). This equipment is of (MEIJI) type and used for testing the microstructure of the specimens.

Digital Infrared Thermal Imaging Camera (Figure 4). This camera is of Chauvin Arnoux type and used for conducting the infrared thermography test for the specimens



Figure 1a. Front View of Mixing Machine

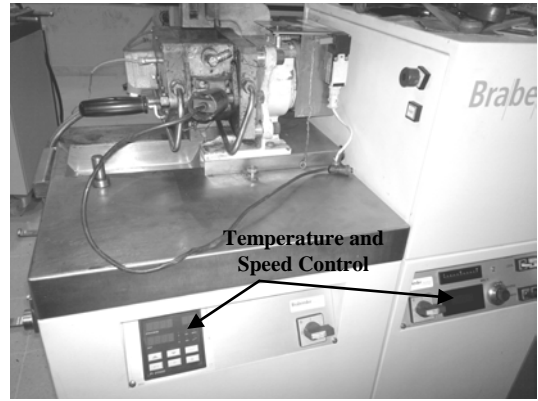


Figure 1b. Side View of Mixing Machine

Figure 1. Plasti Corder BRABENDER used for mixing Bakelite and Polystyrene



Figure 2. Hot Press Machine



Figure 3. Water absorption machine



Figure 4. Thermal Imaging Camera.

2.3 Experimental Procedure

To accomplish this study, Bakelite and polystyrene were mixed in a mixing pan with different proportions. The mixing compositions were based on weight and the proportions of mixing are shown in Table 1.

Table 1. Mixing Proportions

Bakelite (Wt %)	Polystyrene (Wt %)
0	100
10	90
20	80
30	70
40	60
50	50
60	40
70	30

The mixture was then fed into the mixer (Brabender) at a constant speed of 45 m/min to a chamber of a constant temperature (185°C) for 8 minutes. By the end of the mixing step, the mixed materials were in the form of putty-like material. The putty-like material was then put in the mold. The mold is composed of two metallic sheets with 30 × 30 cm size and hollow square sheet (Cavity) of 13 × 13 cm. Then putty-like material was placed in the cavity between these two sheets. Two polyester films were put above and below the material to prevent it from sticking to the metallic sheets.

The mold including the mixed materials was then put in the hot press machine between two preheated hot platens. The material was pressed between the hot platens to get a good and uniform compaction at conditions as shown in Table 2.

Table 2. Hot Pressing Conditions

Segment No.	Force (lb)	Dwell Time (min.)	Temperature (°C)
1	3000	2.0	185
2	15000	2.0	
3	30000	3.0	

The mold was then removed from the pressing machine and allowed to cool to room temperature. The pressed material was then removed from the mold and became a

sheet of 13 × 13 cm and 2 mm thickness. Figure 5 shows samples from the manufactured sheets.

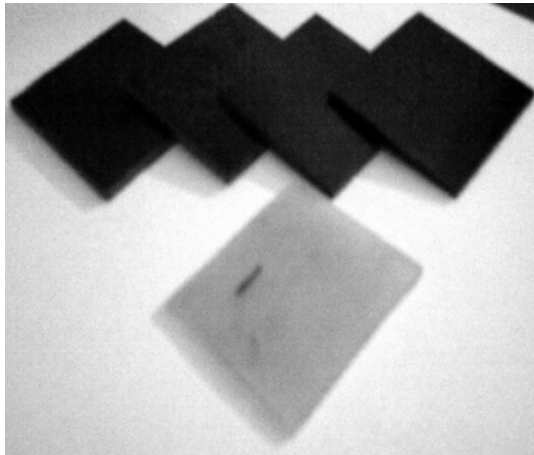


Figure 5. Samples from the Manufactured Sheets.

The sheets of the mixing proportions of (80% bakelite and 20 % polystyrene), (90% bakelite and 10 % polystyrene) and pure bakelite could not be manufactured under these available conditions of the equipment.

Then the microstructure was revealed to test the binding conditions of Bakelite and polystyrene. To accomplish this, the specimens were prepared according to the known standard procedure of grinding and polishing using ethanol as a cooling agent. Other tests were also conducted according to the ASTM standards. For example, water absorption test was accomplished according to ASTM D570 standard, Impact Strength Test according to ASTM D256 standard, Wear Resistance Test according to ASTM D3702 standard, and infrared thermography test was carried out on the manufactured sheets using digital infrared thermal imaging camera. To perform the infrared thermography test, specimens with 30 × 30 mm sheets were cut from the manufactured polystyrene of (20% bakelite and 80% polystyrene sheets), (40 % bakelite and 60% polystyrene sheets) and (60% bakelite and 40% Polystyrene sheets). Then specimens were placed onto a calibrated hot plate. The temperature of the hot plate was set to rise up to 70°C in an increment of 6 °C. The setup of the experiment for one of the ranges is shown in figure 6. While increasing the temperature of the hot plate, infrared images were continuously taken for the surface of the specimens every half second. The taken images for the tested specimens were processed using the camera processor to find the average temperature of the specimens surface versus time. Relative temperature change was expressed by Θ using the following formula:

$$\Theta = T_{avg} - T_o / T_o \dots\dots\dots (1)$$

where

T_{avg} - is the average temperature of specimen surface.

T_o -is the ambient temperature.

And finally, Θ was plotted versus the time up to the steady state

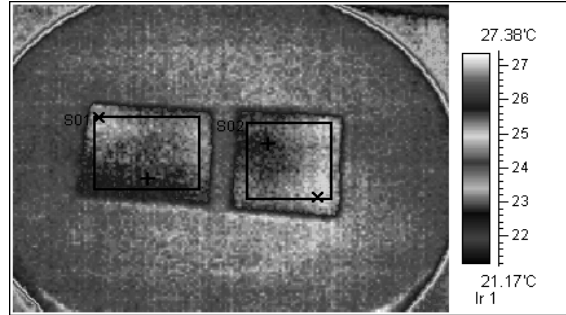


Figure 6. Thermal Image of the manufactured sheets The setup of the experiment for one of the ranges.

3. Results & Discussion

To end up with reliable results, twenty four specimens were manufactured and tested. Their testing results are discussed in the following sections.

3.1. Microstructure

The microstructure after polishing is shown in Figures 7 and 8. Figure 7 indicates that the distribution of mixed materials is homogenous and Figure 8 shows that bonding has occurred between bakelite and polystyrene. This bonding has been reflected positively on the performed tests. The mixing method showed successful results as can be concluded from the bonding.

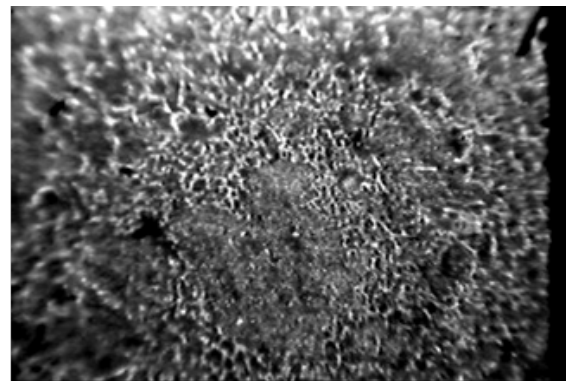


Figure 7. Homogenous Distribution of the Mixed Materials. Magnification 25x

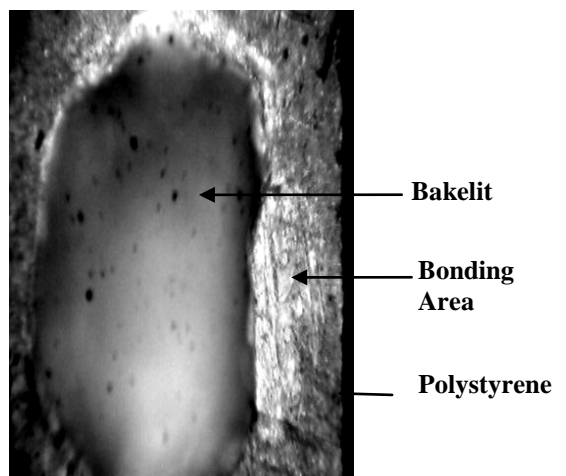


Figure 8. Bonding Between Bakelite and Polystyrene. Magnification 100x.

3.2 Water Absorption

Figure 9 shows the water absorption test results of the specimens. It is clear from this figure that the water absorption percent is increased by increasing the amount of bakelite material in the blend. On the other hand, the minimum percent of absorption was found for the pure polystyrene (0% bakelite). This behavior can be explained by the nature of the chemical structure of the two materials. The polystyrene has less tendency to absorb water than bakelite because its chemical structure contains only carbon and hydrogen, while the bakelite material contains carbon, hydrogen and oxygen.

This behavior is in agreement with Campo [20] who found that the polymers containing only hydrogen and carbon, such as polystyrene, are extremely water resistant, whereas polymeric materials that contain the oxygen group are very susceptible to water absorption.

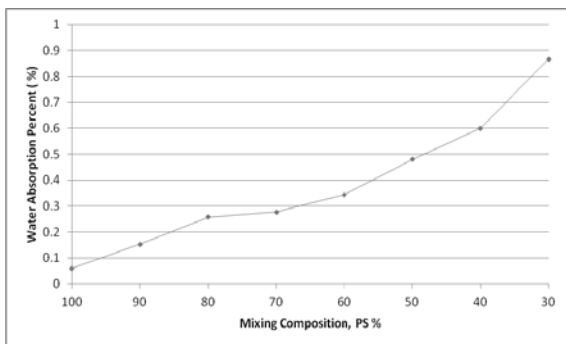


Figure 9. Water Absorption Test Results (PS indicates Polystyrene)

3.3 Impact Test Results

Referring to the impact test results, shown on Figure 10, it is clear that the variation of impact strength values of the tested sheets is about 1 J/m (between 13.5 to 14.5 J/m). This variation is very small and can be considered approximately the same for all mixing compositions. This behavior is due to the similarity in the impact strength of the mixed materials (The theoretical izod impact strength for polystyrene is 15 J/m and the izod impact strength for the bakelite is between 15 - 17 J/m). Moreover, it also indicates that a good bonding between the blended materials was achieved.

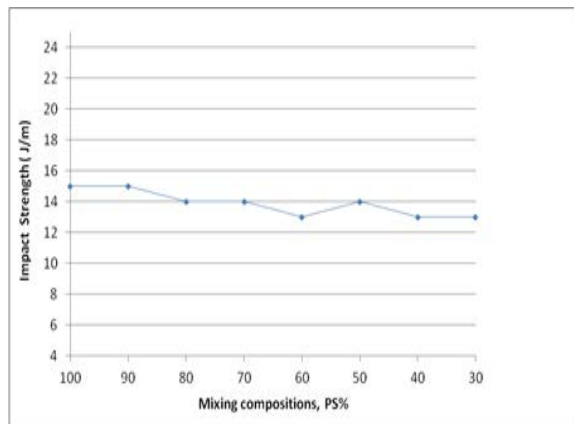


Figure 10. Impact Strength Test Results.

3.4 Wear Resistance Test

The wear resistance test for the manufactured sheets was studied based on the variation of the applied force and the variation of the velocity. The results shown on Figures 11, 12 and 13 indicate the effect of the variation of velocity and the PS % on the wear resistance of the blends for fixed loads. It is obvious from these results that the wear rate for all tested specimens increases with the increase of PS% for the fixed applied force and higher wear rates were obtained after 80% of PS. So, to get best results, the PS% should be less than 80%. Meanwhile, the effect of the velocity at a fixed PS% and Fixed load shows that the increase in velocity increases the wear rate especially when the content of PS exceeds 80% too.

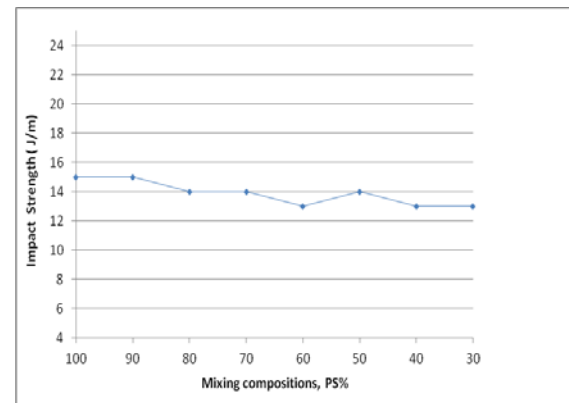


Figure 11. Wear rate at fixed 5N applied force and velocities of 150, 250 and 350 rpm.

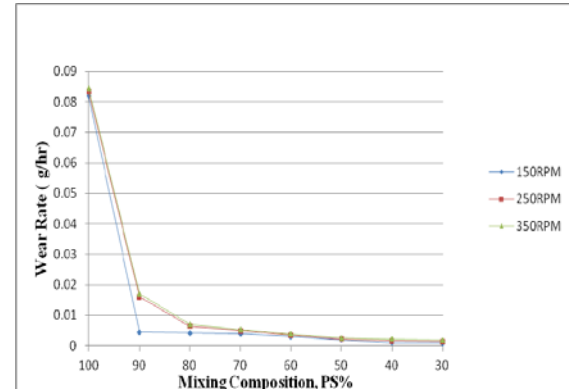


Figure 12. Wear rate at fixed 10 N applied force and velocities of 150, 250 and 350 rpm.

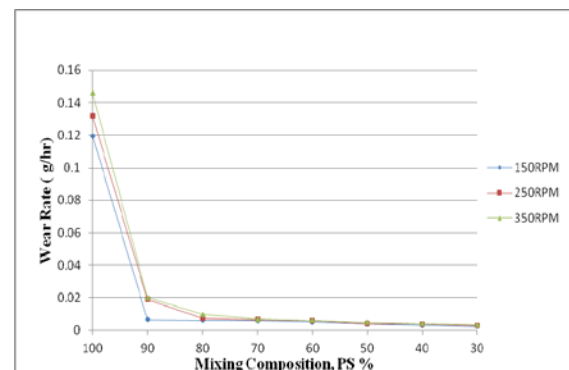


Figure 13. Wear rate at fixed 20 N applied force and velocities of 150, 250 and 350 rpm

The same trend was observed in Figures 14, 15 and 16 which indicate the effect of the load variation for the fixed velocities and different PS content. It is clear that the wear rate for all tested specimens increases with the increase of PS% for the fixed velocity and higher wear rates were obtained after 80% of PS. So, to get best were results, the PS% should be less than 80%. Meanwhile, the effect of the loads at a fixed PS% and Fixed velocity shows that the increase in load increases the wear rate especially when the content of PS exceeds 80% too.

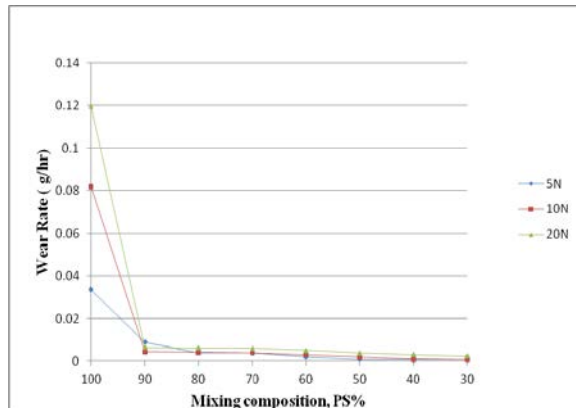


Figure 14. Wear rate at fixed 150 rpm velocity and loads of 5, 10 and 20 N.

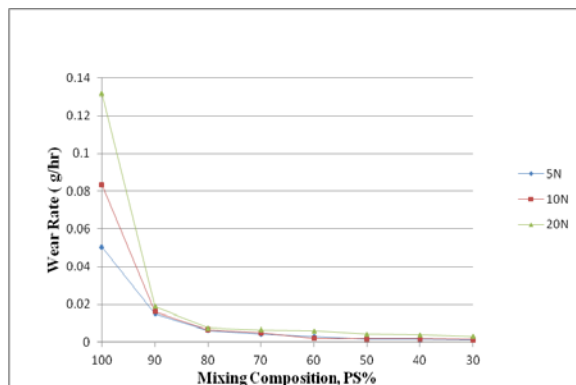


Figure 15. Wear rate at fixed 250 rpm velocity and loads of 5, 10 and 20 N.

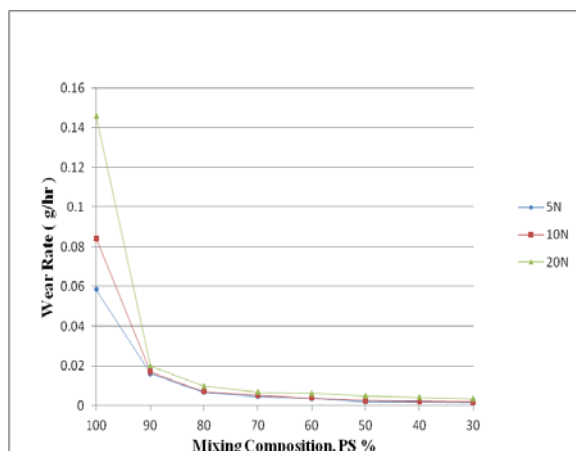


Figure 16. Wear rate at fixed 350 rpm velocity and loads of 5, 10 and 20 N.

It can be also concluded from the figures that the wear resistance of the tested specimens is increased dramatically by adding 10% of bakelite to the mixture, while at higher

percentages than 10% of bakelite the increase in wear resistance was not significant. The reason behind this is that bakelite is a hard material and the cross-linking involves the formation of covalent bonds between the polymer chains and the presence of cross-linked material can have a significant effect on the resulting properties of the material. This is in agreement with Stuart [21] when she explained. Uncross linked material like polystyrene tends to be softer and flexible, while heavily cross-linked polymers tend to be harder and brittle.

3.5. Infrared Thermography Test

Figure 17 shows the relative temperature change (Θ) test results for all tested specimens. It is shown that the relative temperature change of the specimens increases with the increase of the bakelite material in the blend.. Moreover, specimens with higher percentages of bakelite have a higher value of Θ . This behavior is in agreement with heat conductivity change due to a change in the percentages of mixed materials. This may due to the heat conductivity for Bakelite, which is 0.23W/m-°C and for polystyrene, which is 0.13 W/m-°C. Consequently, the material which has higher heat conductivity has a higher value of Θ (specimens which contain higher ratio of high thermal conductivity material will heat faster than those which contain lower ratio) as a results there was a changing in the value of Θ by changing in the composition of manufactured sheets.

From the above results, it is shown that there is a great potential for changing the conductivity of the manufactured sheets and this leads to using them in a various applications that need a certain level of thermal conductivity and insulation properties.

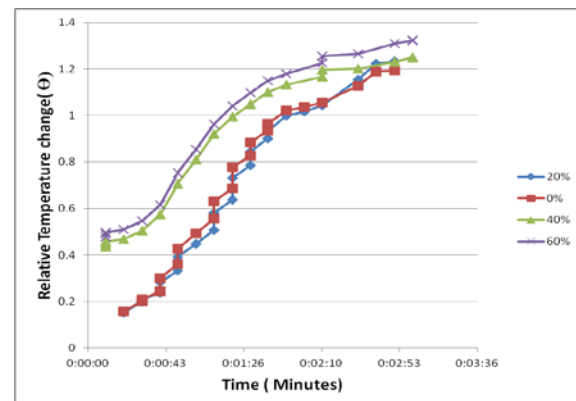


Figure 17. Relative Temperature change.

3.6. Comparison of the results of testing of the Manufactured Sheets and the results of testing of the Commercial Ceramic Tiles

To verify the results of this investigation, commercial ceramic tiles were randomly chosen from the commercial market and subjected to the same tests for comparison purposes.

Wear and water absorption tests were carried out on the ceramic tile at the same testing conditions of the manufactured sheets. Impact test for ceramic tiles was not performed because the sample preparation and testing conditions are totally different between the two materials. Also, according to the Jordanian standards, impact strength

test for ceramic tiles is not required and the testing equipments are not available.

3.6.1. Water Absorption Test Result for Commercial Ceramic Tile

The water absorption percent for the ceramic tile was 10.90% when tested at the same testing conditions of the sheets.

3.6.2. Wear Rate Test Result for Commercial Ceramic Tile

Table 3 Shows the test result at fixed 5, 10 and 20N forces and different velocities 150, 250 and 350RPM.

Table 3. Wear rate test results for the ceramic tile at fixed 5, 10 and 20 N forces and different velocities 150 , 250 and 350 rpm.

Material	Wear Rate (gram/hour) at5N			Wear Rate (gram/hour) at 10N			Wear Rate (gram/hour) at 20N		
	150 RPM	250 RPM	350 RPM	150 RPM	250 RPM	350 RPM	150 RPM	250 RPM	350 RPM
Ceramic Tile	<i>0.0024</i>	<i>0.0027</i>	<i>0.005</i>	<i>0.0024</i>	<i>0.0027</i>	<i>0.0068</i>	<i>0.0028</i>	<i>0.0034</i>	<i>0.0133</i>

Table 4. Wear rate test results for the ceramic tile at fixed 150,250 and 350 rpm velocities and different 5, 10 and 20N forces.

Material	Wear Rate (gram/hour) at 150RPM			Wear Rate (gram/hour) at 250RPM			Wear Rate (gram/hour) at 350RPM		
	5N	10N	20N	5N	10N	20N	5N	10N	20N
Ceramic Tile	<i>0.0024</i>	<i>0.0024</i>	<i>0.0028</i>	<i>0.0027</i>	<i>0.0027</i>	<i>0.0034</i>	<i>0.005</i>	<i>0.0068</i>	<i>0.0133</i>

4. Conclusions

The analysis of the results of the conducted tests led to the following main conclusions:

1. The mixing and manufacturing method helped in achieving a homogeneous distribution and bonding between the mixed materials.
2. The water absorption percent was increased directly by increasing the percent of bakelite material in the blend.
3. The impact strength was almost constant (unsignificant difference) for all mixing compositions because of the similar impact values of the two parents materials and this gave an indication that there was a good bonding between the mixed materials
4. The wear resistance of the manufactured sheets was increased dramatically by adding 10% of bakelite to the mixture, while at higher percentages of bakelite the increase in wear resistance was not significant for all applied forces and velocities.
5. The water absorption percent of the blend was less than the percent of the absorption of the commercial ceramic tiles.
6. The relative temperature change increases with the increase of bakelite in the blend.
7. The wear resistance results of manufactured sheets were close to the results of ceramic tile at (20%) of

Table 4 shows the test result at fixed velocities 150,250 and 350RPM and different applied forces 5, 10 and 20N.

The results in Tables 4 and 5 above were compared to the results of the tested ceramic tile. It was found that the water absorption percent of the manufactured sheets was better than the ceramic tile result. The percent of absorption for the tile was 10.9% and the maximum percent of the manufactured sheets was 0.87%. And wear resistance test results of the manufactured sheets were close to the ceramic tile when the percent of bakelite is 20% at higher bakelite percentages the results were better than those of the tile.

bakelite in the mixture and at higher percent of bakelite the wear resistance became better than that for the ceramic tile.

8. Wear resistance and water absorption tests results of the produced sheets compared to the tested ceramic tile make them of significant interest to the manufacturers to substitute the decoration materials as the later ones are heavy materials and have less potential to change their colors.

References

- [1] Daniel I.M., Hao-Ming H and Shi-Chang W, Failure Mechanics in Thick Composites Under Compression Loading, Journal of composites part B:Engineering, Vol.27, 1996, pp 543-552.
- [2] Lee S.H.and Wass A.M., Compressive Response and Failure of Fiber Reinforced Unidirectional composites, International Journal of Fracture Mechanics, Vol. 100, 1999, pp275-306.
- [3] Jalham Issam S., Jordanian Silica and Cement as a reinforced material for polystyrene matrix composites, journal: Dirasat, Engineering Science, 26 (2), 1999, pp241-250
- [4] Sun CT and Jun AW, Compressive strength of unidirectional fiber composites with matrix nonlinearity, Journal of composites science and technology, Vol.52,1994, pp 577-587
- [5] Akbar Afaghi – Khatibi, lin Ye, and Yiu – Wing Mai, Evaluation of effective crack growth and residual strength of fiber – reinforced metal laminates, Journal of Composite Science and Technology, Vol. 5, 1996, pp 1079-1088

- [6] Abu-Farsakh, G.A., Abdel-Jawad, Y.A., Abu Laila and kh.M., Micromechanical characterization of tensile strength of fiber composite materials, *Journal of mechanics of composite materials and structures*, Vol.7,2000, pp 105-122.
- [7] Mousa A. and Karger-Kocsis, Rheological and Thermodynamical Behavior of Styrene/Butadiene Rubber-Organoclay Nanocomposites, *Journal of macromolecular Material Engineering*, 286 (4), 2001, pp 260-266
- [8] Robinson S.M., Sheridan, M.F., and Ferrardino, The advantages of wollastonite, A Non Traditional Filler in Fluorohydrocarbon elastomers, Presented at meeting of rubber division, American Chemical Society, Savannah, Georgia, 2001.
- [9] Jalham Issam S., The influence of Processing and material parameters on the compressive load capacity of Polystyrene Matrix Reinforced with Jordanian Silica Sand, *Emirates Journal For engineering Research (EJER)*, 8 (2), 2003, pp 21-24.
- [10] Sahnoune F., Cuesta J. M. Lopez and Crespy A., Improvement of the mechanical properties of an HDPE/PS blend by compatibilization and incorporation of CaCO₃, *Journal of Polymer Engineering and Science*, 43(3),2003, pp 647-660
- [11] Chen Zhaobin, Liu Xujun, Lü Renguo and Li Tongsheng, Friction and wear mechanisms of PA66/PPS blend reinforced with carbon fiber, *Journal of Applied Polymer Science*, 105(2), 2007, pp 602-608
- [12] Jalham Issam S., The Influence of Process and Materials Variables on the Surface Properties of Polystyrene Matrix Reinforced with Silica Sand, *Journal of Thermoplastic Composite Materials*, vol. 18, No.6, 2005, pp 529-541
- [13] Friedrich, K., Cyffka, M., On the wear of reinforced thermoplastics by different abrasive papers, *Wear* 103, 1985, p 333-344.
- [14] Friedrich, K., in: K. Friedrich (Ed.), *Friction and wear of polymer Composites*, Composite Materials Series. Vol. 1., Elsevier, Amsterdam Elsevier, Amsterdam, 1986, p 233-237.
- [15] Cirino, M., Friedrich, K., Pipes, R.B., The effect of fiber orientation on the behavior of polymer composite materials, *Wear* 121, 1988, p 127-141.
- [16] Cirino, M., Pipes, R.B., Friedrich, K., The abrasive wear behaviour of continuous fibre polymer composites, *J. Mater. Sci.* 22, 1987, p 2481-2492.
- [17] Jayashree Bijwe, J. Indumathi, J. John Rajesh, and M. Fahim, (2001) "Friction and Wear of Polyetherimide Composites in Various Wear Modes" *Wear*, 249(8), 2001, 715-726.
- [18] Wantinee Viratyaporn, Lehman Richard L., and Joshi Jayant, Impact Resistance of Selected Immiscible Polymer blends. Presented at Society of Plastics Engineers [SPE] Annual Technical Conference Proceedings, OH May Cincinnati, 2007.
- [19] Zhang Huiliang, Sun Shulin, Ren Minqiao, Chen Qingyong, Song Jianbin, Zhang Hongfang, Mo Zhishen, Thermal and mechanical properties of poly(butylene terephthalate)/epoxy blends, *Journal of Applied Polymer Science*, 109(6), 2008, pp 4082-4088
- [20] Campo E. Alfredo, Selection of polymeric material: How to select Design Properties from Different Standards, 1st edition, William Andrews Inc, 2008.
- [21] Stuart Barbara, *Polymer Analysis*, 1st edition, John Wiley and Sons, Ltd, 2002.

Investigating the Applicability of EFQM and KAIIAE in Jordanian Healthcare Organizations: A Case Study

Abdallah Abdallah^{*a}, Ban M. Haddadin^b, Hiba M. Al-Atiyat^b, Leen J. Haddad^b,
Samer L. Al-Sharif^b

^a Talal Abu-Ghazaleh Graduate School of Business (TAGSB) German Jordanian University

Mail Address: P.O. Box 921951 Amman

^b Department of Industrial Engineering, German Jordanian University, Amman, Jordan

Abstract:

This research is set out to analyze the applicability of KAIIAE and EFQM in the Jordanian healthcare organizations. Until 2011, only four Jordanian hospitals applied for the award and only one hospital won it. We chose an elite private Jordanian hospital as a candidate for this research and trained some of its employees on the award's requirements. We then translated the requirements of the award to Arabic and tabulated them into simple Excel sheets. Self-assessment was performed on the entire hospital and the result was a score of 32 out of 100. The score, while seems to be low, is actually high for an organization never considered the award before. The research team put together an action plan that raised the score to 45 or 50 within one year, which is a great score, compared with elite healthcare organizations world wide. This research proves that when simplifying the EFQM requirements and training the hospital personnel, excellence models become very applicable in Jordanian hospitals.

© 2013 Jordan Journal of Mechanical and Industrial Engineering. All rights reserved

Keywords: Healthcare; European Foundation for Quality Management; EFQM; King Abdullah II Award for Excellence; KAIIAE; Accreditation.

1. Introduction

Healthcare organizations worldwide utilize many accreditation systems and excellence models to help achieve high levels of effectiveness and efficiency in their operations. The European Foundation for Quality Management (EFQM) is one example of an excellence model used primarily in all European countries. Many other countries use EFQM in its original format or have its own national version of it. In Jordan, the requirements for King Abdullah II Award for Excellence (KAIIAE), that is applied to private sectors, is identical to that of EFQM. Thus, we will use the terms EFQM and KAIIAE in this report interchangeably.

Numerous European healthcare organizations utilize the EFQM excellence model. In some countries, it is required by law [1]. In Jordan, however, the story is different; KAIIAE receives only 50-60 applications per year from private Jordanian organizations, of which only 2 or 3 are hospitals. In total, only four Jordanian hospitals have applied for the award so far, and one hospital only received the award.

Excellence models initially targeted the manufacturing sector, but slowly found their way to service sectors including healthcare [2]. KAIIAE is not popular for

Jordanian hospitals, as managers find it unimportant since it is not tailored for healthcare. Moreover, EFQM is very generic and does not specifically cover clinical aspects of healthcare institutions [3]. Therefore, Jordanian hospitals focus more on gaining local accreditation from the Healthcare Accreditation Council (HCAC), or international accreditation such that provided by the Joint Commission international (JCI).

In this research, we investigate some reasons behind the lack of applications of EFQM in Jordanian Healthcare organizations, and then we take all the steps necessary for applying it to an elite Jordanian hospital.

1.1. Structure of EFQM Excellence Model

EFQM is a non-profit membership based organization founded in 1988 with the endorsement of the European Commission. The present membership is in excess of 800 European organizations inclusive of healthcare.

EFQM has developed an evaluation approach, termed "Excellence Model" that is implemented via self-assessment. This Excellence Model (2010 version) is made up of 3 parts; The 9 Box Model (Figure 1), The 8 Fundamental Concepts of Excellence, and the RADAR (Figure 2).

* Corresponding author. e-mail: abdallah.abdallah@ju.edu.jo.

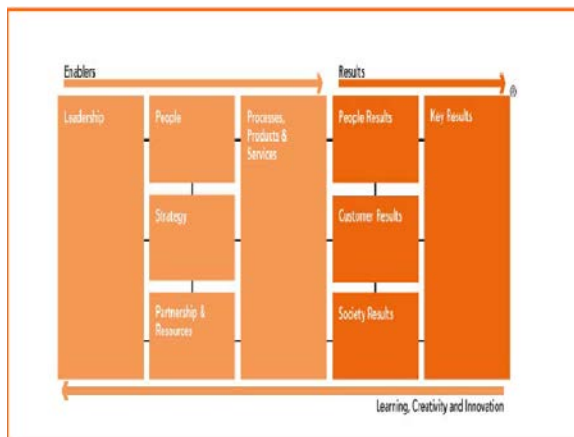


Figure 1. The 9 Box Model

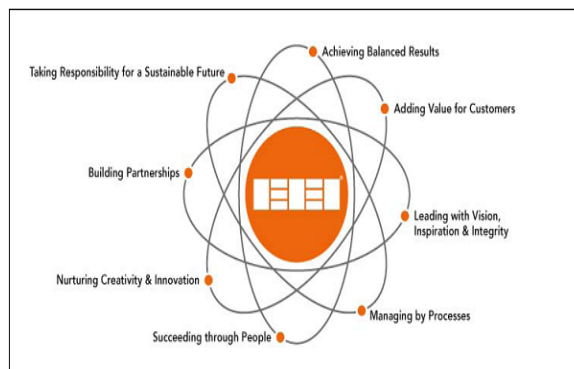


Figure 2. The 8 Fundamental Concepts of Excellence

The 9 Box Model reveals nine criteria classified into two groups: Enablers and Results. Each criterion is divided into few sub criteria, and the final score in a self-assessment is calculated based on the scores of all criteria as shown in Table 1. KAIIE uses the same scoring scheme [4] but each criterion score is divided by 10, which makes the highest possible score in KAIIE 100 instead of 1000.

Table 1. Maximum scores of the 9 criteria

Criteria	Maximum Score
Leadership	10
Strategy	10
People	10
Partnership & Resources	10
Process, Product & services	10
Customer Results	15
People Results	10
Society Results	10
Key Results	15

The fundamental concepts of excellence are basic concepts any institution should develop before applying for the award. They are considered the underlying principles of the EFQM excellence model. These concepts are used to make initial self-assessment to judge the readiness level of the organization to apply for the award.

The RADAR is a measurement tool used to assess and score during the assessment process. It is based on a cycle

of continuous learning and improvement and consists of four elements [5]: Results, Approach, Deployment and Assessment & Review. The application of RADAR logic helps organizations identify, prioritize, plan and implement improvements where needed.

The RADAR logic is considered complex by many assessors. If we add this to the fact that it has to be applied to high number of sub criteria, we will realize how tedious and difficult it is to perform a self-assessment [6].

1.2. King Abdullah II Award for Excellence (KAIIE)

KAIIE is the highest level of recognition of quality in Jordan. It was created to enhance the competitiveness level of Jordanian businesses by promoting quality awareness and performance excellence, recognizing quality and business achievements of Jordanian organizations, and publicizing these organizations' successful performance strategies. The award has shown great success in many organizations that applied for it [7].

For the private sectors, KAIIE uses the exact criteria and sub criteria detailed in the EFQM model. The only difference is the scoring as mentioned in section 1.1.

1.3. Success Drivers and Challenges of Applying for EFQM

EFQM is successful in certain areas where it empowers leaders, increases satisfaction and loyalty of customers, reaches a common sense of purpose throughout the organization, sustains a constant and well managed change, allows employees and stakeholders to be engaged and motivated, establishes an upward flow of ideas and an efficient and effective use of data and operations and lastly produces excellent results, including good financial performance [7].

Most organizations use excellence models as a continuous improvement tool; Goldstein and Schweikhart made that conclusion as a result of studying performance of 220 US hospitals [8]. Other reports also agree with that, especially those studying hospitals in the Basque area (Spain) [9] and in the UK using EFQM [10].

Pakistani healthcare organizations, using excellence models, seem to have higher quality services and enjoy better quality practices [11]. Similarly, in India, many healthcare organizations illustrate successful implementation of various excellence models [12].

EFQM helps Spanish healthcare organizations to create a continuous improvement culture that benefits patients [13]. The article also reveals benefits for staff and key stakeholders. Similar findings are reported in Italy [14].

In Holland, organizations benefit from EFQM by applying it through training and self-assessment before running for the Dutch quality award program. Healthcare organizations, applying this two-step approach, seem to win the Dutch award for Quality in an average of two years [1], which is an indication of successful implementation.

In Germany, healthcare organizations that apply EFQM see noticeable quality improvements [3]. The article, however, highlights some weak aspects of EFQM, such as the general and non-specific nature of the model that does not cover all areas relevant to healthcare. Gómez *et al.* agree with this conclusion and state that EFQM works better in manufacturing

companies than in service organizations such as healthcare [15].

Studying the application of various quality methods including excellence models one may conclude that regardless of the method used, quality success is more related to internal factors than the nature of that method [16]. Similarly, Leggat *et al.* declared that prior to using any such models, healthcare organizations should first focus on enhancing employee skills [17]. As a result, we conclude that excellence models are great tools, but many factors may hinder its application.

In Jordan, The only hospital that won the award is the Specialty Hospital. According to the hospital management, what helped the hospital winning the award is the fact that they were already accredited by HCAC and JCI and received multiple ISO awards before applying for the KAIIE. Most of the documentation required by the award was already enlisted in the policies and practices manuals. Leadership commitment and encouragement of the Specialty Hospital was also an important factor in winning the award.

The hospital faced many challenges, including employees' lack of interest and awareness of the award, the common resistance against learning a new system and due to the employees' current culture which lacked commitment and enthusiasm. The hospital's management revealed, however, that after winning the award such culture gradually improved and employees became more familiar with the terms quality and excellence.

2. Methodology

The methodology used in this research tries to achieve the highest level of success in applying EFQM in a Jordanian healthcare organization, and since very few healthcare institutions applied for it, we found that many preparatory steps had to be performed. The following describes detailed steps of our methodology:

1. Educating the research team on the state of EFQM applicability in Jordanian healthcare organizations. This was achieved by holding many interviews with representatives from the Ministry of Health, King Abdullah II center for excellence, and the only hospital that won the KAIIE in Jordan: Specialty Hospital.
2. Hospital selection: To ensure the highest level of success, we selected a hospital that cares for its performance quality, accredited locally and internationally, yet never attempted to apply for the award.
3. Overcoming the complex nature of EFQM requirements and RADAR scoring scheme: This was a key step to the success of this project. Two major tasks were performed:
 - 3.1. A two-week training program was performed for key employees in the candidate hospital on all details of the award. These trainees were vital for achieving next steps.
 - 3.2. The complex details of the model were translated into an easy-to-use Excel sheet. The sheet was in Arabic language. Each tab in the sheet represents a criterion. The complex RADAR scoring scheme was calculated by Excel without human interference. Figure 3 represents an example of the Excel sheet.

Leadership Criterion							
Sub Criteria							
(1.1) Leaders develop the mission, vision, values and ethics and are role models (20 points)							
Number	Guidance Points	Approach	Deployment	Assessment and Review	Subtotal	Points	Evidence
1/1/1	Leaders establish clear strategic guide lines and unite their employees toward achieving the goals and mission of the organization	50%	100%	0%	50%	1.667	Meeting Minutes
2/1/1	Leaders ensure the future of the institution by defining and delivering the main goal of the existence of the institution which form the basis for the vision, values and work ethics of the organization.	75%	100%	0%	58%	1.934	Orientation process for new employees
3/1/1	Demonstrate a commitment to corporate values and providing a good example of respect, social responsibility, ethical behavior, both internal and external to the organization.	0.00%	0.00%	0.00%	0.00%	0.000	
4/1/1	Support institutional development through shared values, accountability, ethics and culture of the organization, and the culture of trust and openness.	0.00%	0.00%	0.00%	0.00%	0.000	
5/1/1	Ensure staff treated with respect and embrace the highest standards of ethical behavior.	0.00%	0.00%	0.00%	0.00%	0.000	
6/1/1	Creating a culture of shared leadership of the institution, review and develop effective leadership behaviors of individuals	0.00%	0.00%	0.00%	0.00%	0.000	
Total points for Sub criteria		21%	33%	0%	18%	3.61	

Figure 3. Example on the leadership criterion.

The translated Excel sheet is the main stone of this project. The translation minimized the complexity level of the model. The translated sheet was prepared in full agreement with the original EFQM model. Every detail was translated and the score was calculated by using the equations built in Excel.

1. Performing initial assessment of the hospital's performance: In order to judge the readiness of the hospital to apply EFQM, an initial assessment is performed. This assessment is not based on evidence. Rather, it is based on managerial judgment of the level of commitment to the 8 principles of excellence. The hospital needs to score above 25% in this assessment in order to apply for the award. Otherwise, the hospital will be requested to do more basic work in order to bring its score up.
2. Performing a full self-assessment using the Excel sheet produced earlier: This was performed in an accurate method following the exact requirement of EFQM. The score of such assessment represents the level of excellence of the hospital performance.
3. Revealing areas of needed improvements and prioritizing them: the previous step revealed the score in each of the main criteria and sub criteria. Any score, less than a full mark, represents an area of improvement. These areas are prioritized based on their effect on the final score.
4. Designing an action plan to minimize or eliminate performance gaps.
5. Making final recommendations and conclusions for management team.

3. Case Study

The research team spent eight months implementing the prescribed methodology steps. Meeting with representatives from the Ministry of Health and King Abdullah II center of excellence revealed a bleak picture about the applicability of EFQM in Jordanian healthcare organizations. On the other hand, the case of Specialty Hospital represented a success story, largely due to the strong quality inclination of its upper management. Therefore, the team took cautious steps in preparing and encouraging top management of the selected hospital.

Preparation of the Excel sheet was done with two goals in mind: ease of use and automated calculations. This decreased the fear out of the possible users. The sheet was filled in based on data and evidence gathered from all the departments of the hospital. It evaluated strengths and weaknesses (areas for improvement) for each criterion and tabulated as shown in Figure 4.

Strength areas and areas of improvement related to Leadership criterion	
Strength areas	Areas of improvement

Figure 4. Strengths and areas of improvement for each criterion

4. Results and Discussion

4.1. Initial Assessment

This assessment was based on the 8 principles of excellence. The score of the initial assessment was 27/80. This score is above 25%, which is a sufficient indication that the hospital is ready to move to the next step; self-assessment.

4.2. Self-Assessment Scoring

The 9 criteria were analyzed as prescribed by EFQM requirements. For example, the leadership criterion is divided into 5 sub criteria and each sub criterion is divided into a number of activities; let's take the first sub criterion (leaders develop the mission, vision and values and effect and act as role models) as an example. From figure 3, we notice that this sub criterion is divided into 6 activities. Each activity is scored based on 3 scoring tools (Approach, Deployment and Assessment & Refinement) according to the scoring guidelines.

The scoring results of the first activity (set and communicate clear direction and strategic focus; they unite their people in sharing and achieving the organization's core purpose and objectives) are as follows:

1. For the approach, the score is 50% based on the scoring guidelines.
2. For deployment, the score is 100% since the hospital presented comprehensive evidence.
3. For assessment & refinement, the score is 0% since the hospital presented no evidence.

The overall score for this activity is 50% out of the activity overall score or 1.667/3.33.

All other criteria were scored in similar fashion. The overall grade of this self-assessment is 32.4/100. The detailed scores are shown in Table 2 in an ascending manner.

A score of 32.4 out of 100 may seem low, but in fact it is a considerably good score for a hospital in its first self-assessment. To put matters in perspective, most German hospitals score in the mid 20's and some elite German hospitals may score the mid 40's [1].

4.3. Radar Analysis

Figure 5 shows a graphical representation of the criteria's scores; it shows that society results and leadership criteria have the lowest scores; therefore, more attention was paid to these two criteria in order to increase their score.



Figure 5. Radar Analysis

4.4. Cause and Effect

A brain-storming activity and a cause-and-effect diagram were performed to reveal causes of low performance. Figure 6 shows the resulting cause and effect diagram. The figure identifies problems with the overall performance of the hospital. As we can see, the major fish bones that are causing a severe reduction in the hospital performance are: Management, Patients, Strategy and Employees. Finance and Business are two other bones that were considered.

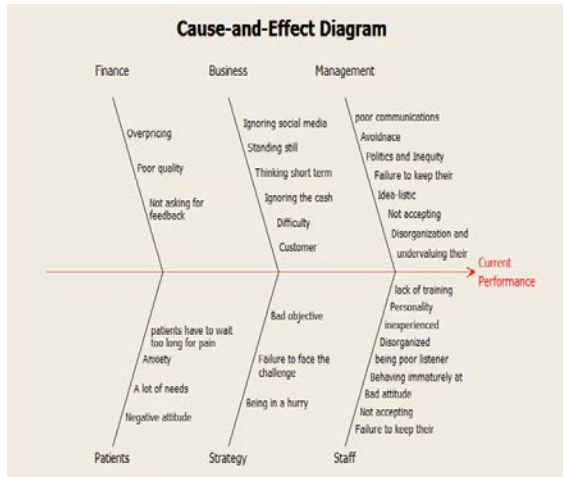


Figure 6. Cause and effect diagram

4.5. Pareto analysis

For all criteria and sub criteria, Pareto chart was conducted to illustrate the gap of the sub criterion to reach the maximum score. Figure 7 shows Pareto chart for leadership. Each column represents the gap of the sub criterion to reach the maximum score. From the chart we conclude that the fifth sub criterion (leaders ensure that the organization is flexible and managers change effectively), the fourth sub criterion (leaders reinforce a culture of excellence with the organization's people) and the first sub criterion (leaders develop the mission, vision, values and ethics and act as role models) are responsible for 80% of the gap. In order to enhance the leadership score, more efforts must be focused on these sub criteria.

Pareto analysis was used for all criteria and was used to prioritize action on these criteria to get the most benefits.

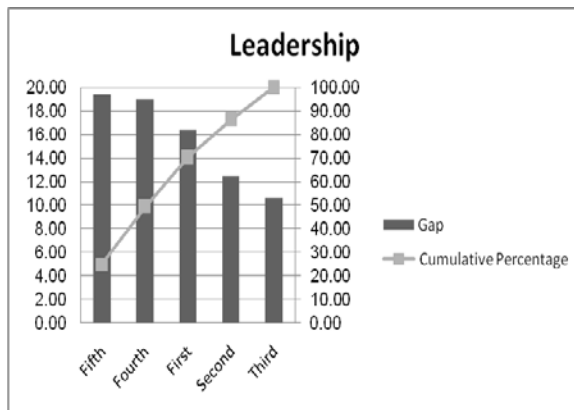


Figure 7. Pareto Analysis for the leadership criterion

4.6. Suggested initiatives

The compiled RADAR analysis, cause and effect diagrams and Pareto analysis for all criteria produced a long list of actions to be performed in order to reach a state of excellence. After meeting with management the team prioritized these actions based on effect and speed of implementation. The team was able to build an action plan that can be implemented within one year and raise the score from 32 to a minimum of 45. In other words, this hospital can join the elite and strongly compete to win the KAIIE within a year time. As an example, let's see some suggested initiatives for the leadership criterion:

1. Managers should create the mission, vision and the strategic values of the hospital required for the long term success and implement these values via appropriate actions and behaviors. They are recommended to be personally involved in ensuring that the *hospital's management system* is created and implemented. (sub criterion 1.1)
2. Management should develop an internal culture of excellence in the hospital and they should personally get involved in ensuring that the *organization's management system* is created, implemented and continuously improved. (sub criterion 1.4)
3. Managers should be more involved through holding monthly meetings for all employees in order to let them express their suggestions and choose the best proposals. (sub criterion 1.5)
4. Managers must use effective communication skills to interact with their customers and external experts at all levels. A process should be established to ensure such activities. (sub criterion 1.5)
5. Managers must act with Integrity and transparency by insuring equal opportunities to all employees and by motivating them to express their innovative ideas and suggestions. A process should be established to ensure such activities. (sub criterion 1.4)

If the suggested improvement initiatives for the leadership criterion are executed, and proven with evidence, the sub criteria score would change as follows:

- The score for sub criterion 1.1 will increase by 2 points.
- The score for sub criterion 1.4 will increase by 4 points.
- The score for sub criterion 1.5 will increase by 6 points.

This will increase the total score by 1.2 points. In similar fashion initiatives for all other criteria were created.

4.6.1. Initiative Scheduling

For each initiative, a schedule (time-line) was created. All schedules were planned to be finished within one year. These action plans represent the starting point of the journey for excellence. Figure 8 shows a Gantt chart, an example for the third leadership suggested initiative. The number of initiatives was high, but the team felt that the initiatives are achievable since the work load is distributed to all departments and personnel of the hospital.

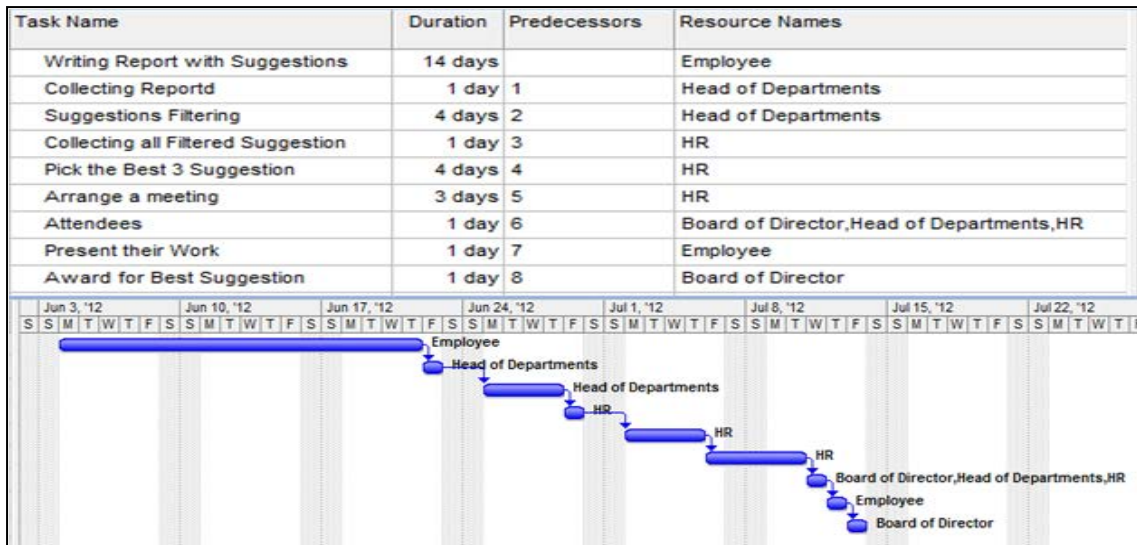


Figure 8. Gantt chart for the leadership criterion

6. Conclusions and Future Work

This research was set out to study the applicability of excellence models in the Jordanian healthcare sector. Working with an elite Jordanian hospital revealed that the upper management had their heart in the right place considering the quality of their services; however, they lacked a rigorous approach to their policies and standards. Most of the actions tackled by different departments are not documented or addressed properly. This affected the hospital's score badly even though it is a simple issue to fix.

After applying the self-assessment tool in many departments, the total score was 32.4/100 which is a good score considering there is no approach in most of the policies set in the hospital. Note that very few hospitals in Europe score up to 750 out of 1000. Therefore, when the proposed initiatives are implemented and yet more work is done by the hospital, it will be able within few years to compete internationally with the finest hospitals in Europe.

The fact that the candidate hospital is already accredited, both locally and internationally, helped in preparing the overall strategy plan of the hospital. This clearly shows that accreditations are in fact the starting steps in the process to reach excellence in hospitals.

The training activity and the creation of the Excel sheet were two key reasons for the success seen in this project. Performing these two tasks took the fear out of quality employees at the hospital. It also simplified the complex requirements of EFQM.

After various visits to the hospital, meetings with the upper management and different department heads and analysis of the current state of the hospital according to the KAIIE standards, we concluded that KAIIE and EFQM are very applicable at Jordanian hospitals. There is no dispute that both excellence models are not in fact tailored for healthcare services; however, they offer a valuable help in creating a continuously improved culture, where a work environment in which employees are able to use their skills is being built, an increase in awareness of quality and excellence and effective communications are seen. This will lead to better processes, resulting in better

service thus higher customer satisfaction and eventually greater revenues.

The main conclusion that is drawn by this study is that EFQM and KAIIE may be applied and won by Jordanian healthcare organizations with the help of proper training and simplification of the award's requirements. Another important conclusion is that EFQM and KAIIE award are used as assessment tools but they do not guarantee excellence. They just reveal performance gaps.

Future work may focus on similar cases to further discuss the applicability of such models. It can also reveal challenges not seen in this research. One area that can extend this research contribution is creating easy-to-use software based on the Excel sheet created in this research. People tend to interact better with a software package than an Excel sheet. User-friendly software, in Arabic, may make excellence models more popular in Jordan and the region.

References

- [1] U. Nabitz, N. Klazinga, J. Walburg, "The EFQM excellence model: European and Dutch experience with the EFQM approach in health care". *International Journal for Quality in Health Care*, Vol. 12, No. 3, 2000, 191-202.
- [2] J.G. Badia, G.J. Solà, E.P. Rodríguez, J. C. Segura, C.M. Molins, "The EFQM excellence model is useful for primary health care teams". *Family Practice*, Vol.18, No. 4, 2001, 407-409.
- [3] J. Moeller, "The EFQM Excellence Model. German experience with the EFQM approach in health care". *International Journal for Quality in Health Care*, Vol. 13, No. 1, 2001, 45-49.
- [4] Z. Abu-Hamattah, T. Al-Azab, M. El-Amyan, "Total quality management achievement: King Abdullah II Award for Excellence of Jordan as a model". *Technovation*, Vol. 23, No. 1, 2003, 649-652.
- [5] J. Moeller, A.K. Sonntag, "Evaluation of health services organizations—German experiences with the EFQM excellence approach in healthcare". *The TQM Magazine*, Vol. 13, No. 5, 2007, 361-367.

- [6] I.A. Rawabdeh, "Jordan Quality Award (King Abdullah II Award for Excellence (KAIIE)): Characteristics, assessment and benchmarking". *Benchmarking: An International Journal*, Vol. 15, No. 1, 2008, 4–24.
- [7] A. Al-Refaie, O. Ghnaimat, M.H. Li, "Effects of ISO 9001 Certification and KAAE on Performance of Jordanian Firms". *Jordan Journal of Mechanical and Industrial Engineering*, Vol. 6, No. 1, 2012, 45-53.
- [8] S.M. Goldstein, S.B. Schweikhart, "Empirical Support for the Baldrige Award Framework in U.S. Hospitals". *Health Care Management Review*, Vol. 27, No. 1, 2002, 62-75.
- [9] A. Arcelay, E. Sánchez, L. Hernández, G. Inclán, M. Bacigalupe, J. Letona, R.M. González, A.E. Martínez-Conde, "Self-assessment of all the health centres of a public health service through the European Model of Total Quality Management". *International Journal of Health Care Quality Assurance*, Vol. 12, No. 2, 1999, 54–59.
- [10] G. Naylor, "Using the Business Excellence Model to develop a strategy for a healthcare organization". *International Journal of Health Care Quality Assurance*, Vol. 12, No. 2, 1999, 37–45.
- [11] F. Vakani, Z. Fatmi, K. Naqvi, "Three-level quality assessment of a dental hospital using EFQM". *International Journal of Health Care Quality Assurance*, Vol. 24, No. 8, 2011, 582–591.
- [12] M. Palani, N. Raja, S.G. Deshmukh, S. Wadhwa, "Quality award dimensions: a strategic instrument for measuring health service quality". *International Journal of Health Care Quality Assurance*, Vol. 20, No. 5, 2007, 363–378.
- [13] S. Jackson, R. Bircher, "Transforming a run down general practice into a leading edge primary care organization with the help of the EFQM excellence model". *International Journal of Health Care Quality Assurance*, Vol. 15, No. 6, 2002, 255–267.
- [14] S. Venero, U. Nabitiz, G. Bragonzi, A. Rebelli, R. Molinari, "A two-level EFQM self-assessment in an Italian hospital". *International Journal of Health Care Quality Assurance*, Vol. 20, No. 3, 2007, 215–231.
- [15] J.G. Gómez, M.M. Costa, Á.R.M. Lorente, "A critical evaluation of the EFQM mode". *International Journal of Quality & Reliability Management*, Vol. 28, No. 5, 2011, 484–502.
- [16] J.A. Alexander, L.R. Hearld, H.J. Jiang, I. Fraser, "Increasing the relevance of research to health care managers: Hospital CEO imperatives for improving quality and lowering costs". *Health Care Management Review*, Vol. 32, No. 2, 2007, 150-159.
- [17] S. G. Leggat, T. Bartram, P. Stanton, "High performance work systems: the gap between policy and practice in health care reform". *Journal of Health Organization and Management*, Vol. 25, No. 3, 2011, 281–297.

Understanding the Linkage between Soft and Hard Total Quality Management: Evidence from Malaysian Manufacturing Industries

Amjad Al-Khalili^{*,a} and Khairanum Subari^b

^a Department of Planning, Studies and Projects Palestine Technical University / Kadoorie (PTUK) Tulkarm, Yaffa Street,
West Bank, P.O. Box 7, Palestine

^b Student Development and Campus Lifestyle, University Kuala Lumpur, Kuala Lumpur, Malaysia Level 3, 1016,
Jalan Sultan Ismail, 50250 Kuala Lumpur, Malaysia

Abstract:

This paper investigates the linkage between TQM two dimensions, namely Soft (ST) and Hard (HT). Few empirical studies examined the interrelatedness between these dimensions especially in the developing economy of Malaysia. Thus, the paper proposed a theoretical multidimensional integrated framework in order to examine the link between TQM dimensions. Seven variables were used to measure ST and Eight variables used for HT. the hypothesis of the study is that there is a significant and positive relationship between the two dimensions. To show the validity of the proposed model, it was tested in 40 ISO 9000 certified Malaysian manufacturing industries. To test the hypothesis, a structured self-administrated questionnaire was developed. It is based on the common five point likert scale for quality management for all the items included in the survey. The multiple regression analysis was used in order to test the corollary hypotheses, utilized from the statistical package for social science. Data analysis indicated: [1] the instrument was valid and reliable; [2] the results supported the proposed theoretical framework; [3] there is a significant and positive link between ST and HT such that they could be linked and integrated together in the same framework if they are implemented and practiced correctly by the quality and production managers; and [4] Malaysian managers have awareness to ST and HT. Results showed that All seven variables of ST were significantly associated with some HT variables. This paper contributes to quality management by: [1] theoretically proposing and empirically investigating the theoretical framework; [2] examining the integration between TQM two dimensions; [3] using the multidimensionality of ST and HT; and [4] the application of this study in the developing economy of Malaysia. It is concluded that ST and HT can be integrated together, the relationship was supported and that Malaysian quality managers can utilize these dimensions if implemented and practiced correctly. This paper provides essential guidelines for Malaysian managers dealing with quality management inside organizations.

© 2013 Jordan Journal of Mechanical and Industrial Engineering. All rights reserved

Key words: Integration; ST; HT; Multidimensional; Questionnaire.

1. Introduction

According to Islam and Haque [10], the definition of TQM is a source of confusion, and there is no consensus on what constitutes TQM. Abdullah and Tari [1] indicated that there is a disagreement about what constitutes the ST and HT elements of quality management. Implementing TQM involves defining and deploying several key elements or factors [26]. Review of TQM literature showed that the key elements of TQM could be classified as "ST" and "HT" quality factors. Both the "hard" practices (such as measurement and analysis, systematic planning, fact-based decision making), and the "soft" practices - or the humanistic factors- (such as visioning

and establishing organization values, recognition of individual and group behavior, empowering workers, teamwork and consensual decision-making) have a mechanism for systematically reexamining and reinforcing their understanding of type especially when organizations put a TQM effort in place [11].

According to Hellsten and Klefsjo [8], TQM is much more than a number of critical factors; it also included other components such as tools and techniques for quality improvement, which is consistent with the view of [24]. Bunny and Dale [4] considered TQM tools and techniques vital to support and develop the quality improvement process. Different views and opinions showed that there were many reasons behind that. The first is from the quality gurus, who often are seen as fathers of TQM do not

* Corresponding author. e-mail: amjad_alkhalili@yahoo.com.

like TQM concept. Another one is that there are several similar names for roughly the same TQM idea. The third, which is probably the most severe one, is that there are many vague descriptions and few definitions of what TQM really is; hence, these reasons are partly related to each other [8]. Based on Evans and Lindsay [6], TQM philosophy consists of two related components: The first one is the management system; the second is the technical system. The management system is concerned with planning, organizing, controlling, and managing human resource processes as they relate to quality products or services. In other words, it is an aspect of ST. On the other hand, the technical system involves the assurance of quality in product design, the planning and design of manufacturing processes, and the controlling of incoming materials, intermediate production and finished goods, in other words, it is aspects of HT. Although these two systems, namely ST and HT, deal with different aspects of quality, they are tightly intertwined and integral to the TQM philosophy, and, therefore, cannot function independently. For instance, the application of statistical methods in improving product quality cannot be successful without management support, employee involvement and teamwork, which are all instilled by a proper management system. As a result, the management system supports the installation of a technical system; in other words, ST supports the use and utilization of HT elements. The view of [28] is that TQM is based on the premise that all activities in a firm contribute to quality. Categories of TQM are the so-called HT and ST aspects. Thus, TQM contributes to both production oriented and employee relations oriented elements.

In sum, ST aspects are the soft dimensions of total quality management. According to Zairi and Baidoun [29], they could be characterized by:

- long-term nature;
- something cannot be switched on and off;
- must be addressed accordingly in the implementation plan;
- intangible factors;
- difficult to measure quality factors;
- initial inputs to the implementation of TQM;
- humanistic factors (people aspects); and
- tacit and behavioral resources [16]

On the other hand, according to Zairi and Baidoun [30], the hard aspects of TQM can be characterized by:

- impact the internal efficiency of the organization;
- focus on TQM tools and techniques, systems, processes
- Considered as tactics rather than strategies;
- utilizes quantitative (technical) methods; and
- the emphasis on the hard aspects reflects the production orientation of the TQM gurus [27].

With reference to the above matters, there is no clear consensus concerning ST and HT content, and this is due to some factors being regarded as ST by some authors and HT by others [31]. Due to these reasons, the purpose of this paper is to introduce the relationship between the two dimensions of TQM, namely, ST and HT, and thus, it will investigate the linkage between them in the developing economy of Malaysia. The ultimate goal of this paper is to answer the following main question:

Is there is any link between ST and HT?

The following sections start with reviewing the literature of ST and HT, proposing the theoretical framework, and empirically testing the hypothesis. The last sections are concerned with data analysis, results, implications and conclusions.

2. Literature Review

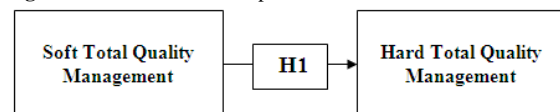
2.1. Theoretical Framework and Study Proposition

To fill the gap concerning the nature of relationship between ST and HT, an empirical study was designed to unravel the gap by testing the relationship between the two main TQM dimensions (ST, HT). To guide the direction of the analysis and test the study hypothesis, a multidimensional theoretical framework was proposed. It was derived from a recent study in quality management area [18], aimed at contrasting the different factors of ST and elements of HT. This study was built based on the suggestion of Rahman and Bullock [18] that:

- ST elements has a direct role on the utilization of HT elements inside organizations; and
- successful organizations are those that apply a combination of ST and HT policies to respond to changing customer requirements.

Hence, the proposed theoretical framework for this study is illustrated in Figure1

Figure1. The Theoretical Proposed Framework.



Source: Rahman and Bullock [18]

Based on the proposed theoretical framework, the main hypothesis of this study reads as follows:

H1: *There is a significant and positive relationship between ST aspects and HT Variables*

Main variables of the study

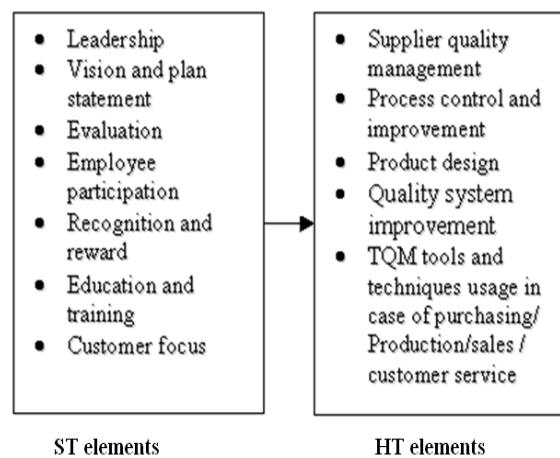


Figure2. Schematic Presentation of the Theoretical Framework

Tata *et al.* [25] recommended using pre-tested constructs from past empirical studies to ensure their validity and reliability. The variables of ST and HT in this

study were mainly adopted from [32], [4], and [14]. Most of the variables included in the questionnaire were based on Zhang *et al.* [32] instrument; this can be justified as: (1) According to [32], the instrument has unique characteristics in that it covers a broader scope of TQM in comparison with other instruments developed by other researchers (Ahire *et al.* [2]); (2) the instrument is integrated to a certain extent in the constructs of many researchers (Saraph *et al.* [19]; Flynn *et al.* [7]; Ahire *et al.* [2]), and this is what researchers recommended to use in future research, a blending of instruments which should yield highly stable, reliable and valid constructs of quality management; (3) it included constructs which were not found in other instruments (i.e., vision and plan statement); (4) it clearly separated the aspects of soft and HT, where most of the variables included are consistent with the literature; (5) researchers can use it because it is empirically tested and validated and can generally be used in different countries since it is developed on the basis of an extensive review of TQM literature [32]; (6) industrial practitioners and managers will also be able to use this instrument to evaluate their TQM implementation so as to target improvement areas and to identify problem areas that should be improved; (7) it described the primary quality management methods, which may be used to assess an organization's present strength and weaknesses with regard to its use of quality management methods [32]; (8) it covered the basic essential elements of all definitions of TQM, which are: the continuous process improvement, people orientation, quantitative methods, and customer focus, which cover both the soft and hard aspects of TQM in a clear picture;. (9) it is valid and reliable and has the highest external validity when it is compared to other instruments such as [19] and the instrument used for testing of its validity and reliability in nine industrial sectors for large sample size; and (10) it included dimensions from the most important models of MBNQA and EFQM.

3. Method

Since the primary objective of this study is to examine relationship, rather than developing new constructs, it used pre tested constructs from past empirical studies. A cross sectional mail survey was developed, consisting of two parts, which relate to the variables ST and HT. The five point likert scale was used for all the items of the questionnaire. The variables, included in the survey, are as described in (Figure 2). To establish the validity and reliability of the questionnaire, two steps were followed. First, a panel of experts evaluated the questionnaire. Based on their suggestions, some items were changed. Second, the revised questionnaire was piloted with 40 ISO 9000 certified Malaysian companies; the data collected from the pilot test were coded and analyzed using the statistical

software (SPSS) to find any unanticipated difficulties, and no significant problems were found. Cronbach's alpha was used to determine the internal consistency of the instrument. All scales were highly reliable and consistent. Then, the proposed theoretical framework was tested in 250 ISO 9000 certified Malaysian manufacturing companies, selected randomly from SIRIM directory [21], which encompassed various industries to generalize the results. The unit of analysis is the manufacturing company. To encourage the respondents to complete and return the questionnaire, several efforts, such as a telephone follow up campaign, a reminder letter, and pre-paid attached postage envelope, were made. A total of 87 companies responded to the postal survey, 8 of them were discarded since they are not completed. The total number of questionnaires accepted for analysis was 79. The final response rate accounted for 32 %, which is considered acceptable when compared with those experienced by others, conducting similar surveys. This can be justified as a considerable success with Malaysian companies and is higher than the suggested minimum in Malhotra and Grover [12], which is 20 percent.

4. Results and Analysis

Testing the hypotheses.

Two steps were followed in order to test the main hypothesis of this study. The first step is the correlation analysis, while the second is the multiple regression technique, which utilized from SPSS.

4.1. Correlation Analysis

Correlation between ST elements

Table 1. Correlation between ST elements (values of r, at p less than.)

0	ST1	ST2	ST3	ST4	ST5	ST6	ST7
ST1	1						
ST2	.78**	1					
ST3	.65**	.62**	1				
ST4	.34**	.34**	.55**	1			
ST5	.23**	.29**	.48**	.31**	1		
ST6	.25**	.28*	.47**	.28*	.13	1	
ST7	.38**	.39**	.55**	.27*	.23*	.76**	1

** Correlation is significant at 0.01 level (2-tailed)

Results show that all ST elements were positively and significantly correlated with each other, except for the correlation between ST5 and ST6. Thus, relationships are as hypothesized.

Correlation between HT Elements

The correlation between HT elements is depicted in Table 2

Table 2. Correlation between HT elements (values of r, at p less than.)

	HT 1	HT 2	HT 3	HT 4	HT 5	HT 6	HT 7	HT 8
HT 1	1							
HT 2	.62**	1						
HT 3	.56**	.84**	1					
HT 4	.56**	.67**	.74**	1				
HT 5	.55**	.67**	.64**	.60**	1			
HT 6	.57**	.57**	.56**	.59**	.81**	1		
HT 7	.47**	.45**	.45**	.49**	.58**	.61**	1	
HT 8	.77**	.62**	.60**	.59**	.49**	.46**	.64**	1

** Correlation is significant at 0.01 level (2-tailed)

Results show that all HT elements were positively and significantly correlated with each other. Thus, relationships are as hypothesized.

Inter item correlation between ST and HT elements

The correlation between the dimensions of ST and HT is depicted in Table 3

Table 3. Correlation between ST and HT elements (Values of r, at p less than.)

	ST 1	ST 2	ST 3	ST 4	ST 5	ST 6	ST 7
HT1	.53**	.55**	.57**	.29**	.17	.48**	.58**
HT2	.49**	.60**	.55**	.16	.14	.47**	.62**
HT3	.54**	.56**	.51**	.22	.19	.47**	.57**
HT4	.50**	.55**	.55**	.33**	.18	.46**	.58**
HT5	.72**	.78**	.62**	.33**	.18	.33**	.47**
HT6	.93**	.91**	.65**	.33**	.24*	.25*	.39**
HT7	.61**	.62**	.89**	.82**	.52**	.45**	.49**
HT8	.45**	.48**	.70**	.39**	.45**	.81**	.82**

** Correlation is significant at 0.01 level (2-tailed).

Table 3 indicated that the dimensions of ST are significantly and positively correlated with HT variables, except for the association between ST5 and (HT1, HT2, HT3, HT4, HT5) and the association between ST4 and (HT2, HT3).

Multiple Regression Analysis

The proposed theoretical framework in this study was multidimensional; hence multiple regression analysis is the best technique for analysis of the multi corollary

hypotheses. Eight multiple regression analyses were conducted in order to assess the relationships between the elements of ST and HT.

The main hypothesis of this study reads as:

H1: There is a significant and positive relationship between ST aspects and HT variables.

Testing of this hypothesis requires postulating 8 different corollary hypotheses; these are:

- H1A: Soft total quality management is positively associated with supplier quality management
- H1B: Soft total quality management is positively associated with process control and improvement
- H1C: Soft total quality management is positively associated with product design.
- H1D: Soft total quality management is positively associated with quality system improvement
- H1E: Soft total quality management is positively associated with total quality management tools and techniques usage in purchasing
- H1F: Soft total quality management is positively associated with total quality management tools and techniques/ production.
- H1G: Soft total quality management is positively associated with total quality management tools and techniques/ sales.
- H1H: Soft total quality management is positively associated with total quality management tools and techniques/ customer service

A detailed explanation of all corollary hypotheses in this study was depicted in appendix A. Eight multiple regression analyses were conducted in order to assess the relationships between the elements of ST and HT. The seven elements of ST were regressed on the eight variables of HT in order to shed light on the association between ST elements and every variable in HT. It is a detailed data analysis that aimed at exploring which elements of ST associated with HT variables. In other words, to examine the utilization of ST into HT. The results of the data analysis summarized in Tables 4 and 5.

Table 4. Effect of ST on HT

R	R ²	Adjust R ²	F	Coefficient
.878	.771	.768	(=255.329, p <0.05)	(β=. 878, p<0.05)

Table 4 indicated that ST and HT, as general constructs, were positively and significantly associated. The detailed data analysis of the elements of ST and HT is depicted in Table 5.

Table 5. The Results of Multiple Regression Analysis of ST to HT. (The values indicated are beta coefficients)

Variables	HT1	HT2	HT3	HT4	HT5	HT6	HT7	HT8
ST1	.09	-.115	.16	.029	.182**	.525*	.009	.019
ST2	.256**	.449*	.28*	.298*	.54*	.493*	.099*	.054
ST3	.226	.302*	.043	.145	.19**	.042	.519*	.160*
ST4	-.01	-.181**	-.070	.062	.015	-.012	.468*	.004
ST5	-.089	-.142	-.010	-.086	-.110	-.025	.088*	.23*
ST6	.13	-.011	.125	.037	-.105	-.043	.039	.46*
ST7	.20	.408*	.30*	.348*	.173**	.036	-.013	.30*
R	.691	.760	.699	.695	.853	.983	.988	.935
R ²	.477	.577	.489	.483	.73	.965	.975	.874
Adjust R ²	.425	.536	.438	.432	.70	.962	.973	.861
F	9.253*	13.85*	9.69*	9.48*	26.69*	279.56*	400.8*	70.24*

Note: Significant levels: * $p < 0.05$; ** $p < 0.10$

With reference to Table 5, it is found that ST1 positively and significantly associated with HT5 ($\beta = .182$, $p < 0.10$) and HT6 ($\beta = .525$, $p < 0.05$), thus, H4E1, H4F1 were supported. ST2 found significantly and positively associated with seven variables of HT, except HT8, namely, HT1 ($\beta = .256$, $p < 0.10$), HT2 ($\beta = .449$, $p < 0.05$), HT3 ($\beta = .28$, $p < 0.05$), HT4 ($\beta = .298$, $p < 0.05$), HT5 ($\beta = .54$, $p < 0.05$), HT6 ($\beta = .493$, $p < 0.05$), and HT7 ($\beta = .099$, $p < 0.05$), hence, H4A2, H4B2, H4C2, H4D2, H4E2, H4F2, H4G2 were supported.

Findings also revealed that ST3, ST7 and ST4 were significantly associated with HT2. Both ST3 ($\beta = .302$, $p < 0.05$) and ST7 ($\beta = .408$, $p < 0.05$) were positively associated, while ST4 ($\beta = -.181$, $p < 0.10$) was negatively associated; thus, H4B3, H4B7 were supported and H4B4 were rejected since it is negatively associated. In addition, both (ST3 and ST7) are found to be positively and significantly associated with HT5 and HT8, thus, hypotheses H4E3, H4E7, H4H3, H4H7 were supported. In addition to ST2, three dimensions of ST, namely, ST3 ($\beta = .519$, $p < 0.05$), ST4 ($\beta = .468$, $p < 0.05$), and ST5 ($\beta = .088$, $p < 0.05$) were found to be positively and significantly associated with HT7, thus, H4G3, H4G4, H4G5 were supported.

ST5 ($\beta = .23$, $p < 0.05$) and ST6 ($\beta = .46$, $p < 0.05$) were found to be positively and significantly associated with HT8, thus, H4H5, H4H6 were supported.

Lastly, ST7 is found to be positively and significantly associated with HT3 ($\beta = .30$, $p < 0.05$), and HT4 ($\beta = .348$, $p < 0.05$), thus, H4C7, H4D7 were supported. Summary of the rejected hypotheses were depicted in Appendix 1

5. Discussion

TQM is a philosophy for continuous improvement. It has two dimensions, namely ST, which focuses on the humanistic aspects, and HT, which focuses on TQM tools and techniques, processes and systems Al-Khalili *et al.* [3].

This study revealed that the relationship between ST and HT was supported. All seven variables of ST were significantly associated with some HT variables. The positive and significant relationship between ST1 and two variables of HT; the positive and significant relationship between ST2 and seven variables of HT; the positive and significant relationship between ST3 and three dimensions of HT; the positive and negative relationship between ST4 and two variables of HT; the positive and significant relationship between ST5 and two variables of HT; the positive and significant relationship between ST6 and one variable of HT; the positive and significant relationship between ST7 and five variables of HT. These significant relationships indicated that Malaysian manufacturing companies have the capability to integrate TQM two sides, namely, ST and HT and, thus, can be more profitable through the implementation and practices of two TQM sides.

Findings in investigation of this relationship (ST – HT) in this study were in line with [18] in their survey in the Australian manufacturing companies; [18] found a significant positive relationship between ST and HT elements. Thus, findings explained that some ST variables have an impact on the diffusion and utilization of HT in Malaysian Manufacturing companies; in other words, findings supported the proposed framework explained in this study and provided evidence that successful organizations are those that apply a combination of ST and HT practices and policies to respond to changing customer satisfaction.

The multidimensionality of some variables also supported, which is consistent with the suggestion by a number of scholars, especially the multidimensionality of TQM ([5]; [23]; [22]).

Figure 3: MBNQA Seven Criteria for Excellent Performance

Source:[On line]

http://www.quality4results.com/enterprise_models_baldrige.php.



Figure 3. MBNQA model [13]

MBNQA model supported the claim that there is an association between the two sides of TQM; the model assumed that there is a link between human resources focus (ST dimension) and process management (HT) from one side, and between them and the performance (business results) from the other side. Findings of this study are also in line with this model, namely MBNQA (Figure 3), where ST7 (customer focus), ST4 (employee participation), which are human resources aspects, in other words, people aspects, have a significant relationship with HT2 (process control and improvement). This means that ST has a direct effect on HT. This, hence, supported the MBNQA model, and also the proposed theoretical framework in this study that ST has direct effect on HT.

The previous support linked the theory as depicted in Figure 1 with the empirical findings of this study regarding the relationship between ST and HT. Furthermore, the existence of a relationship between ST and HT in this study supported Sashkin and Kiser's [20] claim that TQM works when people use basic statistical tools (or HT) and behavioral techniques to account or to collect data in order to analyze and solve problems. In summary, this study found support that there was a positive and significant relationship between the two sides of TQM, especially in the important foundations of TQM which are: (1) tools and techniques that people are trained to use to identify and solve quality programs; and (2) customer as the focus of TQM [20]. This study was consistent with Hung [9] that both ST and HT were the key concepts for successful implementation of TQM, and consistent with Prajogo and Sohal [17] where they verified the proposition that both mechanistic (HT),

and organic (ST) types of practices could coexist under the umbrella of TQM; hence this study supported the multidimensionality of TQM similar to research of Prajogo and Sohal [17].

6. Recommendations for Future Research

Recommendations for future research would address the issues generated from this study. Based on the findings of this empirical study, future research may start from a relatively higher level of knowledge.

Research focusing on the two dimensions of TQM is relatively new. The perspectives are: (a) the effectiveness with which ST and HT practices are implemented. This issue deals with the role of manufacturing companies' top managers, and the quality managers in enhancing the practicing of the two dimensions; and (b) the effectiveness of these practices in producing desired results and their contribution to the performance. Few studies focused on these two issues together to date. The study in the Australian companies by Rahman and Bullock [18] was probably the only study to date examining these issues together. The present study investigated these two dimensions, namely, ST and HT, in the Malaysian industries with different variables. Other researchers are encouraged to do the same in other sectors and firms in other developing and developed countries.

7. Conclusion

This paper investigates the relationship between ST and HT. It attempts to clarify the basics and dimensions of ST and HT found in the literature. The study primary data were gathered using the postal survey; results of this proposition were tested using the multiple regression analysis and supported the proposed framework, hence, ST and HT aspects could be linked and integrated together in the same framework if they are implemented and practiced correctly by the quality and production managers. The importance and usefulness of this paper comes from different aspects. First, it focused on TQM two main dimensions and investigated empirically their linkage in a multidimensional framework. Second, it dealt with quality tools and techniques in depth which are considered as an important element for HT. Moreover, the variables used in this paper were consistent with MBNQA model such as leadership and customer focus (ST elements) and Process management and control which is (HT element). This paper is consistent with Mustafa and Bon's [15] conclusions that the majority of studies agreed that top management leadership and commitment, considered as ST elements, has a crucial role in TQM implementation.

Acknowledgements

Authors of this paper are very grateful to the editor in chief, Prof. Nabil Anagreh and the blind reviewers for

useful comments and suggestions that improved this version of the paper.

References

- [1] M.M .Abdullah, J.J. Tari, "The influence of ST and HT quality management practices on performance". Asian pacific management review, Vol.17, No. 2, 2012, 177-193.
- [2] S.L. Ahire, D.Y.Golhar, M.A. Waller , "Development and Validation of TQM implementation constructs", Decision Sciences, Vol.27, No. 1, 1996a, 23-56.
- [3] A.M. Al khalili, K.Subari, Kamaruddin,S, "Relationships between ISO 9000, ST, HT and Malaysian industries' manufacturing performance: an empirical study", Proceedings of the 4th Mechanical Engineering Research Colloquium (MERC 2005/ I), School of Mechanical Engineering, USM, Penang, Malaysia, 27-29 January, 2005, 184-192.
- [4] H.S. Bunny, B.G. Dale, "The implementation of quality management tools and techniques: A study", The TQM Magazine, Vol.9, No.3, 1997, 183-189.
- [5] J.W.Jr. Dean, D.E. Bowen, "Management theory and total quality: Improving research and practice through theory development", Academy of Management Review, Vol.19, No. 3, 1994, 392-418.
- [6] J.R. Evans, W.M.Lindsay The management and control of quality, Cincinnati, OH. South – western college publishing, 1999
- [7] B.B.Flynn, R.G.Schroeder, S.Sakakibara, "A framework for quality management research and an associated measurement instrument", Journal of Operations Management, Vol.11, No. 4, 1994, 339-366
- [8] U. Hellsten, B. Klefsjo "TQM as a management system consisting of values, techniques and tools", The TQM Magazine, Vol.12, No.4, 2000, 238-244
- [9] R.Y.Y. Hung "The implementation of Total Quality Management Strategy in Australia: Some Empirical Observations", Journal of American Academy of Business, Cambridge, Vol. 5, No. 1/2, 2004, 70-74.
- [10] M.A. Islam , A.F.M.A. Haque "Pillars of TQM implementation in manufacturing organization- An empirical study", Journal of Research in international business and management, Vol.2, No.5 ,2012, 128-141
- [11] F.L.Lewis "Type and Total quality management. Association for psychological type. The electronic college of process innovation. [On line]. [Accessed 15 th May2004]. Available from World Wide Web: <http://www.defenselink.mil/nii/bpr/bprcd/5555.htm>., 1993
- [12] M.K.Malhotra , V. Grover, "An assessment of survey research in POM: from constructs to theory", Journal of Operations Management, Vol.16, 1998, 407-425
- [13] MBNQA Seven Criteria for Excellence Performance. [On line] [Accessed 12th December 2004]. Available from World Wide Web: http://www.quality4results.com/enterprise_models_baldrige.php
- [14] R.E. Mc Quarter, C.H. Scurr, B.G.Dale, P.G. Hillman,"Using quality tools and techniques successfully", The TQM Magazine, Vol.7, No. 6, 1995, 37-42
- [15] E.M.A.Mustafa, A.Bon "Role of top management leadership and commitment in total quality management in service organization in Malaysia: a review and conceptual framework", Elixir International Journal, Vol. 51, No. 1, 2012, 11029–11033.
- [16] T.C. Powell "Total quality management as competitive advantage, a review and empirical study", Strategic Management Journal, Vol.16, No. 1, 1995, 15-37.
- [17] D. Prajogo, A. Sohal "The multidimensionality of TQM practices in determining quality and innovation performance-an empirical examination", Technovation, Vol. 24, 2004b, 443-453
- [18] S. Rahman, P. Bullock, "ST, HT, and organizational performance relationships: an empirical investigation", (*Omega*), The International Journal of Management Science, Vol.33, No.1, 2005, 73-83
- [19] J.V.Saraph , P.G. Benson, R.G.Schroeder "An instrument for measuring the critical factors of quality management", Decision Sciences, Vol. 20, No. 4, 1989, 810-829.
- [20] M. Sashkin, K.J. Kiser. Putting Total Quality Management to work: What TQM means, How to use it & How to sustain it over the long run. Berrett-Koehler Publishers, Inc, 1993
- [21] SIRIM QAS .International Directory of Certified Products and Companies, Shah Alam, Malaysia.
- [22] S.B. Sitkin, K.M. Sutcliffe, R.G. Schroeder "Distinguishing control from learning in total quality management: A contingency perspective", Academy of Management Review, Vol.19, No. 3, 1994, 537-564.
- [23] B.A. Spencer "Models of Organization and Total Quality Management: comparison and critical evaluation", Academy of Management Review, Vol.19, No. 3, 1994, 446-471.
- [24] B. Stephens "Implementation of ISO 9000 or Ford's Q1 award: Effects on organizational knowledge and application of TQM principles and quality tools", The TQM Magazine, Vol.9 No. 3, 1997, 190-200.
- [25] J. Tata, S. Prasad, R. Thorn, "The influence of organizational structure on the effectiveness of TQM Programs", Journal of Managerial Issues, Vol.4, 1999, 440-453
- [26] T., Thiagaragan, M. Zairi, B. Dale "A proposed model of TQM implementation based on an empirical study of Malaysian industry", International Journal of Quality & Reliability Management, Vol.18, No.3, 2001, 289-306
- [27] A. Wilkinson, "The other side of Quality: Soft issues and the Human resource dimension", Total Quality Management, Vol.3, No. 3, 1992, 323-329.
- [28] A. Wilkinson, T., E. Redman, M. Snape, "Managing with Total Quality Management: Theory and Practice", London, MacMillan; 1998
- [29] M. Zairi, S. Baidoun "Understanding the essentials of Total quality management, a best practice Approach – part 1", Working paper series, Bradford University, Australia 03/03,2003a, 1-28.
- [30] M. Zairi, S. Baidoun "Understanding the essentials of Total quality management, a best practice Approach – part 2, Working paper series, Bradford University, Australia 03/05, 2003b,.1-32.
- [31] M.Zairi , A.A. Alsughayir (2011)"The adoption of excellence models through cultural and social adaptations: an empirical study of critical success factors and a proposed model", Total Quality Management and Business Excellence, Vol. 22, No. 6, 2011, 641–654.
- [32] Z. Zhang, AB. Waszink, J. Wijngaard " An instrument for measuring TQM implementation for Chinese manufacturing companies", International Journal of Quality & Reliability Management, Vol.17, No. 7, 2000, 730-755.

Appendix1: Summary of Results of the Corollary Hypotheses

Code: S: supported, R: Rejected

Hypothesis Statement	Result
H1A Soft total quality management is positively associated with supplier quality management.	
H1A1 There is a significant and positive relationship between leadership and supplier quality management	R
H1A2 There is a significant and positive relationship between vision and plan statement and supplier quality management	S
H1A3 There is a significant and positive relationship between evaluation and supplier quality management	R
H1A4 There is a significant and positive relationship between employee participation and supplier quality management	R
H1A5 There is a significant and positive relationship between recognition and reward and supplier quality management	R
H1A6 There is a significant and positive relationship between education and training and supplier quality management	R
H1A7 There is a significant and positive relationship between customer focus and supplier quality management	R
H1B Soft total quality management is positively associated with process control and improvement	
H1B1 There is a significant and positive relationship between leadership and process control and improvement	R
H1B2 There is a significant and positive relationship between vision and plan statement and process control and improvement	S
H1B3 There is a significant and positive relationship between evaluation and process control and improvement	S
H1B4 There is a significant and positive relationship between employee participation and process control and improvement	R
H1B5 There is a significant and positive relationship between recognition and reward and process control and improvement	R
H1B6 There is a significant and positive relationship between education and training and process control and improvement	R
H1B7 There is a significant and positive relationship between customer focus and process control and improvement	S
H1C Soft total quality management is positively associated with product design.	
H1C1 There is a significant and positive relationship between leadership and product design	R
H1C2 There is a significant and positive relationship between vision and plan statement and product design	S
H1C3 There is a significant and positive relationship between evaluation and product design	R
H1C4 There is a significant and positive relationship between employee participation and product design	R
H1C5 There is a significant and positive relationship between recognition and reward and product design	R
H1C6 There is a significant and positive relationship between education and training and product design	R
H1C7 There is a significant and positive relationship between customer focus and product design	S
H1D Soft total quality management is positively associated with quality system improvement	
H1D1 There is a significant and positive relationship between leadership and quality system improvement	R
H1D2 There is a significant and positive relationship between vision and plan statement and quality system improvement	S
H1D3 There is a significant and positive relationship between evaluation and quality system improvement	R
H1D4 There is a significant and positive relationship between employee participation and quality system improvement	R
H1D5 There is a significant and positive relationship between recognition and reward and quality system improvement	R
H1D6 There is a significant and positive relationship between education and training and quality system improvement	R
H1D7 There is a significant and positive relationship between customer focus and quality system improvement	S
H1E Soft total quality management is positively associated with total quality management tools and techniques/ purchasing	
H1E1 There is a significant and positive relationship between leadership and TQM tools and techniques/purchasing	S
H1E2 There is a significant and positive relationship between vision and plan statement and TQM tools and techniques/purchasing	S
H1E3 There is a significant and positive relationship between evaluation and TQM tools and techniques/purchasing	S
H1E4 There is a significant and positive relationship between employee participation and TQM tools and techniques/purchasing	R
H1E5 There is a significant and positive relationship between recognition and reward and TQM tools and techniques/purchasing	R

H1E6 There is a significant and positive relationship between education and training and TQM tools and techniques/purchasing	R
H1E7 There is a significant and positive relationship between customer focus and TQM tools and techniques/purchasing	S
H1F Soft total quality management is positively associated with total quality management tools and techniques/ production.	
H1F1 There is a significant and positive relationship between leadership and TQM tools and techniques/ production	S
H1F2 There is a significant and positive relationship between vision and plan statement and TQM tools and techniques/ production	S
H1F3 There is a significant and positive relationship between evaluation and TQM tools and techniques/ production	R
H1F4 There is a significant and positive relationship between employee participation and TQM tools and techniques/ production	R
H1F5 There is a significant and positive relationship between recognition and reward and TQM tools and techniques/ production	R
H1F6 There is a significant and positive relationship between education and training and TQM tools and techniques/ production	R
H1F7 There is a significant and positive relationship between customer focus and TQM tools and techniques/ production	R
H1G Soft total quality management is positively associated with total quality management tools and techniques/ sales.	
H1G1 There is a significant and positive relationship between leadership and TQM tools and techniques/ sales	R
H1G2 There is a significant and positive relationship between vision and plan statement and TQM tools and techniques/ sales	S
H1G3 There is a significant and positive relationship between evaluation and TQM tools and techniques/ sales	S
H1G4 There is a significant and positive relationship between employee participation and TQM tools and techniques/ sales	S
H1G5 There is a significant and positive relationship between recognition and reward and TQM tools and techniques/ sales	S
H1G6 There is a significant and positive relationship between education and training and TQM tools and techniques/ sales	R
H1G7 There is a significant and positive relationship between customer focus and TQM tools and techniques/ sales	R
H1H Soft total quality management is positively associated with total quality management tools and techniques/ customer service.	
H1H1 There is a significant and positive relationship between leadership and TQM tools and techniques/ customer service	R
H1H2 There is a significant and positive relationship between vision and plan statement and TQM tools and techniques/ customer service	R
H1H3 There is a significant and positive relationship between evaluation and TQM tools and techniques/ customer service	S
H1H4 There is a significant and positive relationship between employee participation and TQM tools and techniques/ customer service	R
H1H5 There is a significant and positive relationship between recognition and reward and TQM tools and techniques/ customer service	S
H1H6 There is a significant and positive relationship between education and training and TQM tools and techniques/ customer service	S
H1H7 There is a significant and positive relationship between customer focus and TQM tools and techniques/ customer service	S

Prediction of surface roughness in Electrical Discharge Machining of SKD 11 TOOL steel using Recurrent Elman Networks

R. DAS^a, M. K Pradhan^{*,b} and C Das^c

^a School of Advanced Sciences, VIT University, Vellore, Tamil Nadu, India

^b Department of Mechanical Engineering, Maulana Azad National Institute of Technology, Bhopal

^c Synergy Institute of Engg. & Tech, Dhenkanal, India

Abstract:

Elman Networks is a one of the dynamic recurrent neural networks. In this research it is used for the prediction of surface roughness in Electrical Discharge Machining (EDM). Training of the models was performed with data from series of EDM experiments on SKD 11 (AISI D2) Tool steel; in the development of predictive models, machining parameters of discharge current, pulse duration and duty cycle were considered as model variables with a constant voltage 50 volt. For this reason, extensive experiments were carried out in order to collect surface roughness dataset. The developed model is validated with a new set of experimental data, and predictive behavior of models is analyzed. The reported results indicate that the proposed model can satisfactorily predict the surface roughness in EDM. And can be considered as valuable tools for the process planning for EDMachining.

© 2013 Jordan Journal of Mechanical and Industrial Engineering. All rights reserved

Keywords: Surface Roughness; Electrical Discharge Machining; Recurrent Elman Networks.

1. Introduction

Due to capability of manufacturing components of any hardness and shape on wide range of conductive engineering materials, electro discharge machining (EDM) is one of the well-established manufacturing methods in modern manufacturing field. In this manufacturing technique, material removal is caused by repetitive minute electric discharges within the electrode-workpiece-dielectric interface. Each discharge, due to high energy concentration, removes from the workpiece surface a small quantity of material in form of molten metal drops and even vapors, meanwhile the discharge location on the workpiece surface is in part stochastic and in part dependent on surface micro relief. The outcome of such a unit-event is the characteristic crater. The mechanism of the crater formation is a complex phenomenon involving several disciplines of science and branches of engineering. The theories revolving around the formation of plasma channel between the tool and the workpiece, thermodynamics of the repetitive spark causing melting and evaporating the electrodes, micro-structural changes, and metallurgical transformations of material, are still not clearly understood. However, it is widely accepted that the mechanism of material erosion is due to intense local heating of the workpiece causing melting and evaporation

of workpiece. Therefore, it is hard to establish a model that can accurately predict the performance by correlating the process parameter.

Surface roughness (Ra) is a significant upshot in the manufacturing process and it materializes a major part in the manufacturing system. Therefore, characterization, prediction, and modeling of quality of EDMed component surface roughness play a vital role. The component, having good surface, improves the fatigue strength, wear resistance and corrosion resistance of the surface. Ra depends on different machining parameters and its prediction and control is a query to the researchers.

Artificial neural networks are simplified models of the central nervous system. They are networks of highly interconnected neural computing elements. In the recent past, neural networks have been shown to be the highly flexible modeling tools surely due to their well-known characteristics of adaptability and non-linear universal mapping approximations. It has the capability to handle problems such as modeling, estimating, prediction, optimization, diagnosis and adaptive control in complex non-linear systems. It is observed that the neural network applications play a very important role in predicting surface roughness in EDM. Recurrent neural networks are useful for storing information about time and particularly suitable for time series prediction [1]. Tsai and Wang [2] applied various neural network architectures for the

* Corresponding author. e-mail: mohanrkl@gmail.com.

prediction of the Ra and MRR in EDM and agreed to the predictions based upon the models. Indurkha and Rajurkar [3] attempted to model a 9-9-2 size back propagation neural network for the prediction of Ra and MRR., where the 9 different machining parameters, such as machining depth, tool radius, orbital radius, radial step, vertical step, offset depth, pulse on time, pulse off time and discharge current are selected as input parameters are used to determine the two outputs Ra and MRR. The model predictions are compared with estimates obtained via multiple regression analysis, and found more accurate and also less sensitive to noise induced in the experimental data than that of multiple regressions model. Panda and Bhoi [4] developed an artificial feed forward neural network to predict MRR of SKD 11 grade steel. This model performs well under the stochastic environment of actual machining conditions without understanding the complex physical phenomena exhibited in EDM, and provides faster and more accurate results. They found that the 3-4-3-1 neural architecture has the highest correlation coefficient and used it for the analysis. Wang et al. [5] combined the capabilities of Artificial Neural Network (ANN) and genetic algorithm to find an integrated solution to the existing problem of modeling and optimization of EDM processes. Markopoulos et al. [6] proposed ANN models for the prediction of Ra of EDMed surfaces. The experiments were conducted on five steel grades, namely a mild steel, a carbon steel, and three alloyed steels, were tested while pulse current (I_p) and the pulse duration (Ton) varied over a wide range. Results revealed that proposed ANNs models can satisfactorily predict the response. Pradhan and Biswas [7] presented a neuro-fuzzy model to predict MRR of AISI D2 tool steel with different process parameter such as I_p , Ton and duty cycle (τ), and the model predictions were found to be in good agreement with the experimental results. Pradhan et al. [8] applied the neural network models namely back-propagation and radial basis function for the prediction of Ra. Using I_p , Ton and τ as input parameters, experiments are conducted on D2 steel. It is reported that former shows slightly better performance than the latter, however latter model is faster. Portillo [9;10] used recurrent neural network approach to detect in advance the degradation of the cutting process due to the memorization capability and the dynamic character of the Elman architecture.

It is observed that the neural network is widely used in EDM process for the prediction of responses and effect of the parameters on them. However recurrent neural network is not used yet for the prediction of Ra in EDM. Though this net has been efficient identification tool in many areas as they have dynamic memories. In this study, recurrent neural network approach, named Elman network [11], is used for the prediction of the center-line average surface roughness, Ra of electrical discharge machined surfaces is discussed. The proposed models use data for the training procedure from an extensive experimental research concerning surface integrity of EDMed D2 steels. I_p , Ton, and τ were considered as the input parameters of the models. The I_p , Ton, and τ varied over a wide range, from roughing to near-finishing conditions. The proposed neural networks trained with the feed forward back propagation algorithm and were proven to be successful, resulting in

reliable predictions, providing a possible way to avoid time and money-consuming experiments.

2. Experimental Details

Experiments were conducted on Electronica Electraplus PS 50ZNC die sinking machine. A cylindrical pure copper was used as a tool electrode (of positive polarity) with a diameter of 30 mm and workpiece materials used were AISI D2 tool steel square plates of dimensions 35 × 35 mm² and thickness 4 mm. Commercial grade EDM oil (specific gravity = 0.763, freezing point= 94°C) was used as dielectric fluid. Lateral flushing with a pressure of 0.3 kg f /cm² was used. Keeping the voltage constant at 50 V, number of experiments was conducted to investigate the effects of I_p , Ton and τ on Ra, where τ is defined as:

$$\tau = \frac{T_{on}}{T_{on} + T_{off}} \times 100 \quad (1)$$

The experimental conditions and the levels of the input parameters are shown in Table 1. Each treatment of the experiment was run for 15 minutes and the Ra was measured.

Table 1. Experimental conditions

Sparking voltage in V	50
Current (I_p), in A	1 5 10 20 30 50
Pulse on Time (Ton), in μ s	5 10 20 30 50 100 150 200 500 750
Duty Cycle (τ) in %	50 85 92
Dielectric used	Commercial grade EDM oil
Dielectric flushing	Side flushing with pressure
Work material	SKD 11 tool steel
Electrode material	Electrolytic pure Copper
Electrode polarity	Positive
Work material polarity	Negative

3. Surface Roughness Measurement

The Ra is used to portray the technical surface quality of an engineering component. It has a very significant influence on the manufacturing outlay of a product. A good quality surface enhances the fatigue strength, corrosion, and wear-resistance of the workpiece. There is a number of ways by which surface roughness of a component is described, such as roughness average (Ra), root-mean-square (rms) roughness (Rq) and maximum peak-to-valley roughness (Ry or Rmax), etc. In this work, Ra is used, which is measured using Talysurf (Taylor Hobson, Surtronic 3⁺). The profilometer was set to a cut-off length of 0.8 mm, filter 2CR, traverse speed 1 mm/second and 4 mm evaluation length. Roughness measurements, in the transverse direction, on the workpieces were repeated four times and average of four measurements of surface roughness parameter values was recorded. The measured profile was digitized and processed through the dedicated advanced surface finish analysis software Talyprofile for assessment of the

roughness parameters. Ra can be defined as the arithmetic value of the profile from centerline along the sampling length. It can be expressed as

$$Ra = \frac{1}{L} \int |y(x)| dx \quad (2)$$

Where L is the sampling length, y is the profile curve and x is the profile direction. The average Ra is measured within L = 0.8 mm. Centre-line average Ra measurements of electro-discharge machined surfaces were taken to provide quantitative evaluation of the effect of EDM parameters on surface finish.

4. Predictive Models for Surface Roughness

Recurrent networks are a special type of the dynamic neural nets. The Elman neural network is a simple recurrent neural network. This network is similar to an architecture proposed by Jordan [12]. Elman network reveals a rich structure that permits them to be highly context-dependent, and also states generalizations across classes of items. Yet, to have a real-time (online) learning ability, standard back propagation (BP) training for Elman network, known as Elman BP [13]. This architecture is standard feedforward architecture with layers of inputs, hidden units, and output units. It is a single hidden layer feedforward neural network. All neurons in one layer are connected with all neurons in the next layer. The outputs of the hidden layer are allowed to feed back to the context layer, and to augment additional units at the input level. Therefore, the input layer is constituted by the input nodes plus these context nodes. The context unit is fully connected with all the hidden units in a forward manner. The neurons in the context layer hold a copy of the output of the hidden neurons. The output of each hidden neuron is copied into a specific neuron in the context layer. The value of the context neuron is used as an extra input for all the neurons in the hidden layer one-time step later. Therefore, the Elman network has an explicit memory of one time lag.

In Elman network, both the input units and context units activate the hidden units. Since the context units are in the initial state, only the input units contribute to the activation of the hidden units at $t - 1$. The hidden units are then fed forward to activate the output units and, at the same time, fed back to activate the context units on the second step at the time t . Now, the context units contain the exact values of those of the hidden units. The information in the context units and input units receive the new input vector to activate the hidden units at time $t + 1$. The hidden units then activate the output units, as well as the context units at time $t + 2$. The above process is repeated at the next time step. Thus, these context units provide the network with information that is recurrent in time.

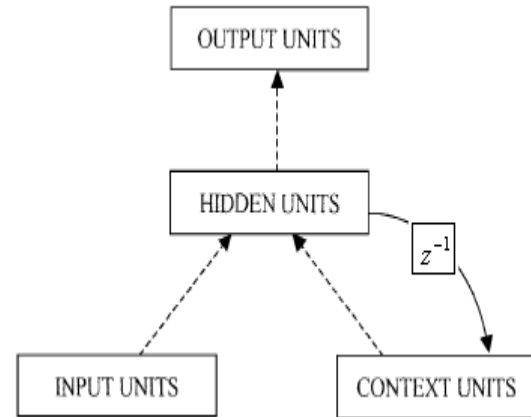


Figure 1. Architecture of the Elman Network.

The structure of an Elman recurrent neural network is illustrated in Fig. 1. Here, I , H , O and z^{-1} are input layer vector, hidden layer vector, context layer vector, output layer vector and unit delay element, respectively. The weight matrix between input layer and hidden layer is $W1$, the weight matrix between context layer and hidden layer is $W2$ and the weight matrix between hidden layer and output layer is $W3$.

At t th iteration,

$$x_i(t) \in I, \quad i = 1, \dots, n$$

$$z_k(t) \in O, \quad k = 1, \dots, l$$

$$y_j(t) \in H, c_j(t) \in C \quad j = 1, \dots, m$$

where i and k are the number of nodes of input layer and output layer respectively and j is the number of nodes of hidden layer and context layer. Considering the activation function $f(\bullet)$ for j th hidden node, the outputs of the neurons in the hidden layer and output layer for time t are can be given by

$$y_j(t) = f \left(\sum_{i=1}^n w1_{ij} x_i(t) + \sum_{j=1}^m w2_{ij} y_j(t-1) \right)$$

,

$$c_j(t) = y_j(t-1)$$

and

$$z_k(t) = f \left(\sum_{j=1}^m w3_{jk} y_j(t) \right)$$

where $w1_{ij} \in W1$, $w2_{ij} \in W2$ and $w3_{jk} \in W3$

For initial step, $y_j(0) = 0$. The context layer input at $t = 1$ leads to $c_i(1) = 0$. The weights are updated according to

$$w(t+1) = w(t) + \eta \Delta w(t)$$

where η is the learning rate.

That minimizes the approximation error E in the output layer is given by

$$E(w) = \frac{1}{p} \sum_{t=1}^p \frac{1}{2} \left(\sum_{k=1}^l [T_k(t) - z_k(t)]^2 \right)$$

where $T_k(t)$ is the target value at t th iteration and p is the length of the training sequence.

Weight coefficient matrix $W1$ and $W3$ can be updated using any of the back-propagation algorithms as done in feedforward neural network. But weight coefficient matrix $W2$ can be adjusted using derivative chain rule [14].

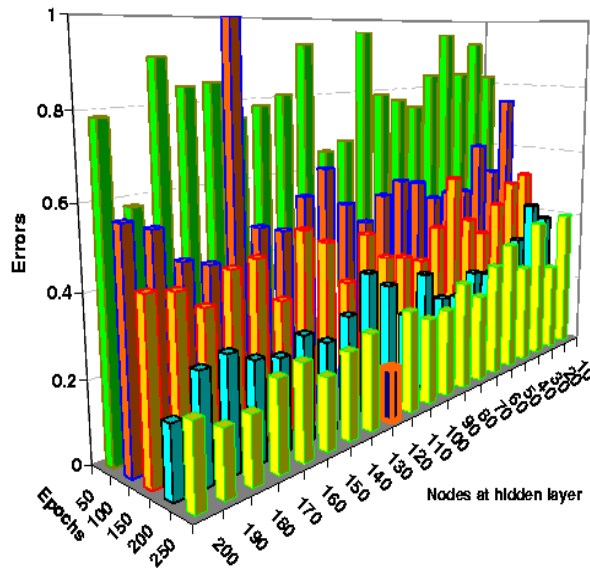


Figure 1. Errors_ Epochs_ Nodes at hidden layer.

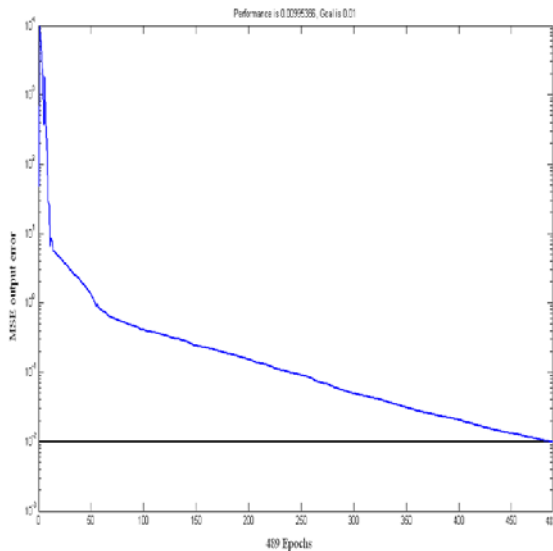


Figure 3: 489 iteration in the Elman's learning process

RNN is observed separately with results obtained by experiments and the average error obtained for the networks. The test result accuracy measured in terms of mean absolute error (MAE) for 9 test data are found to be 0.31355. The experimental results and predicted results of 'Ra' by the RNN were plotted, as shown in Fig 4.

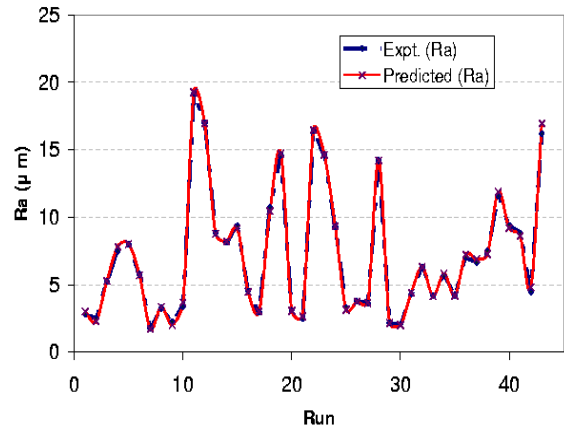


Figure 2. Comparison between experimental and predicted data for Ra.

The variations of prediction error (calculated as the difference between the experimental findings and predicted values) plotted against run for training and validation sets for Elman's model is shown also in the figure 5. Except for an outlier, the validation set exhibits very accurate prediction. The error for the model, calculated as the difference between the experimental findings and predicted values and the pattern of the residual plot, is scattered, which does not shows any pattern/trend that indicates that the model is certainly adequate. A good model fitting this plot should show a random scatter and have no pattern [12]. However, the absolute percentage prediction error is tabulated in Table.2.

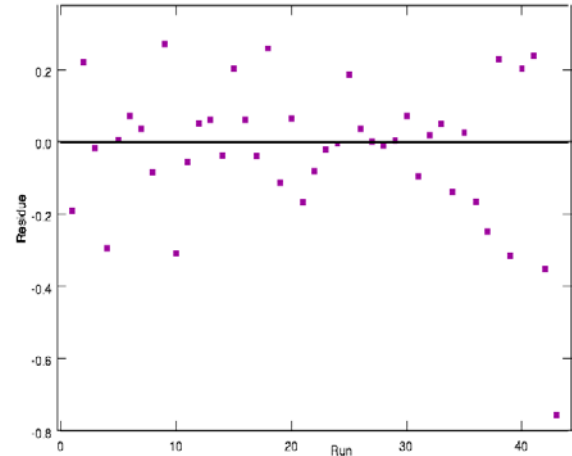


Figure 3. Residual plot vs. Run.

Figure 5 shows the scatter plot of predicted Ra using Elman's network and Experimental Ra, respectively. The correlation coefficients (r) between Experimental and predicted value of Ra is 0.999, from a statistical judgment, the closer this number is to 1, the more powerful the network in correlating the input space to the output space. The plot of Experimental and predicted output is presented in Fig. 6. Since all the points on plot come close to form a straight line, it implies that the data are normal. Therefore, the Elman's network can be used to attain a function that maps input parameters to the desired process outputs in EDM. The predicted values are quite close for most of the data points.

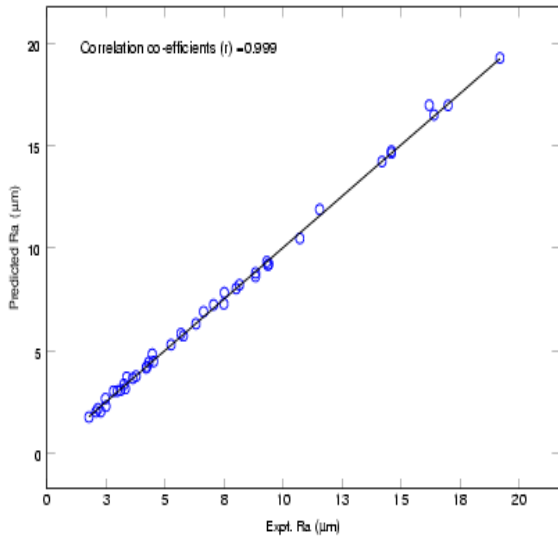


Figure 4. Correlation between experimental data and neural network output.

Table 2. Results from production data sets for surface roughness model

.S. no	Experimental Ra	Eleman's predicted Ra	% error
1	7.06	7.22	2.35
2	6.64	6.88	3.76
3	7.5	7.26	3.07
4	11.56	11.87	2.72
5	9.4	9.19	2.15
6	8.84	8.60	2.67
7	4.46	4.81	7.95
8	16.2	16.95	4.66

5. Conclusion

Elman neural network is discussed in details by predicting Ra. The present study has demonstrated a new application of the Elman recurrent neural network to the prediction of Ra. The Elman network has performed satisfactorily in the prediction of Ra. Instead of conducting actual experiments in EDM for different values of machining parameters, a suitable intelligent system can be used to predict Ra. When a desired Ra is obtained, a confirmation test can then be conducted experimentally to verify the predicted Ra. By using this approach, lengthy and time-consuming experimentation in EDM can be reduced. From our work, the potential of using an intelligent learning system for prediction is evident. Therefore, we believe that ANNs can be used as a powerful tool in manufacturing system, as well as other areas in modern manufacturing industry, so that the development tasks can be performed rapidly and

efficiently with an increase of productivity, consistency and quality.

References

- [1] Elman, J., Finding structure in time. *Cognitive Science* 14, 1990, 179–211.
- [2] Tsai, K. M., Wang, P. "Predictions on surface finish in electrical discharge machining based upon neural network models". *International Journal of Machine Tools Manufacture* Vol. 41, 2001 1385–1403
- [3] Indurkha, Gopal, Rajurkar, K. P. "Artificial Neural Network approach in modeling of EDM process", *Intelligent Engineering Systems Through Artificial Neural Networks*, Vol. 2, 1992, 845-850
- [4] Panda, D.K., and Bhoi, R. K.: "Artificial neural network prediction of material removal rate in electro- discharge machining. *Materials and Manufacturing Processes*" Vol. 20, 2005, 645–672.
- [5] Wang, K., Gelgele, H.L., Wang, Y., Yuan, Q., Fang, M.: "A hybrid intelligent method for modelling the EDM process". *International Journal of Machine Tools and Manufacture* Vol, 43, 2003, 995–999
- [6] Markopoulos, A. P., D. E. Manolakos, and N. M. Vaxevanidis. "Artificial neural network models for the prediction of surface roughness in electrical discharge machining". *Journal of Intelligent Manufacturing* vol. 19, No. 3, 2008, 283-292
- [7] Pradhan, M. K. and Biswas, C. K. "Neuro-fuzzy model on material removal rate in electrical discharge machining in AISI D2 steel", *Proc. of the 2nd International and 23rd All India Manufacturing Technology, Design and Research Conference*, Vol.1, 2008., 469–474.
- [8] Pradhan, M. K, Das R., and Biswas C, K., "Comparisons of neural network models on surface roughness in Electrical Discharge Machining" *Proc. IMechE Part B: J. Engineering Manufacture*, Vol. 223, No- 7, 2009, 801-808.
- [9] Portillo E, Cabanes I, Marcos M, Zubizarreta A. "On the application of recurrent neural network techniques for detecting instability trends in an industrial process". 2007. 242-248.
- [10] Portillo, E., et al. "Recurrent ANN for Monitoring Degraded Behaviours in a Range of Workpiece Thicknesses." *Engineering Applications of Artificial Intelligence* Vol. 22.8, 2009, 1270-1283.
- [11] Jordan, M., I., "Proceeding of Eighth Conference of the Cognitive Science Society", *Attractor dynamics and parallelism in a connectionist sequential machine*. *Cognitive Science Society*, 1986, 531-546.
- [12] Şeker S, Ayaz E, Türkcan E. Elman's recurrent neural network applications to condition monitoring in nuclear power plant and rotating machinery. *Eng Appl Artif Intelligent* . Vol. 16 No.7-8, 2003, 647-656.
- [13] Gruning, "Stack-like and queue-like dynamics in recurrent neural networks," *Connection Sci.*, vol. 18, no. 1, pp. 23–42, 2006.
- [14] Breyfogle, Forrest W. Breyfogle, III, Forrest W. Breyfogle, *Implementing Six Sigma* , John Wiley and Sons, 2003.



الجامعة الهاشمية



المملكة الأردنية الهاشمية

المجلة الأردنية
للمهندسة الميكانيكية والصناعية

JJIMIE

مجلة علمية عالمية محكمة
تصدر بدعم من صندوق البحث العلمي

<http://jjmie.hu.edu.jo/>

ISSN 1995-6665

المجلة الأردنية للهندسة الميكانيكية والصناعية

مجلة علمية عالمية محكمة

المجلة الأردنية للهندسة الميكانيكية والصناعية: مجلة علمية عالمية محكمة تصدر عن عمادة البحث العلمي و الدراسات العليا في الجامعة الهاشمية بالتعاون مع صندوق دعم البحث العلمي في الأردن.

هيئة التحرير

رئيس التحرير

الأستاذ الدكتور نبيل عنقارة

قسم الهندسة الميكانيكية و الصناعية، الجامعة الهاشمية، الزرقاء، الأردن.

الأعضاء

الأستاذ الدكتور ناصر الحنيطي
الأستاذ الدكتور سهيل كيوان
الأستاذ الدكتور محمود زعل ابو زيد
الأستاذ الدكتور محمد أحمد حمدان
الأستاذ الدكتور إبراهيم الروابدة
الأستاذ الدكتور امين الربيدي

مساعد رئيس هيئة التحرير

الدكتور خالد الوديان
الدكتور اسامة منيزل
الدكتور أحمد الغندور

فريق الدعم

تنفيذ وإخراج

م.مهند عقدة

المحرر اللغوي

الدكتور قصي الذبيان

ترسل البحوث إلى العنوان التالي

رئيس تحرير المجلة الأردنية للهندسة الميكانيكية والصناعية

عمادة البحث العلمي والدراسات العليا

الجامعة الهاشمية

الزرقاء - الأردن

هاتف : 00962 5 3903333 فرعي 4147

Email: jjmie@hu.edu.jo

Website: www.jjmie.hu.edu.jo